Na^+ AND Ca^{2+} CHANNELS IN THE LYSOSOME: OPENING THE GATE TO THE CELL'S RECYCLING CENTER

by

Xiang Wang

A dissertation submitted in partial fulfillment
of the requirements for the degree of
Doctor of Philosophy
(Molecular, Cellular, and Developmental Biology)
in the University of Michigan
2013

Doctoral Committee:

Associate Professor Haoxing Xu, chair
Professor Richard I. Hume
Professor John Y. Kuwada
Assistant Professor Kwoon Y. Wong
Associate Professor X.Z. Shawn. Xu

To my parents, my husband and my baby,

for their love and support,

and for the joy they bring to my life.

ACKNOWLEDGEMENT

I would like to take this opportunity to thank all the people who have made this dissertation possible, and who have made my graduate life wonderful.

First and foremost, I would like to express my sincerest gratitude to my advisor Dr. Haoxing Xu, for his tremendous guidance, support and encouragement throughout my graduate studies. His passion and dedication have always inspired me; his hard-working has instilled in me the value of efforts; his scientific rigor and research philosophy have influenced me to grow as a critical and independent scientist; and his patience and support has helped me overcome the difficulties during my study. I feel extreme fortunate to be his student, and I hope one day I would be as good a scientist and mentor as Dr. Haoxing Xu. I also would like to thank all the former and current members from Dr. Xu's lab. This thesis would not have been possible without their generous assistance, passionate scientific discussion and strong support. They are all wonderful friends and colleagues for me and I can hardly expect more from them. I want to thank Dr. Xianping Dong and Dr. Xiping Cheng for being my first supervisor and teaching me many techniques essential for my research. For my research work, I have a close collaboration with Dr. Xianping Dong, Dr. Xiaoli Zhang, Dr. Dongbiao Shen, Mohammad Samie, Xianran Li, Andrew Goschka and Taylor Dawson. I greatly enjoyed working together with them and deeply appreciate their important contributions to my thesis work. I also want to thank Qiong Gao, Abigail Garrity, Dr. Wuyang Wang, Tony Zhuo, Nick Rydzewski, Cathy Dong, Qi Zhang, Eric Mills, Brian Eisinger, Lily Hu, Meiling Liu and all other lab members, for all the help and support, and for sharing pleasures and joys with me.

I owe my great gratitude to the members of my thesis committee, Dr. Richard Hume, Dr. John Kuwada, Dr. Shawn Xu, Dr. Kwoon Wong. They are always ready to help and have offered invaluable suggestions and support for both my research and my career.

It's a pleasure to thank all the labs in the department of MCDB, especially Hume lab, Kuwada lab, Collins lab, Akaaboune lab, Shafer lab and Duan lab for sharing reagents and thoughts with us. I want to thank Dr. Amy Chang to offer me the opportunity to rotate in her lab. I also want to thank Ms. Mary Carr and Ms. Diane Durfy for their generous help to make my graduate life much easier.

I appreciate all the contributions from my collaborators at University of Michigan, Drs. Hollis Showalter, Yafei Jin, Leslie Satin, Jianhua Ren, Peter Arvan for the TPC project, Dr.

Yanling Zhang, Dr. Lois weisman and her lab members, Dr. Miriam Meisler and her research group for the TRPML1-PI(3,5)P_2 project. I also would like to thank Dr. Michael Zhu from University of Texas Health Science Center, Houston, Dr. Dejian Ren and his research group in University of Pennsylvania and Dr. David Clapham in Children's Hospital Boston for the generous help on the TPC project.

I am very grateful to have many friends, who have offered support and care for me, and shared many moments with me. I deeply value their friendship and they have made my graduate life a joyful journal.

Most importantly, I owe my deepest gratitude to my family: my parents, my husband Dr. Dongbiao Shen and my son Ethan Shen. They always have belief in me. Undoubtedly, their love and support are the genuine drive for me. I feel extremely lucky to have them in my life.

Finally, I appreciate the financial support from Rackham predoctoral fellowship.

PREFACE

In Chapter 1, part of section 1.3 is modified from an invited review [(Dong, Wang, and Xu. TRP channels of intracellular membranes. *J. Neurochem.* 113, 313-328 (2010)). Chapter 2 and chapter 3 are reprinted from a published paper (Wang*, Zhang* et al. TPC proteins are phosphoinositide- activated sodium-selective ion channels in endosomes and lysosomes. *Cell* 151(2):372-83 (2012), with minor modifications. Xiang Wang and Dr. Xiaoli Zhang performed some electrophysiology experiment together. The content of Chapter 4 is modified from a published paper (Dong*, Shen*, Wang*, et al. $PI(3,5)P_2$ controls membrane trafficking by direct activation of mucolipin Ca^{2+} release channels in the endolysosome. *Nat Commun.* 1:38 doi: 10.1038/ncomms1037 (2010)). The content of Chapter 5 is from a submitted manuscript (Samie, Wang, et al. A Ca^{2+} channel in the lysosome regulates large particle phagocytosis via focal exocytosis.) and a published paper (Dong*, Wang*, et al. Activating mutations of the TRPML1 channel revealed by proline scanning mutagenesis. *J. Biol. Chem.* 284, 32040–32052 (2009). **Fig. 3.1** and **Fig. 3.2** were prepared by Dr. Xianping Dong, Dr. Xiaoli Zhang and Xiang Wang. **Fig. 2.4B, F; Fig. 2.10A; Fig. 3.3A**; **Fig. 3.5A** were prepared by Dr. Xiaoli Zhang; **Fig. 2.4C-E; Fig. 4.1; Fig. 5.2** were prepared by Dr. Xianping Dong; **Fig. 2.3A**, **Fig. 2.4A**, **Fig. 2.8E** were prepared by Xianran Li; **Fig. 2.7A-C**; **Fig. 2.8B** were prepared by Mohammad Samie and Andrew Goschka; **Fig. 2.9A; Fig. 3.5B-E**; **Fig. 4.4B** were prepared by Dr. Dongbiao Shen; **Fig. 4.4E** were prepared Taylor Dawson.

TABLE OF CONTENTS

LIST OF FIGURES

LIST OF ABBREVIATIONS

BAPTA: 1,2-bis(o-aminophenoxy)ethane-N,N,N',N'-tetraacetic acid

BAPTA-AM: BATPA acetoxymethy

cADPR: cyclic ADP-ribose

CaM: calmodulin

Ca_V: voltage-gated Ca^{2+} channel

CICR: calcium induced calcium release

EE: early endosome

EEA1: early endosome antigen 1

EGFP: enhanced green fluorescent protein

EGTA: ethylene glycol-bis(2-aminoethylether)-N,N,N′,N′-tetraacetic acid

EGTA-AM: EGTA acetoxymethy

Endolysosome: endosome and lysosome

ER: endoplasmic reticulum

E_{rev}: reversal potential

GOF: gain-of-function

GPN: glycyl-L-phenylalanine-2-napthylamide

hTPC2: human two-pore channel 2

IP_3: inositol trisphosphate

IP_3R: inositol trisphosphate receptor (IP_3 receptor)

KO: knock-out

Lamp-1: lysosome-associated membrane protein 1

LEL: late endosome and lysosome

LL: di-leucine

LSD: lysosomal storage disease

ML1: TRPML1, mucolipin-1

ML4: type IV Mucolipidosis

mTPC2: mouse two-pore channel 2

MVB: multi-vesicular body

NAADP: nicotinic acid adenine dinucleotide phosphate

Na_V: voltage-gated Na^+ channel

NHE: Na^+/H^+ exchanger

NPC: Niemann-Pick disease, type C

PM: plasma membrane

PI: phosphatidylinositol

PI(3,5)P_2: phosphatidylinositol 3,5-bisphosphate

PI(4,5)P_2: phosphatidylinositol 4,5-bisphosphate

PIKfyve: FYVE finger-containing phosphoinositide kinase

Pro: proline

RyR: ryanodine receptor

SNARE: soluble NSF attachment protein receptor

SR: sarcoplasmic reticulum

Syt VII: synaptotagmin VII

TFEB: transcription factor EB

TGN: trans-Golgi network

TM: transmembrane

TPC: two-pore channel

TRP channels: Transient receptor potential channels

TRPML: the mucolipin family of the TRP channels

V-ATPase: vacuolar-type H^+-ATPase

VAMP7: vesicle-associated membrane protein 7

ABSTRACT

Lysosomes primarily serve as the cell's "garbage disposal and recycling center", and are recently found to be involved in many important cellular functions. Lysosomes are also ion stores enriched with H^+, Ca^{2+}, and Na^+. While it's well known that the lysosomal ionic homeostasis is essential for its proper functions, the properties of ion transporters and channels residing on lysosomal membranes are barely understood, largely due to the lack of a reliable functional assay. Recently our lab has established a unique lysosomal patch-clamp method to directly record from native lysosomal membrane. Taking advantage of the technique, I discovered two novel lysosomal Na^+-selective channels (Two-Pore-Channels TPC1 and TPC2), which are previously thought to be Ca^{2+} release channels, triggered by the second messenger NAADP. Using an integrative approach, I further demonstrated that TPCs are not activated by NAADP, but instead by $PI(3,5)P_2$, a lysosome-specific phosphoinositide that regulates lysosomal ion homeostasis and membrane trafficking. TPCs represent the first intracellular Na^+-selective channels, although their functions are not characterized. In addition, my colleagues and I found that $PI(3,5)P_2$ also activates TRPML1, a principle lysosomal Ca^{2+} channel. Loss-of-function mutations in human *TRPML1* cause type IV Mucolipidosis (ML4), a childhood neurodegenerative disease. My results showed that increasing TRPML1's activity alleviated lysosomal trafficking defects in $PI(3,5)P_2$-deficient cells, suggesting that $PI(3,5)P_2$ controls Ca^{2+}-dependent membrane trafficking by regulating TRPML1. To study the role of TRPML1 in membrane trafficking, I focused on the involvement of TRPML1 in Ca^{2+}-dependent lysosomal exocytosis, a universal process important for many cellular functions, including cellular clearance, plasma membrane repair and phagocytosis. I found that gain-of-function mutations of TRPML1 caused a dramatic increase in lysosomal exocytosis. During particle uptake in macrophages, lysosomal exocytosis is required to provide membrane supplies to facilitate phagosome formation. By whole-cell recordings and newly developed whole-phagosome recordings, I found that upon particle binding, TRPML1-associated lysosomes are delivered to the newly-formed phagosomes via lysosomal exocytosis in a Ca^{2+}-dependent manner. Overall, my thesis work has characterized two types of important channels (TPCs and TRPMLs) in the lysosome, identified their first endogenous activator $PI(3,5)P_2$, and explored their functions in lysosomal biology.

KEY WORDs: $PI(3,5)P_2$, NAADP, lysosomes, patch-clamp technique, TPCs, TRPML1, Na^+ channel, Ca^{2+} channel, membrane trafficking, lysosomal exocytosis

CHAPTER 1
Introduction

1.1 Lysosomes: cellular clearance and recycling center

Lysosomes are ubiquitous intracellular organelles, primarily serving as the cell's "garbage disposal and recycling center". Consistently lysosomes are enriched with a variety of acidic hydrolase, and mediate the degradation and recycling of biomaterials. Recent studies have revealed that lysosomes have much broader functions, including membrane trafficking, signal transduction, plasma membrane repair, cholesterol homeostasis and cell-death (Saftig and Klumperman, 2009). The diverse functions and the dynamic interactions with endocytic, autophagic, phagocytic and exocytosis pathways have placed the lysosome at a center point of cellular catabolism.

The study on lysosomes can be traced back to over one century ago. In 1893, Metchnikoff (Nobel laureate in 1908) first discovered that during phagocytosis, the engulfed particles can be digested by an acidic intracellular compartment (reviewed in (Tauber, 2003)). In the 1950s, Christian de Duve identified the "lysosome" as a membrane-enclosed compartment containing acidic hydrolases (De Duve, 1963; De Duve, 1966), and was awarded with a Nobel Prize in 1974. The next milestone for lysosomal research was the discovery of the first lysosomal storage disease (LSD). In 1963, Hers revealed that Pompe disease was caused by genetic defects in a lysosomal enzyme α-glucosidase, which is involved in glycogen catabolism (Hers, 1963). LSDs describe a group of inherited metabolic disorders that result from lysosomal enzyme deficiencies or defects in lysosomal membrane proteins (Platt et al., 2012), including Niemann-pick disease and Mucolipidosis type IV (mutations in TRPML1, discussed below). Thus far, there are more than 50 types of LSDs identified with a combined birth frequency of about 1 in 7500 (Poupetova et al., 2010). Numerous studies into these diseases have provided valuable insights into the complex and fundamental functions of lysosomes. The lysosome-related storage have also been recognized as a pathological feature contributing to other commonly acquired neurodegenerative diseases, such as Alzheimer's disease, Huntington's disease, and Parkinson's disease (Giacomello et al., 2011; Harris and Rubinsztein, 2012; Mazzulli et al., 2011; Tofaris, 2012).

The lysosome performs its function through dynamic membrane fusion and fission (i.e.

membrane trafficking) (See **Fig. 1.1**). During endocytosis, the extracellular macromolecules and plasma membrane proteins are first delivered to early endosomes, where they are either sorted to recycling endosomes to be trafficked back onto the plasma membrane or further transported into late endosomes and lysosomes for degradation (Maxfield and McGraw, 2004). Late endosomes and lysosomes are hard to be distinguished by common molecular markers, e.g. Lamp1 (lysosome-associated membrane protein 1). Thus in this introduction, they may collectively be called endolysosomes. In endolysosomes, the recycled materials are either released into the cytosol via membrane transporters/channels, or delivered to the *trans*-Golgi network via retrograde trafficking (a membrane fission event) (Huotari and Helenius, 2011). In phagocytosis, phagosomes are fused with lysosomes to degrade invading pathogens or apoptotic cells (Luzio et al., 2007b). Beyond the degradation and recycling function, lysosomes also undergo Ca^{2+}-dependent exocytosis (fusion with the plasma membrane) in most, if not all cells (Andrews and Chakrabarti, 2005; Reddy et al., 2001) (Discussed in section 1.7.). This process serves various functions, such as the plasma membrane repair (Reddy et al., 2001), neurite outgrowth (Arantes and Andrews, 2006), and phagosome formation (Czibener et al., 2006). Recent studies also showed that following the starvation-induced autophagy, proto-lysosomes bud off from reformation tubules of autolysosomes, and go through a maturation process to become functional lysosomes. This process, termed as autophagic lysosome reformation, is used to recycle lysosomes and to maintain lysosomal homeostasis (Chen and Yu, 2013; Yu et al., 2010).

1.2 Lysosomal ionic homeostasis

Lysosomes are enriched with H^+, Ca^{2+}, and Na^+, and it has long been known that lysosome ion homeostasis is essential for the proper functioning of lysosomes (Luzio et al., 2007a; Mindell, 2012; Morgan et al., 2011; Scott and Gruenberg, 2011) (See **Fig. 1.2**). However, our understanding about the flux and functions of luminal ions are primitive.

Along the endocytic pathway, progressive acquisitions of different ion channels and transporters considerably change the luminal ionic nature of endosomes and lysosomes. Gradual acidification happens from early endosomes (pH 6.0), late endosomes (pH 5.5) to mature lysosomes (pH 4~5) (Demaurex, 2002; Luzio et al., 2007a; van der Goot and Gruenberg, 2006). In contrast, luminal Ca^{2+} concentration first drops significantly from the newly formed endocytic vesicles (2 mM in the extracellular milieu) to mature early endosomes (~0.003 mM, 20 min after endocytosis) (Gerasimenko et al., 1998); then the Ca^{2+} concentration gradually increase to ~0.5

mM in lysosomes (Christensen et al., 2002). Like Ca^{2+} ions, the Cl^- concentration also decreases from ~130 mM in extracellular fluid to ~20 mM in the early endosomes (Hara-Chikuma et al., 2005), and then increases when early endosomes mature into late endosomes, although no reliable estimation has been made (Weinert et al., 2010). The luminal concentrations of K^+ and Na^+ in late endosomes and lysosomes are reported to be ~60 mM and 20 mM, respectively, but later section will discuss the problems with this estimation (Ohkuma et al., 1983; Steinberg et al., 2010). Considering nature of lysosomes, The trace metal ions Fe^{2+}/Fe^{3+} and Zn^{2+} are also very important for the degradation and recycling functions of lysosome (Dong et al., 2008; Kiselyov et al., 2011), although this thesis will not focus on these ions.

1.2.1 The prominent feature of lysosomes: acidic lumen

The primary functions (degradation and recycling) of lysosomes are highly dependent on maintaining an acid luminal environment (pH ~4-5), which is established by a vacuolar (V)-type H^+-ATPase (Mindell, 2012; Ohkuma et al., 1982). In translocating H^+ into the lumen, the V-ATPase is electrogenic, and thus generates membrane potential (lumen-positive potential) that may inhibit further acidification (Harikumar and Reeves, 1983; Ohkuma et al., 1983). For the V-ATPase to fully acidify the lysosome lumen, counterion flux is necessary to dissipate the membrane potential. Theoretically, this counterion pathway can be accomplished by anion influx into lysosomes, cation efflux from lysosomes, or both. The role of counterion flux for the lysosomal acidification has long been established (Cuppoletti et al., 1987; Ohkuma et al., 1983; Van Dyke, 1993). However, the carrying ions and the channels/transporters responsible for ion flux are still illusive. The current view for dissipating the lumen-positive potential is K^+ efflux through a cation channel/transporter (Steinberg et al., 2010) or by Cl^- influx through ClC-7, a Cl^-/H^+ antiporter (Graves et al., 2008; Kornak et al., 2001; Weinert et al., 2010). This issue will be further discussed in this section and section 1.3.

Besides being required for digestive functions of hydrolases, the establishment of acidic lumen is also essential for endosomal trafficking, such as the maturation from endosomes to lysosomes (Clague et al., 1994), and cargo sorting, including the dissociation of internalized receptor-ligand complexes in endosomes (Marshansky and Futai, 2008). In addition, the formation of intraluminal vesicles in multivesicular bodies (MVB)/late endosomes is also dependent on the luminal low pH (Falguieres et al., 2008).

1.2.2 Cl^-: not just supporting lysosomal acidification

The primary role of Cl^- ions is traditionally thought to establish the counterion flux to support lysosomal acidification, probably through ClC-7 (Kasper et al., 2005a; Kornak et al., 2001). ClC-7 belongs to the ClC chloride channel/transporter family. The ClC family has nine known members, including four Cl^- channels functioning on the plasma membrane, and the other five (ClC-3-7) $2Cl^-/H^+$ antiporters residing on the intracellular membranes (Jentsch et al., 2005; Planells-Cases and Jentsch, 2009). Among these, ClC-3, ClC-4 and ClC-5 are localized on endosomes, and are reported to mediate counterion flux, since disruptions of their activities cause increased pH in endosomes. But these transporters are not broadly expressed (Gunther et al., 1998; Hara-Chikuma et al., 2005; Mohammad-Panah et al., 2003; Piwon et al., 2000).

ClC-7 is the only member in ClC family localized on the lysosome (Kasper et al., 2005a), and is ubiquitously expressed (Brandt and Jentsch, 1995). ClC-7 is responsible for the Cl^-/H^+ antiporter activity in the lysosome (Graves et al., 2008), but it's still controversial whether ClC-7 is essential for maintaining lysosomal pH. siRNA-knockdown of ClC-7 in some cell lines resulted in increased lysosomal pH (Graves et al., 2008). However, other results from ClC-7 knockout mice showed normal lysosomal pH (Kasper et al., 2005a; Lange et al., 2006; Steinberg et al., 2010). Although lysosomal acidification is intact, deletions of ClC-7 or its β-subunit Ostm1 cause severe lysosomal storage disease and osteopetrosis in mice and humans. Therefore, ClC-7 mediated Cl^- flux must be actively serving some other functions beyond just providing a counterion pathway.

Since either Cl^-/H^+ antiporters or simple Cl^- channels can provide a counterion pathway to support acidification, the next interesting question is whether the energy-expensive electrogenic antiporter provides functional advantages over a simple Cl^- channel? Studies from Jentsch lab (Weinert et al., 2010) were aimed to address this question. They generated knock-in mice with ClC-7 carrying a point mutation that converts the Cl^-/H^+ antiporter to an uncoupled Cl^- channel. Although the Cl^- conductance and low pH of lysosomes were maintained in mice carrying the uncoupled ClC-7, these mice still recapitulated much of the phenotypes seen in ClC-7 knockout mice with milder severity (Weinert et al., 2010). A similar experiment of ClC-5 conducted also in Jentsch lab (Novarino et al., 2010) has showed similar results. Although for ClC-5, the uncoupled mutant rescued the acidification defects in lysosomes from total knockout mice, proximal tubular endocytosis was still impaired in the uncoupled ClC-5 mice, as seen in knockout mice (Novarino et al., 2010). These experiments clearly showed that the

Cl^-/H^+-coupling of ClC-7 is essential for maintaining lysosomal functions, probably due to the higher level of Cl^- in lysosomes from wild-type mice, compared with uncoupled mutant (Weinert et al., 2010).

What are the possible functions of Cl^- ions beyond lysosomal acidification? First, besides maintaining the acidic pH in lysosomes, Cl^- ions may actively regulate lysosomal pH. Majumdar et al. (Majumdar et al., 2011; Majumdar et al., 2008; Majumdar et al., 2007) found that lysosomes in the quiescent microglia are incompletely acidified (pH ~6) and fail to degrade amyloid Aβ peptides. Upon activation, CLC-7 is recruited to lysosomes to promote the acidification (pH~5) and thus facilitate the degradation of Aβ peptides. Second, Cl^- ions may be involved in endolysosomal trafficking and sorting processes. For example, Cl^- has been shown to regulate receptor-ligand interactions for transferrin (Byrne et al., 2010). Third, Cl^- may participate in lysosomal degradation by modulating the activity of lysosomal hydrolases, such as cathepsin C (Wartosch et al., 2009). Last but not the least, the flux of Cl^- or coupled Cl^-/H^+ may exert local secondary effects on other ions (Steinberg et al., 2010) which may have direct impacts on the lysosomal functions.

1.2.3 Basic monovalent cations: K^+ and Na^+

In the physiological context, K^+ and Na^+ are the major and essential monovalent ions, with K^+ as the primary ion intracellularly, while Na^+ as the primary ion extracellularly. K^+ and Na^+ are involved in numerous fundamental functions via a variety of K^+/Na^+ ion channels and transporters. For example, K^+ and Na^+ are the principle ions mediating action potentials across the cell membrane in the nervous system: Na^+ entry into cells causes membrane depolarization, while K^+ efflux from cells causes membrane repolarization.

However, compared with the essential roles of K^+/Na^+ homeostasis across the cell membrane, our understandings about the two cations across the lysosomal membrane are very limited. Although it has been long speculated that cation counterflux may function to shunt proton-pumping currents, the supporting evidence does not appear until recently (Steinberg et al., 2010). Steinberg et al. performed experiments in living macrophages, and revealed that lysosomal acidification is supported by the efflux of the luminal cation, presumably K^+ (Mindell, 2012; Steinberg et al., 2010). This lead to the next more basic question: is there suitable K^+ electrochemical gradient across the lysosome membrane? The same group (Steinberg et al., 2010) also measured $[K^+]_{luminal}$ and $[Na^+]_{luminal}$ to be ~60 mM and 20 mM, respectively, based on

null-point titration, indicating the major cation in lysosomes is K^+. However, with this measurement, the electrochemical gradients for both K^+ and Na^+ across the lysosomal membrane are quite small, due to the high $[K^+]_{cytosol}$ and low $[Na^+]_{cytosol}$. More importantly, down the electrochemical gradient, what happens is K^+ influx into lysosomes, rather than the hypothesized efflux of K^+ in the counterion pathway. On the other hand, my thesis work has provided the first direct measurement from isolated lysosomes with atomic absorption spectrometry, and found that Na^+ is the major cation in the lysosomal lumen. This result leads to a more reasonable working model that the Na^+ efflux facilitates lysosomal acidification due to the large Na^+ gradient. In addition, the nature of lysosomal lumen is still unknown. For example, is it water-based, matrix-based, or a combination of both? These questions need to be taken into consideration when we discuss lysosomal ionic composition and flux. Therefore, more extensive and thorough work is needed to better understand the basic properties of lysosomes, which would have a huge impact on lysosomal biology. Meanwhile, identification of possible lysosomal K^+/ Na^+ channels/transporters certainly would facilitate our understanding of lysosomal ion stores. My thesis work has identified the first intracellular Na^+ channels two-pore channels (TPCs). Together with the measurement that Na^+ is the major cation in lysosomes, the discovery has provided the opportunity to study Na^+ homeostasis and its functions.

1.2.4 Lysosomal Ca^{2+} signaling

ER (endoplasmic reticulum) is an established Ca^{2+} store mediating intracellular Ca^{2+} signaling through IP_3 receptors (IP_3Rs) and ryanodine receptors (RyRs). $[Ca^{2+}]$ in the ER lumen is estimated to be ~0.5-2 mM (Miyawaki et al., 1997), compared with well maintained low level of cytosolic Ca^{2+} (~100 nM) (Tsien et al., 1982). Endosomes and lysosomes have recently emerged as new intracellular Ca^{2+} stores, because of appreciable amounts of Ca^{2+} in these compartments (endosomes: ~ 3-600μM (Gerasimenko et al., 1998), lysosomes: ~ 400-600 μM, (Christensen et al., 2002; Lloyd-Evans et al., 2008)), and the essential roles of endolysosomal Ca^{2+} in membrane trafficking and Ca^{2+} signal transduction (Galione and Churchill, 2002).

Ca^{2+}-dependence of membrane traffic

Ca^{2+} is a key regulator of synaptic vesicle fusion with the plasma membrane during neurotransmission (see **Fig. 1.1**). Upon membrane depolarization, Ca^{2+} ions enter cells through the voltage-gated Ca^{2+} channels and bind to the Ca^{2+} sensor synaptotagmin (Syt)-Ⅰ. The Ca^{2+}

binding of Syt-Ⅰ causes its conformational change and finally triggers SNARE (Soluble N-ethylmaleimide-sensitive factor Attachment protein REceptor) complex mediated membrane fusion. Similarly, Ca^{2+} is also considered to regulate intracellular membrane trafficking (Hay, 2007), although the regulation mechanisms are barely understood. The basic steps of fusion (tethering, docking, priming, and bilayer fusion) and the fusion machinery (SNAREs, phosphoinositides, and Rabs) involved are similar for intracellular membrane trafficking and neurotransmitter release (Martens and McMahon, 2008; Suudhof, 2008; Tsien et al., 1982), but the molecular players are distinct.

Both *in vitro* and i*n vivo* studies suggest that the luminal Ca^{2+} release is critical for endolysosomal membrane trafficking. *In vitro* fusion assays using cell extracts from yeast or mammalian cells have shown that both homotypic and heterotypic fusions between endolysosomes are inhibited by BAPTA, but not EGTA. Although both are strong Ca^{2+} chelators, BAPTA binds Ca^{2+} ions at least one hundred times faster than EGTA (Chen et al., 2002; Hay, 2007). The increased sensitivity of endolysosomal fusion to BAPTA versus EGTA has been widely interpreted as evidence to support that local Ca^{2+} release from luminal store is essential, and that the putative action site is extremely close (estimated to be < 20 nm) to the Ca^{2+} release site (Chen et al., 2002; Hay, 2007; Pryor et al., 2000). In vivo experiments using membrane permeable forms of chelators, i.e., BAPTA-AM and EGTA-AM in intact cells, have further demonstrated that intraluminal Ca^{2+} release is required for many steps of intracellular transport, such as retrograde trafficking from endolysosomes to *trans*-Golgi-network (TGN) (Burgoyne and Clague, 2003; Chen et al., 2002; Hay, 2007). Upon localized juxta-organellar Ca^{2+} elevation, distinct Ca^{2+} sensors are employed to trigger different membrane fusion and fission events. For example, the exocytosis of lysosomes is mediated by Syt-Ⅶ with C2-type Ca^{2+} binding sites (Reddy et al., 2001). Calmodulin (CaM), an EF-hand cytosolic protein, has been shown to play important roles in fusions between endocytic compartments (Hay, 2007; Peters and Mayer, 1998; Pryor et al., 2000), although how CaM is recruited to various intracellular vesicles is still not clear.

Juxta-organellar luminal Ca^{2+} release also regulates membrane fission/budding events (Hay, 2007; Luzio et al., 2007a; Luzio et al., 2007b). Membrane fissions actually share many common mechanisms with fusions. For example, Ca^{2+}, Rab proteins and phosphoinositides (PIPs) can regulate both membrane fission and fusion (Hay, 2007; Luzio et al., 2007a; Luzio et al., 2007b; Roth, 2004). Luminal Ca^{2+} dependence of membrane fission is supported by that

BAPTA-AM, but not EGTA-AM, inhibited vesicle budding *in vitro* (Ahluwalia et al., 2001). The Ca^{2+} effector protein involved in the fission process is not known.

Role of Ca^{2+} in signal transduction and organellar homeostasis

The Ca^{2+} signaling of endolysosomes is involved in many important cellular functions such as autophagy and pancreatic hormone release (Gomez-Suaga et al., 2012; Zhao et al., 2012). The best characterized pathway for mobilizing lysosomal Ca^{2+} stores is via intracellular second messenger NAADP (Nicotinic Acid Adenine Dinucleotide Phosphate) in many cell types [(Galione et al., 2010), more discussion in section 1.4]. NAADP induces lysosomal (acidic store) Ca^{2+} release initially, and then trigger further Ca^{2+} release from ER, a process referred to as Ca^{2+}-induced Ca^{2+} release (CICR) (Cancela et al., 1999; Guse and Lee, 2008). This interesting observation has brought up a question: whether there is universal communications between ER and endolysosomal Ca^{2+} stores. For example, ER and mitochondria as Ca^{2+}-storing organelles have close contacts and Ca^{2+}-signaling coupling (de Brito and Scorrano, 2008; Rizzuto et al., 2009). Although long speculated, three recent studies have revealed a close bidirectional communication of Ca^{2+} signaling between ER and lysosomes (Friedman et al., 2013; Kilpatrick et al., 2013; Lopez-Sanjurjo et al., 2013). Extensive and dynamic ER-lysosome contacts are also observed using 3D EM and live imaging (Friedman et al., 2013; Kilpatrick et al., 2013; Lopez-Sanjurjo et al., 2013). Besides signal transduction, another consequence of endolysosomal Ca^{2+} release is a reduction of $[Ca^{2+}]_{lumen}$, which may also modulate the ionic homeostasis, such as luminal pH (Cosker et al., 2010; Morgan, 2011).

In summary, endolysosomal Ca^{2+} signaling has multiple cellular functions. Accumulated evidence has connected dysfunction of the Ca^{2+} stores with lysosomal storage disorders (Cheng et al., 2010; Lloyd-Evans et al., 2008; Shen et al., 2012), acute pancreatitis (Gerasimenko et al., 2009), Alzheimer's disease (Coen et al., 2012) and Huntington's disease (Giacomello et al., 2011). However, many questions regarding endolysosomal Ca^{2+} signaling remain: What proteins mediate the Ca^{2+} release? Which trafficking cues activate the release channels? What proteins are the Ca^{2+} sensors? The mucolipin subfamily of transient receptor potential (TRPMLs) proteins serve as candidates for endolysosomal Ca^{2+} release channel, since TRPMLs are Ca^{2+} permeable channels localized on the endolysosomal membranes, and activated by a key regulator in membrane trafficking- $PI(3,5)P_2$. The role of TRPMLs in endolysosomal Ca^{2+} release will be further discussed in section 1.5, 1.6 and chapter 4 and 5.

1.2.5 Electrical properties of lysosomes

The electrical potentials across the endolysosomal membranes are not precisely known. Based on studies of synaptic vesicles (Van der Kloot, 2003) and phagosomes (Steinberg et al., 2007), the transmembrane potentials are presumed to be positive in the lumen (relative to the cytosol) and are likely to be between +30 and +110 mV (see **Fig. 1.2**). A recent measurement found the lysosomal potential is ~19 mV using FRET-based indicators (Koivusalo et al., 2011). The positive potential of lysosomes provides a driving force for Ca^{2+} release into the cytosol.

1.3 Diverse ion channels and transporters residing on the endosomes and lysosomes

The maintenance of ionic homeostasis and the accomplishment of ionic functions require a collection of ion channels and transporters. The intense studies of these ion channels/transporters have been greatly prompted by the recognition of lysosomal ionic functions, the discovery of new lysosomal ion channels/transporters, together with the linking between lysosomal transmembrane proteins with a number of diseases. However, our understandings about endolysosomal ion channels/transporters are still preliminary. Molecular identities underlying a lot of lysosomal conductance are still lacking (see **Fig. 1.2**). Moreover, the functions of known lysosomal ion transporters/channels are barely understood, largely due to the lack of a reliable functional assay for the intracellularly-localized membrane channels, as the patch-clamp technique that has been extensively employed for ion channel studies is mostly limited to the plasma membrane channels. Recently our lab established a modified patch-clamp method (see **Fig. 1.3**) (Dong et al., 2008), which allows us to perform electrophysiological recordings directly on native lysosomal membranes. This technique, referred to as lysosome patch-clamp, has opened a new avenue for the study of ion channels/transporters in the lysosome (see chapter 2 for further discussion). Below is a summary of our current understandings about these "gateways" to lysosomes.

1.3.1 Ion transporters involved in endolysosomal acidification

Primary driver of acidification: V-ATPase

As mentioned above, the V-ATPase is the primary driver along the endocytic pathway that pumps H^+ into the lumen against the electrochemical gradient at the expense of ATP (with a stoichiometry of 2~4 H^+/ATP) (Forgac, 2007; Johnson et al., 1982; Kettner et al., 2003;

Marshansky and Futai, 2008). In transporting H^+, V-ATPase is electrogenic, resulting in accumulation of positive potential at the luminal side.

The V-ATPase is composed of 14 subunits, including a soluble ATP-hydrolysing complex (V_1) and a transmembrane H^+-translocaing complex (V_0). The proton pump is structurally and functionally similar to the mitochondrial F_0F_1 ATP synthase (Forgac, 2007; Marshansky and Futai, 2008). As an essential player in organellar acidification, V-ATPase is regulated in different ways. For example, different subunits compositions are found in different tissues or subcellular organelles (Toei et al., 2010). Yeast Studies showed that the isoform of V-ATPase targeting to vacuoles is 4~5 folds more efficient than the one on the Golgi, which is consistent with the less acidic lumen of the Golgi (pH 6.0-6.7) (Kawasaki-Nishi et al., 2001; Manolson et al., 1994). In addition, V-ATPase is reported to undergo reversible dissociation of its V_1 and V_0 subcomplex in response to different metabolic status (Kane, 1995; Wieczorek et al., 2000). Moreover, V-ATPase is also regulated by cytosolic pH (Forgac, 2007) and regulatory proteins, including protein kinase A (PKA) and protein kinase C (PKC) (Alzamora et al., 2010; Nanda et al., 1992). Besides providing an acidic environment, emerging evidence has also indicated that V-ATPase is directly involved in membrane trafficking during endocytosis and exocytosis. Interestingly, a recent study has identified V-ATPase as a component of mTOR complex (a master growth regulator) pathway by showing that the luminal amino acids are sensed by V-ATPase, which is necessary for amino acid-mediated activation of mTOR1 (Zoncu et al., 2011). It is worth noting that despite the essential roles of V-ATPase, no direct functional assays (patch-clamp recording) on V-ATPase have been reported in mammalian cells yet, with only a few electrophysiological analysis for the V-ATPase in plant and yeast cells (Kettner et al., 2003; Rienmuller et al., 2012; Yabe et al., 1999).

Modulators of organellar pH: NHEs

Na^+/H^+ exchangers (NHE) represent a family of electroneutral monovalent cation-proton transporters. In the family, NHE 6-9 are primarily present on endosomes and the trans-Golgi network (Nakamura et al., 2005; Orlowski and Grinstein, 2007), but there are no NHEs in lysosomes. Although direct electrophysiology measurements are lacking, the intracellular NHEs are thought to dissipate the organellar pH gradient to transport Na^+ or K^+, and thereby contribute to the adjustment of both pH and salt concentrations (Nakamura et al., 2005; Orlowski and Grinstein, 2007). Experimentally, intracellular NHEs are shown to be involved in vacuole fusion

(Qiu and Fratti, 2010), cytosolic pH regulation (Rodriguez-Rosales et al., 2009) and vesicle trafficking (Bassil et al., 2011). For example, NHE8 is reported to regulate late endosomal morphology and function (Lawrence et al., 2010).

Counterion flux: what are the underlying molecular pathways?

The luminal-positive-potential generated by the V-ATPase needs to be dissipated by counterion flux to facilitate further acidification. As discussed above, the efflux of K^+ or Na^+, and/or the influx of Cl^- can fulfill this function. For the molecular identities of the Cl^- pathway, the CFTR (cystic fibrosis transmembrane conductance regulator) represents a long debated candidate (reviewed in (Haggie and Verkman, 2009a)) and now is thought unlikely to be a key component in the organellar acidification, especially in lysosomes (Haggie and Verkman, 2009b). On the other hand, the intracellular ClC antiporters appear to be promising (Edwards and Kahl, 2010), although lysosomal acidification seemed to be normal in ClC-$7^{-/-}$ cells (see above discussion, (Kasper et al., 2005a; Lange et al., 2006; Steinberg et al., 2010; Weinert et al., 2010)). Thus far, no K^+ or Na^+ channels on the lysosome have been identified yet. My thesis work has provided the first Na^+ channel candidate (TPC proteins) for cation counterflux.

H^+ leaks: uncharacterized conductance

V-ATPase inhibitors (such as bafilomycin A1) cause alkalization of acidic organelles, which indicates the existence of H^+ leaks, and reveals that the H^+-leak rates are different in distinct acidic compartments (Paroutis et al., 2004). The current model is that the luminal pH set point is primarily determined by the H^+ pump/H^+ leak balance, and the ratio of H^+ pump/H^+ leak is higher in organelles with the more acidic luminal environments (Demaurex, 2002; Paroutis et al., 2004). Our understandings about the H^+ leaks are at very preliminary stage, and both the conductance properties and molecular identities need to be further investigated.

Mysterious ion transporters for Ca^{2+} uptake in endolysosomes

It is well known that Ca^{2+} uptake in the ER is primarily by the SERCA (sacro-endoplasmic reticulum Ca^{2+}-ATPase) pump, and Ca^{2+} leaks out through RyRs (Laporte et al., 2004). In stark contrast, the machinery for Ca^{2+} filling in endolysosomes is barely understood, particularly in the animal kingdom.

Regarding the ionic flux in the acidic stores, far more is known in plants, yeast and protist vacuoles. In these organisms, the Ca^{2+}-refilling in the acidic stores is accomplished by a higher affinity vacuolar Ca^{2+}-ATPase and a lower affinity Ca^{2+}/H^+ exchanger (CAXs) with a stoichiometry of 2-3H^+/Ca^{2+} (Cunningham, 2011; Pittman, 2011). As for endolysosomal Ca^{2+} pump, there are a few reports proposing that a P-type Ca^{2+}-ATPase (Ezaki et al., 1992; Goncalves et al., 2000; Hicks and Parsons, 1992) or SERCA3-like pump (Lopez et al., 2005; Lopez et al., 2006; Papp et al., 1992) might be on some types of acidic stores based on pharmacological studies, however, it's far from clear yet. What we do know about endolysosomal Ca^{2+} store is that the H^+ gradient helps in establishing the Ca^{2+} gradient, because disruption of H^+ gradient by NH_4Cl or the V-ATPase inhibitor bafilomycin A1 leads to depletion of the Ca^{2+} store (Christensen et al., 2002; Lloyd-Evans et al., 2008; Luzio et al., 2007a; Yamasaki et al., 2004). By analogy with the vacuolar machinery, the simplest explanation for the above observations is the presence of a Ca^{2+}/H^+ exchanger. Since the CAX proteins are absent from higher vertebrates (Pittman, 2011), the new proteins acting as Ca^{2+}/H^+ exchangers in mammals need to be identified. Another plausible scenario for Ca^{2+} refilling is Na^+/H^+ exchangers coupled with Na^+/Ca^{2+} exchangers, i.e., a Na^+ gradient is first established by the dissipation of H^+ gradient (e.g. by a reverse action of NHE), which in turn drives Ca^{2+} uptake. In mammals, there are three families of CaCAs (Ca^{2+}/cation antiporters), including NCX (Na^+/Ca^{2+} exchangers), NCKXs (Na^+/Ca^{2+}-K^+ exchangers) and CCX (Ca^{2+}/cation exchangers) (Altimimi and Schnetkamp, 2007; Lytton, 2007). Although some reports showed that NCKX might contribute to Ca^{2+} refilling in chromaffin granules (Pan et al., 2008) and melanosomes (Lamason et al., 2005), more work remains to be done to clarify the putative roles of Ca^{2+}/cation antiporters. In addition, the potential functions of Ca^{2+} pumps/exchangers need to be cautiously explained by considering the their interactions with the positive luminal potential and high H^+ gradient.

In summary, the machinery for endolysosomal Ca^{2+} uptake in mammalian cells remains in the hypothetical stage. Detailed and more specific pharmacological characterization is needed to probe potential Ca^{2+} pumps or exchangers. Also, the Ca^{2+} refilling mechanisms may not be universal for endolysosomes in different tissues.

1.3.2 Ion channels residing on the endosomes and lysosomes – a growing community

An increasing number of ion channels are found to be localized on intracellular vesicles along the endocytic pathway. Functional studies suggest that many of those channels are not simply

passive cargo, but instead play active roles in membrane fusion and fission, signal transduction, and vesicular homeostasis. The two established ion channel families on endolysosomes are TRPMLs (Dong et al., 2008) and TPCs (two pore channels) (Calcraft et al., 2009). Unlike other channels localized both at the plasma membrane and intracellularly, these two types of channels are primarily expressed on the endolysosomes, and are the focus of my thesis work, which will be discussed in detail later.

TRPV2

Initially reported to be a temperature-activated Ca^{2+}-permeable non-selective cation channel in somatosensory neurons (Caterina et al., 1999), TRPV2 is also localized to intracellular vesicles (Kanzaki et al., 1999). Based on a proteomic study revealing the presence of TRPV2 in the early endosome, Saito et al. (Saito et al., 2007) tested the hypothesis that TRPV2 is an endosomal Ca^{2+} channel for Ca^{2+}-dependent membrane fusion. Using an elegantly modified patch-clamp technique, Saito et al. successfully measured endogenous ionic currents (I_{EE}) in the isolated enlarged early endosome, which was made possible after endosomal fusion was genetically promoted. I_{EE} is activated by reductions in the luminal pH and Cl^- concentration, which usually occur within 20 min post-endocytosis (Gerasimenko et al., 1998). The pharmacological properties of I_{EE} resemble those of I_{TRPV2} studied in heterologous systems. To ultimately prove the hypothesis, however, more experiments are necessary to show that TRPV2 is the underlying channel for the endogenous I_{EE}.

TRPM2

Initially characterized as a plasma membrane Ca^{2+}-permeable channel gated by free cytosolic ADP-ribose (ADPR) (Perraud et al., 2001), recent evidence suggests that TRPM2 is also localized in the LEL compartment (**Fig. 1.4**) (Lange et al., 2009). Rather than simply being a cargo in the degradative pathway, TRPM2 can function as a lysosomal Ca^{2+} release channel in response to cytosolic ADP-ribose in pancreatic ß cells (Lange et al., 2009) and dendritic cells (Sumoza-Toledo et al., 2011). TRPM2-deficient dendritic cells were found to show impaired maturation and severely compromised chemotaxis (Sumoza-Toledo et al., 2011). Plasma membrane TRPM2 is reportedly activated by high concentration (μM) of NAADP (Beck et al., 2006) or by increases in $[Ca^{2+}]_i$ (Du et al., 2009), it is conceivable that TRPM2 might also has a role in lysosomal NAADP (working at nM range) signaling or in Ca^{2+}-induced Ca^{2+} release

(CICR).

$P2X_4$

Initially identified as a plasma membrane non-selective cation channel activated by ATP and other nucleotides, $P2X_4$ is also expressed in lysosomes (Qureshi et al., 2007). Studies showed that $P2X_4$ is upregulated at the cell surface through the exocytosis of lysosomal $P2X_4$. However, it is not clear that whether $P2X_4$ functions as a lysosomal channel.

Summary

An increasing number of putative ion channels/transporters primarily expressed on the endolysosomes are found to be involved in many physiological processes or disease conditions, such as DIRC2 (disrupted in renal carcinoma 2) (Savalas et al., 2011) and LAPTM4B (lysosomal-associated transmembrane protein 4B) (Kasper et al., 2005b; Li et al., 2010; Shao et al., 2003), although their intracellular functions are far from clear yet. In the future, the advancement in understanding endolysosomal ion channels/transporters is expected in the following areas:

(1) Tissue and organellar expression pattern will be defined for most endolysosomal channels.
(2) The intracellular activities of the putative ion channels/transporters will be characterized by extensive functional assays (including patch-clamp recordings and Ca^{2+} imaging). Agonists and antagonists of intracellular channels may provide useful tools for measuring their functions and dissecting their cellular roles.
(3) Real-time live imaging methods will be used to investigate the roles of intracellular channels in lysosomal physiology. Local Ca^{2+} transients may be capture by endosome-targeted Ca^{2+} sensors (such as a genetically-encoded Ca^{2+} indicator GCaMP3 fused with lysosomal channel TRPML1, GCaMP3-TRPML1 (Shen et al., 2012)), and may be correlated with membrane trafficking events.
(4) More information will be revealed for the electric properties of intracellular compartments and vesicles. Ion imaging methods will be applied to accurately measure luminal ion concentrations at both basal and stimulated states.
(5) Molecular identities underlying the ionic conductance will be discovered in the lysosomes and their activation and functions will be further investigated.

Last but not least, recent studies have blurred the boundaries between the plasma and intracellular ion channels. For example, some plasma membrane channels are found in intracellular organelles (e.g. TRPV1) (Dong et al., 2010b), and intracellular channels, e.g. IP_3 receptor in the ER (Dellis et al., 2006)) can be detected at the plasma membrane. These observations have brought up an important question: how to prevent channels from being active at the wrong subcellular location? One plausible hypothesis is that the channel activities at different subcellular locations are dependent on compartment-specific lipid compositions. For example, $PI(4,5)P_2$ is required for the functioning of many plasma membrane ion channels (Suh and Hille, 2008), but this lipid is usually excluded from endocytic vesicles (Poccia and Larijani, 2009; Roth, 2004), which may serve as a mechanism to keep the plasma membrane channels inactive intracellularly. On the other hand, TRPML1 as an endolysosomal channel, is shown to be activated by endolysosome-specific $PI(3,5)P_2$ (part of my thesis work (Dong et al., 2010a)), while inhibited by $PI(4,5)P_2$ (Zhang et al., 2012a) and sphingomyelin (Shen et al., 2012) at the plasma membrane.

1.4 NAADP signaling and Two-pore channels

1.4.1 NAADP mediates Ca^{2+} release from intracellular acidic compartments.

Ca^{2+} release from intracellular stores induced by second messengers upon extracellular stimuli represents an important mechanism for Ca^{2+} signaling. It is well known that the second messengers inositol trisphosphate (IP_3) and cyclic ADP-ribose (cADPR) mobilize Ca^{2+} release from the S/ER store, targeting IP_3 receptors (IP_3Rs) and ryanodine receptors (RyRs), respectively (Berridge et al., 2000). It was until a decade ago that nicotinic acid adenine dinucleotide phosphate (NAADP) was identified as the most potent Ca^{2+} mobilizing messenger (acting at < 1 nM concentration) (Lee and Aarhus, 1995), which evokes Ca^{2+} release from a completely novel intracellular compartments, acidic stores (Churchill et al., 2002). This discovery has not only recognized acidic organelles as indispensible Ca^{2+} stores, but has also provided a critical probe to dissect this unknown Ca^{2+} store-associated signaling pathway.

The Ca^{2+}-releasing phenomenon by pyridine nucleotide metabolites in sea urchin egg homogenates was first described by Lee and his colleagues in 1987 (Clapper et al., 1987). Their follow-up work further identified that the Ca^{2+}-mobilizing molecule, whose targeting and properties are distinct from IP3 and cADPR, is NAADP (Lee and Aarhus, 1995). Then in 2002, the studies from Churchill et al. demonstrated that NAADP mobilizes calcium release from the

reserve granule, a lysosome-related organelle in sea urchin eggs (Churchill et al., 2002). To identify the NAADP-sensitive compartments, Churchill et al. used bafilomycin A1 (the V-ATPase inhibitor) and GPN (a substrate of cathepsin C, causing osmotic disruption of lysosomes) to deplete acidic organelles without affecting S/ER Ca^{2+} stores (thapsigargin sensitive). Bafilomycin A1 and GPN have subsequently been found to disrupt NAADP-sensitive stores in many mammalian cell types (Brailoiu et al., 2006; Kinnear et al., 2004; Macgregor et al., 2007; Yamasaki et al., 2004), strengthening the concept that NAADP induces Ca^{2+} release from acidic stores. The nature of the acidic stores is generally assumed to be lysosomes, although some studies indicated that endosomes (Menteyne et al., 2006) and dense core vesicles (Mitchell et al., 2003) may also be included.

NAADP triggered local Ca^{2+} release from lysosomes is hypothesized to be coupled with ER Ca^{2+} release, a process referred to as calcium-induced calcium release (CICR) (Cancela et al., 1999). The NAADP-induced Ca^{2+} signaling has been linked with a variety of physiological processes. For example, in pancreatic acinar cells, the brain gut peptide cholecystokinin (CCK) is shown to recruit the NAADP pathway (Yamasaki et al., 2005); while in pancreatic β cells, NAADP is thought to mediate the Ca^{2+} signaling in the insulin secretion (Arredouani et al., 2010; Masgrau et al., 2003). In addition, the roles of NAADP signaling have also been suggested in cardiac (Macgregor et al., 2007) and smooth muscle contractions (Boittin et al., 2002; Kinnear et al., 2004), neurotransmitter release and neurite outgrowth (Brailoiu et al., 2006; Brailoiu et al., 2003), and activation of platelets (Lopez et al., 2006) and T-lymphocytes (Berg et al., 2000).

Since the discovery of the Ca^{2+}-mobilizing messenger NAADP, there has been a natural interest to search for the putative NAADP receptor(s). This receptor is hypothesized to be a NAADP-activated Ca^{2+} channel, located on the endolysosomes (acidic stores). Several candidate ion channels have been implicated (Guse and Lee, 2008), including TRPM2 (Beck et al., 2006; Lange et al., 2009) and TRPML1 (Zhang and Li, 2007), although the evidence was not strong. Separate studies have also indicated that thapsigargin-sensitive stores and RyRs are involved in NAADP signaling in some cell types (Dammermann and Guse, 2005; Gerasimenko et al., 2003). Then in 2009 three groups (Brailoiu et al., 2009; Calcraft et al., 2009; Zong et al., 2009) independently reported that a new family of ion channels, termed two-pore channels (TPCs), might be the underlying molecules mediating NAADP signaling, which appeared to be a hallmark discovery. This finding was immediately discussed in a number of review articles (Galione et al., 2009; Guse, 2009; Guse and Lee, 2008; Patel et al., 2010; Zhu et al., 2010a; Zhu

et al., 2010b), and many of the physiological functions previously ascribed to the NAADP signaling were thought to be mediated by TPCs (Arredouani et al., 2010; Rybalchenko et al., 2012). But the conclusion is challenged by follow up studies (Lin-Moshier et al., 2012; Walseth et al., 2012), and definitive evidence that TPCs are directly activated by NAADP is still lacking. Surprisingly, using lysosomal patch-clamp techniques, my thesis work has demonstrated that TPCs are Na^+-selective channels with little Ca^{2+} permeability and they can be activated by $PI(3,5)P_2$, but not NAADP. Ca^{2+} imaging results have further demonstrated that NAADP signaling is intact in TPCs-knock out cells. Below our current knowledge and results regarding TPCs will be summarized and discussed.

1.4.2 Two-pore channels- the long-sought NAADP receptors?

The family of two-pore channels contains three members (TPC1-3). In 2000 the first member TPC1 was cloned by homology screening a rat kidney cDNA library based on the voltage-gated cation channel superfamily, to which TPCs belong (Ishibashi et al., 2000). The founding members of this superfamily are the voltage-gated Na^+ (Nav) and Ca^{2+} channels (Cav) (Yu and Catterall, 2004). Their primary α subunits are composed of four homologous repeats of 6 transmembrane domains (6TMD, i.e. segments S1 to S6, 24 TMD in total). α subunits of voltage-gated K^+ channels (Kv), on the other hand, contains only one repeat of 6TMD, and tetrameric assemblies are required for functional channels. For a 6TMD channel, S4 region usually containing multiple positively charged amino acid residues, is thought to serve as voltage sensor, while S5 and S6, together with a membrane-reentrant loop between the two segments (called the pore-loop) form the ion conducting pore. The 6TMD channels (e.g. Kv) appear to be the basic pore-forming structural unit, and the 24TMD channels (e.g. Cav and Nav) are generated from the basic unit by gene duplications during evolution. This hypothesis immediately raised an interesting question: do the intermediate duplication of 12 TMD channels exist in the genome? The newly cloned two-pore channels have perfectly answered the question, with two predicted repeats of 6TMD (12TMD in total), homologous to the pore-forming domains of Cav and Nav. TPC genes exist in most species from plant to animal, although they are absent in the well studied model organisms of *C. elegans* and *Drosophila*. Present in some mammals (e.g. cows and horses), TPC3 appears to be absent in rats, mice and humans (Patel et al., 2010; Zhu et al., 2010c) (This thesis will mainly focus on mammalian TPC1 and TPC2). Ever since the first report of TPC proteins in rat, the channel functions in animals have been enigmatic. For a

long time, the plant TPC1 was the only TPC protein that has been functionally characterized (Peiter et al., 2005).

Mammalian TPC1 and TPC2 are probably expressed in most tissues as revealed by Northern blot, with higher levels in the liver and kidney (Calcraft et al., 2009; Ishibashi et al., 2000; Zong et al., 2009). Early efforts failed to detect channel functions using electrophysiology in various heterologous expression systems (Ishibashi et al., 2000). A turning point was when the three broadly consistent reports came out in 2009, proposing that TPCs might mediate NAADP-evoked Ca^{2+} release from acidic stores (lysosomes) (Brailoiu et al., 2009; Calcraft et al., 2009; Zong et al., 2009). Unlike their homologs of the plasma-membrane-localized Cav and Nav, TPCs are actually localized in intracellular endosomes and lysosomes (Calcraft et al., 2009; Morgan et al., 2011), although their individual localizations are generally not overlapped with each other. TPC2 is mainly expressed in late endosomes and lysosomes (**Fig. 1.4**), while TPC1 is more broadly distributed across the endosomes, and chicken TPC3 may be largely in recycling endosomes. The intracellular localizations and their sequence homology to Cav made TPCs promising candidates as NAADP receptors. These work represent a major step forward in our understandings of TPC expressions and functions, and have provided evidence supporting the intriguing idea that TPCs are the long-sought NAADP receptors. The difference between the three reports focused on whether the ER store is coupled with TPC-mediated Ca^{2+} release. It was suggested that the difference might be due to different cell types and variations in the levels of heterologous expression (Morgan et al., 2011). But it needs to be pointed out that the studies were largely based on indirect measurements, and the definitive assay that NAADP directly activates the specific conductance of TPC channels was lacking.

The intracellular localization of TPCs hindered the application of electrophysiology to examine their channel properties, however three subsequent reports (Brailoiu et al., 2010; Pitt et al., 2010; Schieder et al., 2010) made efforts to overcome the difficulties. All three studies suggested TPC2 is activated by NAADP, although the TPC2 currents were shown to be K^+-permeable (Pitt et al., 2010), Cs^+-permeable (Brailoiu et al., 2010), or Ca^{2+}-selective (Schieder et al., 2010), which were inconsistent with each other.

In summary, the hypothesis that TPCs serve as NAADP receptors was quickly accepted, although the direct measurements of NAADP-activated TPC currents remain to be elucidated. Therefore, TPCs are proposed to mediate NAADP-evoked Ca^{2+} signaling in many physiological processes, including NAADP-regulated plasma membrane excitability (Calcraft et al., 2009;

Moccia et al., 2004), muscle contraction (Tugba Durlu-Kandilci et al., 2010), insulin secretion (Arredouani et al., 2010) and muscle differentiation (Aley et al., 2010). Assumed to be endolysosomal Ca^{2+} channels, TPCs are also hypothesized to be involved in luminal pH regulation of endolysosomes (Morgan et al., 2011), and intracellular membrane trafficking (Ruas et al., 2010). It is worth mentioning that human genetic studies have identified TPC2 as a regulator of pigmentation in North Europeans, which is consistent with TPC2 functions in the melanosome (Sulem et al., 2008). Melanosomes are lysosomal-related organelles in melanocytes, which produce and release melanin to keratinocytes for pigmentation.

In stark contrast with the popular views, my thesis work has discovered that TPCs are Na^+-selective channels with little Ca^{2+} permeability and they can be activated by $PI(3,5)P_2$, but not NAADP, using established lysosomal-patch clamp recordings (Dong et al., 2008; Dong et al., 2010a), Ca^{2+} imaging and mouse genetics. In my view, this work may represent a critical correction to this field, and has established a new dimension for TPC studies as the first intracellular Na^+ channels.

1.5 TRPML1: a principle Ca^{2+} channel in endolysosomes

The mucolipin subfamily of transient receptor potential (TRP) cation channels (TRPMLs) includes three members in mammals, i.e., TRPML1-3 (also called MCOLN1-3). Loss-of-function mutations of human *TRPML1* cause type IV Mucolipidosis (ML4), a childhood neurodegenerative lysosomal storage disorder (LSD) manifested by psychomotor retardation and retinal degeneration (Bargal et al., 2000; Bassi et al., 2000; Sun et al., 2000). At the cellular level, membranous lipids are accumulated in enlarged vacuolar structures (lysosomes), suggesting defective lysosomal biogenesis and trafficking. Disruption of mouse *TRPML1* (Venugopal et al., 2007), *C. elegans TRPML* (*Cup-5*) (Fares and Greenwald, 2001; Hersh et al., 2002) and *Drosophila TRPML* (Venkatachalam et al., 2008) all result in behavior defects and cellular defects that are reminiscence of ML4.

Unlike other plasma membrane TRP channels, TRPMLs are mainly localized in intracellular endosomes and lysosomes (Abe and Puertollano, 2011; Cheng et al., 2010), consistent with the defective endolysosomal functions shown in TRPML1-deficient cells. However, the mechanisms of TRPML1' essential roles in endolysosomal functions remain elusive. Fortunately, the recent development of the whole-endolysosome patch-clamp technique from our lab (Dong et al., 2008) has conquered the difficulties in assessing intracellular channels,

and provided insights in channel properties and their activation mechanisms (Dong et al., 2008; Dong et al., 2010a; Shen et al., 2012). Moreover, the newly identified activating or surface-expressing trafficking mutants (Grimm et al., 2007; Kim et al., 2007; Nagata et al., 2008; Shen et al., 2012; Xu et al., 2007) of TRPMLs have allowed the use of whole-cell recordings to study channel functions. Taken together, these studies have revealed that TRPML1 is an inwardly rectifying $Ca^{2+}/Fe^{2+}/Zn^{2+}$-permeable cation channel that is activated by an endolysosomal-specific phosphoinositide, $PI(3,5)P_2$ (part of my thesis work, please see chapter 4). Therefore, TRPML1 represents an ideal candidate channel mediating cation/heavy metal ions release from endolysosomes, in response to $PI(3,5)P_2$ elevation or other unidentified cellular cues.

Studies using animal models and cell lines with the disruption of *TRPML1* have uncover critical roles of TRPML1 in multiple cellular functions including endocytosis, endolysosomal membrane trafficking, lysosomal ion homeostasis, lysosomal exocytosis, and autophagy (Cheng et al., 2010; Grimm et al., 2012). Moreover, recent identification of several small-molecule activators of TRPMLs has made it possible to dissect the role of TRPML1 in those cellular functions (Grimm et al., 2012; Grimm et al., 2010; Shen et al., 2012). The development of an endolysosomal-targeted genetically-encoded Ca^{2+} indicator, GCaMP3-TRPML1 may allow one to correlate the local, transient Ca^{2+} release to membrane fusion/fission (Shen et al., 2012). In addition, molecular and biochemical analyses have indicated several potential proteins that interact with TRPML1, defining its molecular signaling context. For example, two-pore channel (TPC) proteins might form heteromeric channels with TRPML1. Several Ca^{2+} sensors are indicated to function downstream of TRPML1, including ALG-2, Synaptotagmin VII and calmodulin. Lysosome associated protein transmembrane (LAPTM) proteins are found to interact with TRPML1 by a yeast two-hybrid screen (Vergarajauregui et al., 2011). Last but not least, dynamic interactions with other intracellular organelles have ensured that the lysosome is a central point of convergence in diverse cellular processes and a variety of diseases. As the principle Ca^{2+} release channel in endolysosomes, TRPML1 may serve as a gateway to understand lysosomal functions and disease mechanisms, including ML4 and LSDs.

1.5.1 Structural aspects and expression patterns of TRPML1

TRPMLs contain six putative transmembrane domains (S1-S6) with the amino (NH2)- and carboxyl (COOH)-terminus facing the cytosol, and are predicted to form tetramers as functional

channels. S5 and S6 are presumed to form the channel pore and gate. By proline-substitution screening around this region, I have identified several gain-of-function mutations that lock the channel at a non-gated open stage (please refer to chapter 5). My colleagues and I have also identified the poly-basic domain in the N terminus of TRPML1 as the PIP_2-binding domain, mediated by seven positively-charged amino acids. My colleagues Zhang et al. have further found this domain is also involved in the inhibitory effects of $PI(4,5)P_2$ on TRPML1, and proposed that Arg41-43 mainly mediate the $PI(4,5)P_2$ binding, while Arg61 and Lys 62 mediating the $PI(3,5)P_2$ binding (Zhang et al., 2012a).

TRPML1 is ubiquitously expressed in every tissue (Cheng et al., 2010; Slaugenhaupt, 2002) and mainly co-localizes with late endosomal and lysosomal (LEL) markers (> 80%, see **Fig. 1.4**) (Cheng et al., 2010; Dong et al., 2009; Puertollano and Kiselyov, 2009). The LEL localization is also supported by gradient fractionation studies on both endogenous and heterologously-expressed proteins (Kim et al., 2009; Zeevi et al., 2009). Although primarily localized in LELs, TRPML1-GFP is also detected in EEA-1 positive early endosomes (Cheng et al., 2010), and TRPML-specific channel activity can be measured in inside-out patches derived from the plasma membrane in TRPML1-GFP-overexpressing HEK 293 cells (Zhang et al., 2012a). Two di-leucine (LL) motifs, situated separately with one each at the N- and C- terminus, are shown to mediate the trafficking of TRPML1 to the LEL (Vergarajauregui and Puertollano, 2006). Mutations in both di-leucine motifs ($L^{15}L/AA$-$L^{577}L/AA$) result in a significant increase in the surface expression of TRPML1 and whole-cell TRPML1 currents (Shen et al., 2012; Zhang et al., 2012a).

1.5.2 Pore properties of TRPML1 channels

The first electrophysiologically characterized wild-type TRPML channel was TRPML3 (Kim et al., 2007; Kim et al., 2008; Xu et al., 2007). Although the majority of heterologously-expressed TRPML3 proteins are vesicular, a small portion of them are able to traffic to the plasma membrane and give rise to whole-cell currents (I_{TRPML3}) (Cuajungco and Samie, 2008; Grimm et al., 2007; Kim et al., 2007; Martina et al., 2009; Nagata et al., 2008; Puertollano and Kiselyov, 2009; Xu et al., 2007). I_{TRPML3} is an inwardly-rectifying Ca^{2+}permeable cation current. Mutations in the mouse *TRPML3 (A419P)* result in the *varitint-waddler (Va)* phenotype (Cuajungco and Samie, 2008; Puertollano and Kiselyov, 2009). *Va* mice are deaf, exhibit circling behavior and have pigmentation defects. Compared with the wild-type, much larger currents are seen in cells

expressing TRPML3^{A419P} (TRPML3^{Va}). The TRPML3^{Va} channel exhibits similar pore properties as wild-type TRPML3, but with altered gating behavior, suggesting that *Va* is a channel gain-of-function mutation (Cuajungco and Samie, 2008; Grimm et al., 2007; Kim et al., 2007; Martina et al., 2009; Nagata et al., 2008; Puertollano and Kiselyov, 2009; Xu et al., 2007). Similarly, the proline substitution at the homologous position in *TRPML1* (*V432P* or *TRPML1*$^{Va)}$ leads to large inwardly rectifying non-selective whole-cell currents that is permeable to both monovalent (Na^+, K^+, Cs^+) and divalent (Ca^{2+}, Mg^{2+}) cations (Dong et al., 2008; Xu et al., 2007).

Recently, our lab (Dong et al., 2008) has developed an endolysosomal patch-clamp method to record directly from isolated LELs which were pharmacologically enlarged (from 0.1-0.5 to 2-3 μm) with the small compound vacuolin-1. With this method, lysosomal I_{TRPML1} largely resembles $I_{TRPML1\text{-}Va}$, suggesting that although TRPML1 is likely to be locked at non-gated open state, the activating mutation is still a valid approach for characterizing the pore properties of TRPML1. TRPML1 exhibits significant permeability to Ca^{2+}, serving as a potential conduit for Ca^{2+} release from LELs (Cheng et al., 2010). In addition, I_{TRPML1} is also permeable to divalent heavy trace metals, such as Fe^{2+}, Zn^{2+}, Cu^{2+} (Dong et al., 2008), which may have important implications in lysosomal functions and ML4 disease (Altarescu et al., 2002; Eichelsdoerfer et al., 2010). It is worth noting that although TRPML1 appears to be important for LEL pH regulation (Martina et al., 2009; Soyombo et al., 2006; Venkatachalam et al., 2008), none of the TRPMLs is H^+-permeable (Cheng et al., 2010; Xu et al., 2007), suggesting that the effect of TRPMLs on the luminal pH is most likely to be secondary.

1.5.3 TRPML1 in membrane trafficking

The roles of TRPML1 in intracellular membrane trafficking associated with the LELs have been extensively studied both *in vitro* and *in vivo* (reviewed in Refs. (Abe and Puertollano, 2011; Cheng et al., 2010; Puertollano and Kiselyov, 2009)). As discussed above, accumulating evidence supports the essential role of Ca^{2+} release from endososmes and lysosomes in membrane trafficking (Morgan et al., 2011). However, the channels responsible for the Ca^{2+} release remain mysterious. TRPML1 (or TRPMLs), the principle Ca^{2+} channel(s) localized on LELs, are natural candidates for endolysosomal Ca^{2+}-release channels .

TRPML1 may be involved in multiple processes in membrane trafficking, including endosome maturation, lysosome reformation, LEL-to TGN retrograde trafficking, autophagy and lysosomal exocytosis. Studies showed that both the transport of fluid-phase markers to

lysosomes, and the lysosomal degradation of internalized growth factor receptors (e.g. PDGFR) were delayed in TRPML1$^{-/-}$ cells (Thompson et al., 2007; Vergarajauregui et al., 2008), suggesting a role of TRPML1 in the maturation process from endosomes to LELs via membrane fusion.

TRPML1 may participate in lysosome reformation, a process also referred to as lysosome biogenesis. Loss-of-function of *Cup-5* (the orthologue of *TRPML1*) in *C. elegans* causes enlarged vacuoles containing both endosome and lysosome markers (Fares and Greenwald, 2001). Similar observations were also found in ML4 cells (Cheng et al., 2010). These enlarged vacuoles were considered to be the hybrids of endosomes and lysosomes, suggesting that TRPML1 is necessary for lysosomal reformation. Recent studies also reported that lysosome biogenesis is under the regulations of mTOR (Zoncu et al., 2011), a master regulator of cell growth and metabolism, and TFEB (Roczniak-Ferguson et al., 2012; Sardiello et al., 2009), a lysosome-associated transcription factor. While TFEB is shown to transcriptionally regulate TRPML1 (Medina et al., 2011; Sardiello et al., 2009), *Drosophila* trpml is shown to be required for TORC1 activation (Wong et al., 2012), suggesting TRPML1 may interact with mTOR/TFEB signaling to regulate lysosome biogenesis.

Retrograde trafficking from the LEL to the TGN is used to reutilize the products from lysosomal degradation or recycle the shuttle proteins, such as M6PR (Luzio et al., 2007b). It has been shown that in ML4 cells, the retrograde trafficking of LacCer from TGN to LELs is delayed or blocked (Chen et al., 1998; Pryor et al., 2006). Similar trafficking defects are also seen in PI(3,5)P_2-deficient cells, suggesting the physiological relevance of PI(3,5)P_2 and TRPML1 (Zhang et al., 2007b). Interestingly Niemann-Pick type C (NPC) cells also exhibits similar LEL-to-TGN trafficking defects, which can be attenuated by increasing TRPML1 activity (Shen et al., 2012).

Autophagy is a lysosome-mediated degradation process for damaged organelles and unnecessary macromolecules. The cytosolic components are first sequestered into autophagosomes, which then fuse with lysosomes to form autolysosomes, where autophagic substrates are degraded (He and Klionsky, 2009). TRPML1 deficiency is shown to cause accumulation of autophagosomes, which are due to either increased autophagic flux or impaired fusion with lysosomes (Vergarajauregui et al., 2008). Decreased degradation of autophagy is also observed in TRPML-deficient Drosophila and mouse neurons (Curcio-Morelli et al., 2010;

Micsenyi et al., 2009; Vergarajauregui et al., 2008). The impaired autophagy might underlie the neuronal cell death and neurodegeneration in ML4 (Cheng et al., 2010).

In addition, TRPML1 may also mediate Ca^{2+}-dependent lysosomal exocytosis. My thesis work has provided evidence to support this hypothesis.

1.5.4 TRPML1 in vesicular ion homeostasis

In the endo-lysosome system, H^+, Ca^{2+} and membrane fusion have been found to be interconnected (Luzio et al., 2007a; Luzio et al., 2007b). In addition to Ca^{2+}, TRPML1 is also permeable to other cations in the LEL lumen and thus may have functions distinct from Ca^{2+} signaling. ML4 or TRPML1 knockdown cells appear to have an overly acidified pH in LEL compartments，though these findings are highly controversial (Miedel et al., 2008; Soyombo et al., 2006). Given that TRPML1 exhibits no permeability to protons, the defects in lysosomal pH regulation must be secondary to the absence of TRPML1 (Cheng et al., 2010).

TRPML1 is also permeable to Fe^{2+}, Zn^{2+} and other heavy trace metals (Dong et al., 2008). ML4 mutant cells exhibit a cytosolic Fe^{2+} deficiency and a concurrent lysosomal Fe^{2+} overload, suggesting that the iron efflux pathway is blocked in ML4 cells and that TRPML1 is essential for lysosomal Fe^{2+} release (Dong et al., 2008). Under oxidative conditions, lysosomal Fe^{2+} overload may dramatically increase the production of reactive hydroxyl radicals (OH, Fenton reaction), which in turn facilitates the formation of lipofuscin (also called aging pigment) (Kurz et al., 2008).

In summary, TRPML1 participate in multiple endolysosome-mediated functions including signal transduction, ionic homeostasis, and more than one aspect of membrane trafficking. A major challenge of TRPML research is to understand how one single TRPML protein can play such diverse roles. Multiple ionic conductances in a single membrane channel may certainly contribute to multifaceted functions. In addition to their divalent permeability, TRPML1 is also permeable to Na^+ and K^+ (Xu et al., 2007). TRPML1 may therefore regulate organelle dynamics by regulating endolysosomal membrane potentials. Rabs and PIPs exist in 'microdomains' in the membranes of endolysosomes, participating in multiple functions by recruiting distinct effector proteins (Poccia and Larijani, 2009) ((Poccia and Larijani, 2009; Stenmark, 2009). TRPML1 may differentially associate with Rabs, PIPs, and Ca^{2+} sensors (for example, CaM, Syt, and ALG-2), affording TRPML1 the ability to generate multiple cellular outputs.

1.6 PI(3,5)P_2, a signature lipid in endolysosomes.

Phosphoinositides (PIs) function as signaling molecules, and determine the identities of different intracellular membranes. In mammalian cells, phosphoinositides can be reversibly phosphorylated at three hydroxyl groups, in total, generating seven members (Di Paolo and De Camilli, 2006). These phosphoinositides are all concentrated on the cytosolic side of membrane bilayers with distinct localizations. While PI(3)P is mainly found on early and late endosomes, newly formed phagosomes and autophagosomes (Poccia and Larijani, 2009; Roth, 2004), PI(4)P is mainly localized on the Golgi (Levine and Munro, 1998). While PI(3,4)P_2 and PI(3,4,5)P_3 are generated transiently upon activation of plasma membrane receptors (Dewitt et al., 2006), PI(4,5)P_2 is relatively abundant on the plasma membrane and is the best characterized PI involving in a variety of plasma membrane specific functions. Finally, PI(3,5)P_2, the most recently identified phosphoinositide, is produced in late endosomes and lysosomes (LELs) using PI(3)P as the substrate (see **Fig. 1.1, Fig. 1.4**) (Zhang et al., 2012b; Zolov et al., 2012).

PI(3,5)P_2, a low abundance PI, makes up only ~ 0.04% of total cellular PIs in non-stimulated conditions (Dove et al., 2009; Zolov et al., 2012), which is ~1% of PI(4,5)P_2, and ~20% of PI3P. The level of PI(3,5)P_2 is tightly regulated spatially and temporally by the action of the specific kinase and phosphatases. Mammalian PIKfyve (Fab1 in yeast), a PI 5-kinase, converts PI3P to PI(3,5)P_2, and is the only enzyme shown to generate PI(3,5)P_2 (Ho et al., 2012; Sbrissa et al., 1999; Zolov et al., 2012). Generation of PI(3,5)P_2 requires a protein complex composed of PIKfyve, the scaffolding protein Vac14 (Dove et al., 2002; Jin et al., 2008), the PI(3,5)P_2 5-phosphatase Fig4 (Duex et al., 2006a; Rudge et al., 2004), a PIKfyve activator Vac7 (Bonangelino et al., 1997; Gary et al., 2002) and a negative regulator Atg18 (Dove et al., 2004; Efe et al., 2007). Since PIKfyve is mainly localized in late endosomes and lysosomes (Ikonomov et al., 2001; Zhang et al., 2012b), PI(3,5)P_2 is likely to have the similar LEL localization (Dove et al., 2009; Ho et al., 2012; Zhang et al., 2007b). Although the overall level of PI(3,5)P_2 is low, upon stimulation, the concentration in microdomains where PIKfyve is enriched may rapidly and transiently increase up to ~10 μM, similar level to those of PI(4,5)P_2 on the plasma membrane (Botelho et al., 2008; Ikonomov et al., 2009).

Mutations in *Vac14* and *Fig4* genes in mice, which result in roughly a 50% decrease in total PI(3,5)P_2 level, lead to profound neurodegeneration (Chow et al., 2007; Jin et al., 2008; Zhang et al., 2007a). Moreover, mutations in human *Fig4* underlie Charcot-Marie-Tooth type 4J neuropathy and are present in selected cases of amyotrophic lateral sclerosis (Chow et al., 2007).

Global knockout of *PIKfyve* causes preimplantation lethality (Ikonomov et al., 2011), however, a newly generated mouse model carrying a hypomorph of *PIKfyve* (~10% of the wild type PIKfyve protein) may provide more insights in the role of PIKfyve (Zolov et al., 2012). Yeast Fab1 and its regulators are localized in the vacuole and late endosomes (Bonangelino et al., 1997; Cooke et al., 1998; Duex et al., 2006a; Duex et al., 2006b; Gary et al., 2002). Consistent with this localization, the loss of Fab1 causes defects in retrograde traffic from vacuoles to the Golgi (Dove et al., 2004), vacuole membrane fission (Duex et al., 2006b) and vacuole acidification (Bonangelino et al., 2002). Similarly, mammalian $PI(3,5)P_2$-deficient cells from Fig4- or Vac14-knockout mice, exhibit defects in multiple LEL-associated cellular processes, including enlarged vacuoles/LELs (de Lartigue et al., 2009; Jefferies et al., 2008; Zhang et al., 2012b; Zhang et al., 2007a), defects in retrograde traffic from early endosomes to *trans*-Golgi network (Rutherford et al., 2006), impaired degradation of EGF receptor (de Lartigue et al., 2009), defects in autophagy (Ferguson et al., 2009; Rusten et al., 2007) and disrupted ionic homeostasis in LELs (Shen et al., 2011). These phenotypes are reminiscent of the cellular defects observed in TRPML1-deficient cells (Cheng et al., 2010), suggesting TRPML1 may functionally interact with the $PI(3,5)P_2$ signaling pathway and mediate LEL-associated functions, which would be discussed later as part of my thesis work.

$PI(3,5)P_2$ is proposed to perform its functions through at least three mechanisms (Di Paolo and De Camilli, 2006; Dove et al., 2009; Ho et al., 2012). First, as the signature phospholipid in LELs, $PI(3,5)P_2$ determines the physical properties and the fusogenic potential of endolysosomal membranes. Second, $PI(3,5)P_2$ may function as co-receptors together with membrane proteins in the recruitment of downstream cytosolic effectors. For example, Atg18 is the first identified $PI(3,5)P_2$ effector protein, that may mediate retrograde trafficking after its binding with $PI(3,5)P_2$ in yeast (Obara et al., 2008). Third, $PI(3,5)P_2$ may directly regulate the activity of membrane proteins, such as ion channel and transporters. The plasma membrane isoform $PI(4,5)P_2$ has been shown to be required for the activation or regulations of many plasma membrane ion channels, including TRP channels and voltage-gated $Na^+/K^+/Ca^{2+}$ channels (Suh and Hille, 2008). Similarly, my thesis work has shown that $PI(3,5)P_2$ activates both TPC channels and TRPML channels on the endolysosomes, regulating Na^+ and Ca^{2+}release through these channels, respectively.

1.7 Ca^{2+}-dependent lysosomal exocytosis

Lysosomes have been traditionally regarded as terminal compartments along the endocytic pathway. However it was recently shown that lysosomes undergo exocytosis in response to an increase of intracellular Ca^{2+} in most, if not all cell types (Andrews, 2000; Coorssen et al., 1996; Ninomiya et al., 1996; Rodriguez et al., 1999; Rodriguez et al., 1997) . This discovery has immediately attracted considerable interest to study the molecular mechanisms and physiological roles of this ubiquitous, Ca^{2+}-regulated lysosomal exocytosis pathway.

Similar to the exocytosis of synaptic vesicles, lysosomal exocytosis has two sequential steps. First, lysosomes are recruited to the close proximity of the cell surface in a Ca^{2+}-independent manner (Jaiswal et al., 2002). Then in response to intracellular Ca^{2+} elevation, the pool of docked lysosomes fuse with the plasma membrane via SNARE proteins in a few seconds (Andrews, 2000; Jaiswal et al., 2002; Tucker et al., 2004). During this step, synaptotagmin VII (Syt VII) is identified as the Ca^{2+} sensor (Gao et al., 2000; Gut et al., 2001; Martinez et al., 2000), while VAMP7 is the lysosomal v-SNARE interacting with the plasma membrane t-SNAREs SNAP-23 and syntaxin 4 (Rao et al., 2004). Syt VII, localized in lysosomes, is a ubiquitously expressed member of the synaptotagmin family, and contains two high-affinity Ca^{2+}-binding C2 domains (C2A and C2B) (Andrews, 2005; Sudhof and Rizo, 1996). Syt VII-deficient mice developed a form of autoimmune myopathy similar to the human diseases polymyositis/dermatomyositis. Cells from those mice showed defects in lysosomal exocytosis, phagocytosis and membrane resealing (Chakrabarti et al., 2003; Czibener et al., 2006; Roy et al., 2004; Zhao et al., 2008). Accumulating studies have identified essential roles of lysosomal exocytosis in numerous physiological processes, including plasma membrane repair (Andrews, 2005; Reddy et al., 2001), bone resorption (Zhao et al., 2008), neurite outgrowth (Arantes and Andrews, 2006), neurotransmitter release (Chen et al., 2005; Dou et al., 2012; Liu et al., 2011; Zhang et al., 2007b), axonal remyelination (Chen et al., 2012), phagocytosis (Czibener et al., 2006) and cellular clearance (Medina et al., 2011).

Lysosomal exocytosis can be monitored by Lamp1 (Lysosomal-associated membrane protein 1) surface staining using an antibody against a luminal epitope of Lamp1, or by measuring the activity of released lysosomal-specific enzymes (e.g. β-hexosaminidase) (Reddy et al., 2001). The critical trigger for lysosomal exocytosis is the local Ca^{2+} increase, presumably from lysosomal Ca^{2+} release under physiological conditions (Czibener et al., 2006; Liu et al., 2011; Tapper et al., 2002). However, definitive evidence to support this hypothesis is still

lacking, and more essentially, the ion channel(s) responsible for Ca^{2+} release from lysosomes remains elusive. TRPML1, as a lysosomal Ca^{2+}-permeable channel, may serve a perfect candidate for this job. Defects in lysosomal exocytosis were reported in TRPML1-deficienct cells, although the application of ionomycin (a Ca^{2+} ionophore, causing Ca^{2+} influx from extracellular space) to induce exocytosis may mask the function of TRPML1 as a potential lysosomal Ca^{2+} release channel. In addition, a very recent study showed that TFEB, a transcription factor and master regulator for lysosomal biogenesis, increases lysosomal exocytosis in a TRPML1-dependent manner (Medina et al., 2011). My thesis work has provided evidence to support that TRPML1-mediated Ca^{2+} release may induce lysosomal exocytosis. I screened several gain-of-function mutations in TRPML1 with constitutive Ca^{2+} permeability, and found that cells expressing these gain-of-function mutants of TRPML1 showed increased lysosomal exocytosis. To directly test the involvement of TRPML1, I also developed a whole-cell patch-clamp method to "detect" the plasma membrane insertion of TRPML1 during particle uptake-induced exocytosis, and further confirmed the prominent role of TRPML1 in this fundamental process.

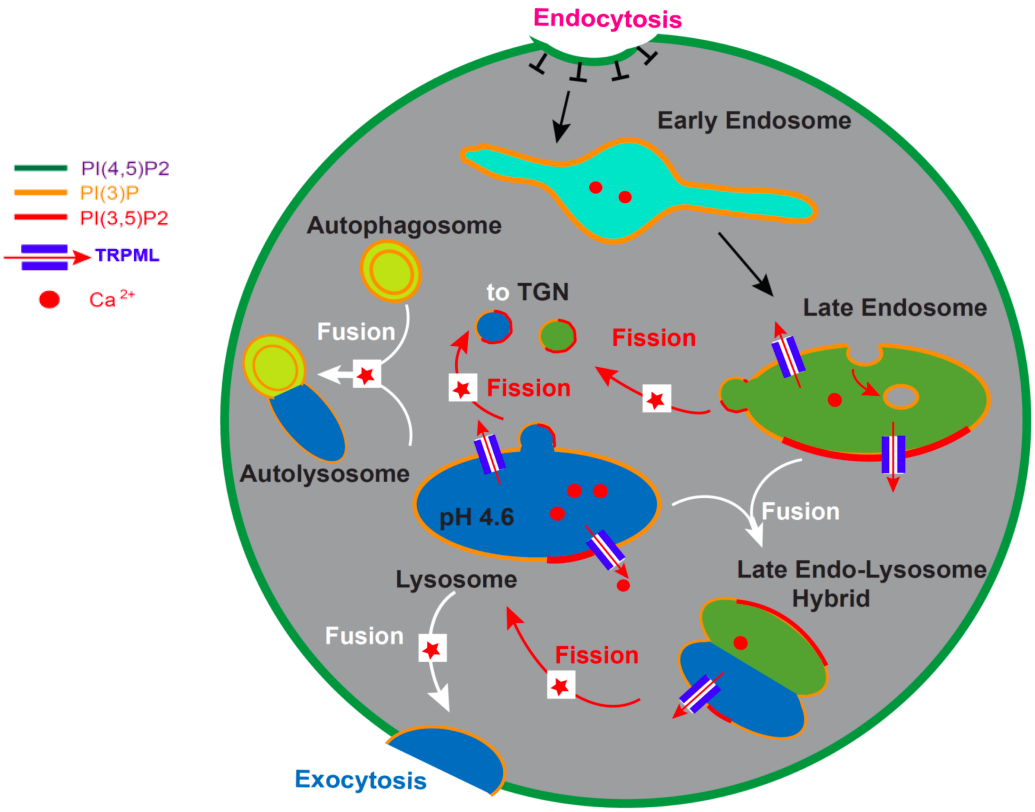

Figure 1.1. PI(3,5)P_2 and TRPML1 in endolysosomal membrane trafficking

Intracellular compartments in the endocytic pathways undergo cargo-dependent maturation (indicated by black arrows), membrane fusion (white arrows), and fission/budding (red arrows). PI(3)P is localized in early endosomes. PI(3,5)P_2 is presumed to be produced in late endosomes and lysosomes (LELs) . Endolysosomes are Ca^{2+} stores, with a luminal Ca^{2+} concentration estimated to be approximately 0.5 mM. Lysosomal pH is ~ 4.6. In endolysosomes, TRPML-mediated intra-endosomal Ca^{2+} release may trigger homotypic and heterotypic fusion. Early endosomes (pH 6.0; PI(3)P;) are derived from the primary endocytic vesicles after endocytosis. Early endosomes can undergo maturation through membrane trafficking to become late endosomes (pH 5.5; PI(3)P + PI(3,5)P_2). Late endosomes can fuse with lysosomes (pH 4.5; PI(3)P+PI(3,5)P_2 to form the hybrids. Lysosomes can be reformed from the hybrids in a fission-dependent mechanism. Besides fusion with late endosomes, lysosomes also fuse with

autophagosomes to form autolysosomes, or fuse with the plasma membrane in exocytosis. TRPML1-3 channels are predominantly localized in LELs. Activation of TRPML channels by $PI(3,5)P_2$ may induce intralysosomal Ca^{2+} release. Retrograde transport vesicles, derived from LELs upon membrane fission, transport lipids and proteins in a retrograde direction to the *trans*-Golgi Network (TGN). Stars indicate membrane fusion and fission processes that are reportedly defective in both TRPML1-deficient and $PI(3,5)P_2$-deficient cells. Adapted from reference (Dong et al., 2010a).

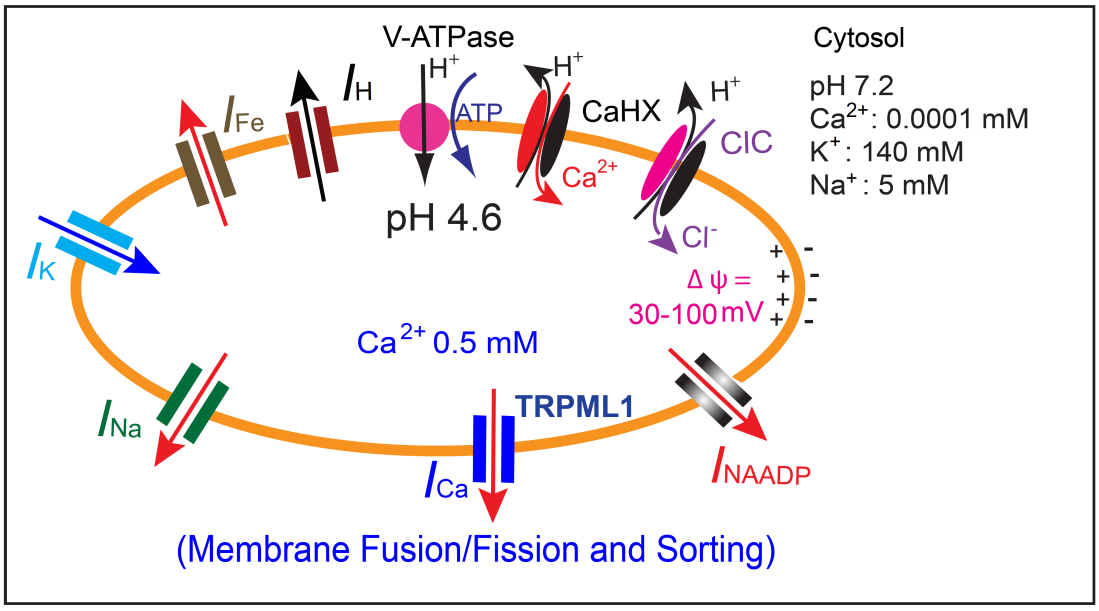

Figure 1.2. Ion channels and transporters in endolysosomes.

The prominent feature of endolysosomes is their acidic lumen (lysosomal pH: 4~5), which is established by the V-type ATPase. The existence of H^+ leak is supported by the luminal alkalization caused by inhibiting V-ATPase function, although the conductance is not characterized. The $[Ca^{2+}]$ in lysosomes is ~0.5 mM, which presumably is maintained by an unidentified H^+-Ca^{2+} exchanger, due to the sensitivity of the Ca^{2+} store to the H^+ gradient. NAADP is a newly identified second messenger, and is reported to trigger lysosomal Ca^{2+} release via unknown receptors. TPCs are proposed to be the NAADP receptors. The Cl^- conductance in endolysosomes is mediated by ClC Cl^-/H^+ antiporters (ClC3-6 in endosomes; ClC-7 in lysosomes). The Cl^- flux was thought to mediate counterion flux to support lysosomal

acidification, but emerging evidence has demonstrated that the ClC-mediated Cl^- flux is actively serving some other important functions beyond just pH regulation. A putative lysosomal K^+ release channel was also proposed to provide counterion flux to facilitate lysosomal acidification, although the electrochemical gradient of K^+ across the lysosome membrane might be low, or opposite. The Fe^{2+} release conductance is important for lysosomal functions, which may be mediated by the Fe^{2+}-permeable channel TRPML1. TRPML1 is also the principle Ca^{2+}-permeable channel primarily localized in late endosomes and lysosomes. The role of TRPML1-mediated Ca^{2+} signaling has been studied in vesicular ion homeostasis and intracellular membrane trafficking, including lysosome biogenesis, lysosomal exocytosis and autolysosome formation.

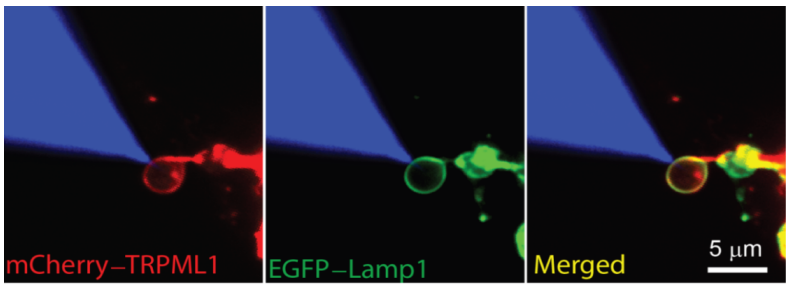

Fig.1.3. Illustration of a whole-lysosome recording configuration on an isolated lysosome. The mCherry–TRPML1 and EGFP–Lamp1 (lysosomal marker) are co-localized on the membrane of an isolated enlarged lysosome. The patch pipette is filled with rhodamine B dye (shown in blue for clarity). Adapted from reference (Dong et al., 2008).

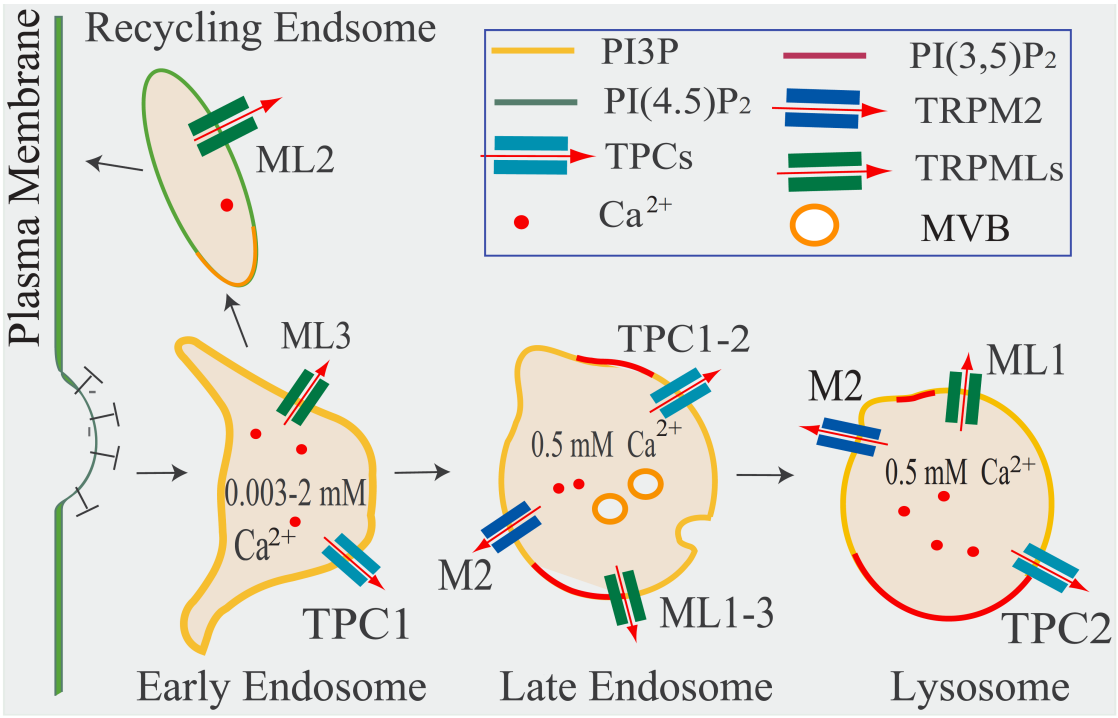

Figure 1.4. The distribution of ion channels (TRPMLs and TPCs) and phosphoinositide (PI3P, PI(3,5)P_2) along the endocytic pathway.

PI3P mainly resides in early and late endosomes, while PI(3,5)P_2 is on late endosomes and lysosomes. TRPML channels (TRPML1-3) are primarily expressed in late endosomes and lysosomes (LELs), while TRPML2 and TRPML3 are also associated with recycling and early endosomes, respectively. TPC2 is mainly localized in the LELs, and TPC1 is mainly associated with early and late endosomes. TRPM2 is expressed in specific cell types, and resides in LELs as well as the plasma membrane. The concentration of Ca^{2+} stores associated with each vesicle type is also indicated. Figure is adapted from reference (Shen et al., 2011).

CHAPTER 2

TPC proteins are phosphoinositide-activated sodium-selective ion channels in endosomes and lysosomes

Abstract

Mammalian Two-Pore-Channels (TPC1, 2; *TPCN1, TPCN2*) encode ion channels in intracellular endosomes and lysosomes and were proposed to mediate endolysosomal calcium release. By directly recording TPCs in endolysosomes from wild-type and TPC double knockout mice, here we show that, in contrast to previous conclusions, TPCs are in fact sodium-selective channels activated by $PI(3,5)P_2$. Moreover, the primary endolysosomal ion is Na^+, not K^+, as had been previously assumed. These findings suggest that the organellar membrane potential may undergo large regulatory changes, and may explain the specificity of $PI(3,5)P_2$ in regulating the fusogenic potential of intracellular organelles.

Introduction

Two pore channel proteins (TPC1, 2; *TPCN1, TPCN2*) (Calcraft et al., 2009; Morgan et al., 2011) are localized in intracellular endosomes and lysosomes (collectively endolysosomes) previously inaccessible to conventional patch clamp assays. Consistent with this localization, human genetic studies have identified TPC2 as a regulator of pigmentation (Sulem et al., 2008) and a number of recent studies suggest that TPCs mediate Ca^{2+} release from endolysosomes in response to an elevation of the potent Ca^{2+}-mobilizing second messenger, nicotinic acid adenine dinucleotide phosphate (NAADP) (Brailoiu et al., 2009; Calcraft et al., 2009; Ruas et al., 2010; Zong et al., 2009) (but also see ref. (Guse, 2009)). Unlike plasma membrane localized Na_V and Ca_V channels, the primary structures of TPCs contain two, instead of four, 6 transmembrane (6TM) domains (Yu and Catterall, 2004). Like Na_V and Ca_V channels, they contain multiple positively charged amino acid residues in their voltage sensor domains and negatively-charged amino acid residues in their pore domains, but their intracellular localization has prevented characterization of basic channel properties such as selectivity and gating.

$PI(3,5)P_2$ is an endolysosome-specific phosphoinositide (PIP) of low abundance (Dove et al., 2009; Shen et al., 2011). Upon cellular stimulation, PI 5-kinase PIKfyve/Fab1 phosphorylates PI(3)P to increase $PI(3,5)P_2$ from low nM to μM concentrations (Dove et al., 2009; Shen et al., 2011). Human mutations in $PI(3,5)P_2$-metabolizing enzymes and their regulators result in muscle and neurodegenerative diseases such as amyotrophic lateral sclerosis (ALS) and Charcot-Marie-Tooth (CMT-4B, CMT-4J) disease (Chow et al., 2007). $PI(3,5)P_2$-deficient cells have enlarged endolysosomes/vacuoles, suggestive of impaired ion homeostasis and/or defective membrane trafficking (Chow et al., 2007; Dove et al., 2009; Kerr et al., 2010; Shen et al., 2011). We recently found that TRPML1 mediates $PI(3,5)P_2$-dependent Ca^{2+} release from endolysosomes (Dong et al., 2010a). However, $PI(3,5)P_2$ deficiency results in a much more severe phenotype than TRPML1 mutations, suggesting that there are additional $PI(3,5)P_2$ effectors (Shen et al., 2011). Here, we find by direct patch-clamp of endolysosomal membranes, that $PI(3,5)P_2$ specifically activates TPCs. TPC-mediated currents are selective for Na^+, which we demonstrate is the predominant cation in the lysosome. TPCs represent the first intracellular Na^+-selective channels and suggest a new model for ion channel control of endolysosomal fusion.

Results

$PI(3,5)P_2$ activation of a large endogenous current in the endolysosome.

Cells were pretreated with vacuolin-1, a lipid-soluble polycyclic triazine (Huynh and Andrews, 2005) that can selectively increase the size of endosomes and lysosomes from < 0.5 μm to up to 5 μm (Dong et al., 2010a). The enlarged endolysosomes were manually isolated and then patch clamped in the whole-endolysosome configuration (**Fig. 2.1A**; **Fig. 2.2**). We previously reported that TRPML1 was the primary $PI(3,5)P_2$-activated conductance (reversal potential, E_{rev} ~ 0 mV) in the endolysosomes of human fibroblast (Dong et al., 2010a). However, in several other cell types including skeletal muscles (data not shown) and macrophages, we observed that bath (cytoplasmic) application of diC8 $PI(3,5)P_2$ (abbreviated as $PI(3,5)P_2$) , a water-soluble analog of $PI(3,5)P_2$ (Dong et al., 2010a), activated a distinct whole-endolysosome conductance with an E_{rev} > + 60 mV (defined as I_X; **Fig. 2.1B**). Strongly inwardly-rectifying TRPML-like currents ($I_{TRPML-L}$; (Dong et al., 2010a)) were also present in macrophages, but $PI(3,5)P_2$-activated $I_{TRPML-L}$ was often masked by I_X due to its positive E_{rev}. $I_{TRPML-L}$ could be activated by SF-51 (100 μM (Grimm et al., 2010); **Fig. 2.1B**). $I_{TRPML-L}$, but not I_X, was dramatically reduced in *TRPML1*$^{-/-}$ macrophages (**Fig. 2.1C**). In 9 out of 23 enlarged endolysosomes isolated from non-transfected COS-1 cells, high concentrations of $PI(3,5)P_2$ (10 μM) activated I_X, which was distinct from $I_{TRPML-L}$ activated by 1 μM $PI(3,5)P_2$ (Dong et al., 2010a) or SF-51 (**Fig. 2.1D**).

$PI(3,5)P_2$ activates recombinant TPC1 and TPC2 channels in the endolysosome.

To search for the identity of the protein mediating I_X, a number of fluorescently-tagged putative intracellular channels or transporter-like lysosomal membrane proteins were transfected into COS-1 cells. As described below, endolysosomes from TPC1- and TPC2-transfected cells exhibit large I_X. The majority (> 80%) of vacuolin-1-treated TPC2-positive vacuoles were Lamp-1^+ (**Fig. 2.3A**), confirming that TPC2-positive vacuoles were enlarged late endosomes and lysosomes (LELs). In TPC2 (hTPC2)-positive enlarged LELs isolated from transfected COS1 cells, little or no basal currents were detected in the whole-endolysosome configuration (**Fig. 2.3B)**. Bath application of $PI(3,5)P_2$ rapidly activated hTPC2-mediated currents (I_{TPC2}; E_{rev} = + 83 ± 3 mV; **Fig. 2.3B**), but not those that expressed a mutant hTPC2 carrying a charge-reversal mutation in the putative pore domains

(D276K; **Fig. 2.4A, B**); I_{TPC2} gradually declined upon the washout of $PI(3,5)P_2$ (**Fig. 2.3B**) with variable time courses (depending on treatment time). The I-V and E_{rev} of I_{TPC2} are similar to the endogenous $PI(3,5)P_2$-activated I_X.

$PI(3,5)P_2$-dependent activation of I_{TPC2} was dose-dependent (EC_{50}= 390 ± 94 nM; **Fig. 2.3C**). I_{hTPC2} was inhibited > 80% by the $PI(3,5)P_2$ chelators (Nilius et al., 2008; Suh and Hille, 2008) poly-L-lysine and anti-$PI(3,5)P_2$ antibody (**Fig. 2.4C, D**). Other phosphoinositides, PI(3)P, PI(5)P, $PI(3,4)P_2$, $PI(4,5)P_2$, and $PI(3,4,5)P_3$, did not activate I_{TPC2} (10 μM; **Fig. 2.3D**; **Fig. 2.4E**). Thus $PI(3,5)P_2$ activated I_{TPC2} with striking specificity. In contrast, 1 μM $PI(3,5)P_2$ failed to activate the lysosome-localized (Lange et al., 2009) recombinant TRPM2 channel (**Fig. 2.4F**) or modulate the endogenous outward currents that were present in a subset of endolysosomes isolated from INS1 pancreatic β-cells (**Fig. 2.4G**). TPC1, also localized in the endolysosome (Calcraft et al., 2009) (but primarily in Lamp-1-negative compartments; **Fig. 2.4A**), was also activated by $PI(3,5)P_2$ (**Fig. 2.3E**).

TPC-mediated currents are Na^+-selective.

The measured E_{rev} of I_{TPC} under standard recording conditions (with a low pH modified Tyrode's solution in the pipette/lumen and a K^+-based solution in the bath/cytosol) dictates that the channels are selective for Na^+, Ca^{2+}, or H^+, but not K^+. Increasing the luminal pH from 4.6 to 7.4 had minimal effects on I_{TPC2} (**Fig. 2.5A; Fig. 2.6A**) and I_{TPC1}. Conversely, replacement of luminal cations (Na^+, K^+, Mg^{2+}, and Ca^{2+}) with $NMDG^+$ at pH 4.6 completely abolished inward I_{TPC2} (**Fig. 2.6B**), suggesting that I_{TPC2} is impermeable to H^+ or $NMDG^+$. Under bi-ionic conditions (luminal Na^+, pH 7.4; cytoplasmic K^+), the E_{rev} of I_{TPC2} was + 89 ± 5 mV (n=8; see **Fig. 2.5A**). In contrast, under reversed bi-ionic conditions (luminal K^+, pH 7.4; cytoplasmic Na^+), the E_{rev} of I_{TPC2} was -68 ± 3 mV (n = 5; see **Fig. 2.5B**). These results indicated that I_{TPC2} was selective for Na^+ over K^+. Consistent with this conclusion, switching cytoplasmic K^+ to Na^+ in the presence of luminal Na^+ resulted in a leftward shift of the Erev and the appearance of large outward currents (**Fig. 2.5A**). Addition of 2 mM Ca^{2+} to the luminal side of the symmetric Na^+ solutions did not result in any significant change of the E_{rev} or the amplitude of the inward currents (**Fig. 2.6C**), suggesting that luminal Ca^{2+} contributed insignificantly to inward I_{TPC2}. Consistently, under bi-ionic conditions (luminal isotonic Ca^{2+}, pH 4.6 or 7.4; cytoplasmic Na^+), the E_{rev} of I_{TPC2} was -68 ± 2 mV (n = 12; **Fig. 2.6D**), in dramatic contrast to the E_{rev} of I_{TRPML1} (+ 47 ± 2 mV, n = 3; **Fig. 2.6E**). With

cytoplasmic K^+, however, a small inward I_{TPC2} could be resolved with luminal isotonic Ca^{2+} (105 mM), but not $NMDG^+$ (**Fig. 2.6B, D**), suggesting a very limited Ca^{2+} permeability for TPC2. By estimating the permeability ratios based on E_{rev} measurements, we determined the sequence of ion permeability or selectivity of I_{TPC2} as $Na^+ > Li^+ >> Ca^{2+} >> K^+ \sim Cs^+$ (**Fig. 2.5C** & **Fig. 2.6F**). P_{Ca}/P_{Na} and P_K/P_{Na} were about 0.10 and 0.03, respectively, which are similar to the values for canonical Na_V channels (0.08-0.11) (Favre et al., 1996; Hille, 1972). Consistent with the low P_K/P_{Na}, with a mixture of K^+ and Na^+ at both luminal and cytoplasmic sides, the Na^+-dependence of E_{rev} was fit with a Nernstian slope of 57 mV per 10-fold change of $[Na^+]_{cyto}$ (**Fig. 2.5D**). Taken together, these ion substitution analyses demonstrate that TPC2 is a highly Na^+-selective channel in the endolysosome.

Because the S4 segments of TPC1 and TPC2 contain several positively-charged amino acid residues, we investigated the voltage-dependence of I_{TPC}. Unlike canonical Na_V and Ca_V channels, I_{TPC} was not directly activated by membrane depolarization. Instead, in response to a step voltage protocol, $PI(3,5)P_2$-activated I_{TPC} inactivated at negative voltages (**Fig. 2.6G**), with I_{TPC1} exhibiting faster inactivation than I_{TPC2} (**Fig. 2.5E**). Inactivation recovered rapidly after a brief pulse to positive voltages (**Fig. 2.6H**). Although being Na^+ selective, I_{TPC2} was insensitive to the Na_V blocker, TTX (**Fig. 2.6I**), but was sensitive to low concentrations of the nonselective Ca_V blocker, verapamil, in a voltage-dependent manner (**Fig. 2.5F**).

Na^+ is the major cation in the lysosome.

The existence of Na^+-selective channels in the lysosome was unexpected because the lysosomal lumen, like the cytosol and the ER lumen (Morgan et al., 2011), has been presumed to contain high K^+ and low Na^+ (Morgan et al., 2011; Steinberg et al., 2010), suggesting the lack of a significant Na^+ or K^+ concentration gradient across the lysosomal membrane. To directly measure the ionic composition of the lysosome lumen, we enriched the lysosome fraction of HEK293T cells using density gradient centrifugation (Dong et al., 2010a; Graves et al., 2008) (**Fig. 2.8A**; **Fig. 2.7A**), and then determined the ratios of major cations (Na^+, K^+, Ca^{2+}, and Mg^{2+}) using Inductively Coupled Plasma Mass Spectrometry (ICP-MS) analysis. All centrifugation steps were performed at 4 ºC (1 h in the sucrose gradient + 2.5 h in the iodixanol gradient; see **Fig. 2.8A**). At this temperature, the rate of ion transport across the lysosomal membrane is expected to be extremely low. In addition, the sucrose -based homogenization buffer contains few ions. Thus, lysosomal ion

transporters/exchangers are not likely to be operative. Hence, we presume that the lysosomal ion composition is largely maintained during the isolation procedure. Similar approaches have been used to determine ionic compositions in a number of intracellular organelles, including mitochondria and synaptic vesicles (Cohn et al., 1968; Schmidt et al., 1980). Although the absolute concentrations of ions could not be accurately measured due to the lack of information about lysosome volume, this approach allowed us to determine the relative abundance/ratios of the total, but not free ions in the lumen. Interestingly, the K^+/ Na^+ and Ca^{2+}/ Na^+ ratios were only about 0.01 (**Fig. 2.7B**), which were not significantly affected by the trace amount of ions in the buffer (**Fig. 2.8B**). Similar results were obtained from human fibroblasts and mouse macrophages. Thus Na^+ is the predominant cation in the lumen of the lysosome (estimated to be ~ 140-150 mM, assuming that its lumen is iso-osmotic relative to the cytosol, and all the cations are osmotically-active) (**Fig. 2.7B**), indicating that in contrast to previous indirect measurements (Morgan et al., 2011; Steinberg et al., 2010), a large Na^+ concentration gradient is present across the lysosomal membrane.

To directly test whether the lysosomal lumen is a high Na^+-compartment, isolated lysosomes were treated with TPC agonists. Application of $PI(3,5)P_2$, but not $PI(4,5)P_2$, significantly increased the K^+/ Na^+ ratios (**Fig. 2.7C**). Similarly, in isolated TPC2-mCherry lysosomes loaded with Sodium Green (**Fig. 2.8C**), a Na^+-sensitive dye (Carrithers et al., 2007), $PI(3,5)P_2$, but not $PI(4,5)P_2$ application significantly decreased Sodium Green fluorescence (**Fig. 2.7D**). These results suggest that sustained activation of TPCs may reduce luminal Na^+ content. Consistent with the lysosome being a high Na^+ compartment rather than high K^+, when $PI(3,5)P_2$ was included in the pipette solution, a large I_{TPC2} was observed under the lysosome-attached configuration (**Fig. 2.7E**) in which the lysosomal content and hence the Na^+ gradient were maintained. Collectively, these results suggest that TPC-mediated Na^+ flux in response to a localized increase in $PI(3,5)P_2$ may rapidly depolarize endolysosomal membranes (luminal-side positive ~ + 30-110 mV at rest (Dong et al., 2010b; Morgan et al., 2011)), and facilitate membrane fusion (**Fig. 2.8D**). Consistently, TPC2-positive compartments were significantly enlarged in COS1 cells transfected with WT, but not D276K mutant hTPC2 (**Fig. 2.8E, E'**), suggesting that TPC2-expressing endolysosomes might have increased fusogenic potentials.

TPC1 and TPC2 underlie endogenous TPC-like currents in the endolysosome.

Mice lacking *TPC1* or *TPC2* were generated and crossed to make double knockout (*TPC1*$^{-/-}$/*TPC2*$^{-/-}$) mice (**Fig. 2.9A**). In our targeting strategy, the first exons of the *TPC1* and *TPC2* genes were deleted, and the resulting recombinant transcripts failed to generate I_{TPC} (**Fig. 2.10A**). In vacuoles isolated from *TPC1*$^{-/-}$/*TPC2*$^{-/-}$ primary macrophages, PI(3,5)P_2 activated $I_{TRPML-L}$, but Na^+-selective (I_{TPC}-like; I_{TPC-L}) currents were absent (**Fig. 2.9B**). In contrast, PI(3,5)P_2 activated I_{TPC-L} in the majority (> 90%) of vacuoles in *WT* (**Fig. 2.9C)** and *TRPML1*$^{-/-}$ (**Fig.** 2.**1C**) macrophages. The current amplitudes of $I_{TRPML-L}$ were not significantly different in *TPC1*$^{-/-}$/*TPC2*$^{-/-}$ compared to *WT* macrophages (**Figs. 2.1B, 2.9B, D**), but were dramatically reduced in *TRPML1*$^{-/-}$ macrophages (**Figs. 2.1C, 2.9D**). Although $I_{TRPML-L}$ and I_{TPC-L} are both activated by PI(3,5)P_2, their I-V's and E_{rev}'s differed significantly from each other. When we analyzed PI(3,5)P_2-activated currents at – 30 mV, large differences were noted between *WT, TRPML1*$^{-/-}$, and *TPC1*$^{-/-}$/*TPC2*$^{-/-}$ macrophages (**Fig. 2.9E**). Consistently, the PI(3,5)P_2-activated current was selective for Na^+ over Ca^{2+} (**Fig. 2.10B**). Collectively, these results suggest that I_{TPC-L} is mediated by TPC2 and/or TPC1.

Discussion

The lysosomal lumen has been presumed to contain high K^+ and low Na^+ (Morgan et al., 2011; Steinberg et al., 2010), which would suggest the lack of a significant Na^+ or K^+ concentration gradient across the lysosomal membrane. These conclusions contrast directly with the high Na^+/low K^+ (like that of the extracellular media) we have found here using subcellular fractionation of organelles, which has been successfully applied to measure ionic compositions in a number of intracellular organelles, including mitochondria and synaptic vesicles (Cohn et al., 1968; Schmidt et al., 1980). Because the isolation procedures were performed at 4 ºC using a homogenization buffer that limits ion exchange, the lysosomal ion composition is presumed to be largely maintained. Indeed, lysosome fractions prepared using this protocol are of relatively normal size (lysosome swelling could be caused by the loss of luminal ions) and are functional (Graves et al., 2008; Radhakrishnan et al., 2008). Finally, the significant Na^+-selective current observed in the lysosome-attached configuration provides an independent verification that the lysosome lumen contains high concentrations of Na^+. It is worth mentioning that although a putative lysosomal K^+ release channel was proposed to provide counter ion flux for lysosomal acidification (Steinberg et al., 2010), such a scenario

is unlikely to occur due to the high cytosolic K^+, hence the low or opposite electrochemical gradient of K^+ across the lysosome membrane. Instead, the existence of a large Na^+ gradient and lysosomal Na^+ channels are more likely to fulfill this function (counter-ion flux).

What is the purpose of Na^+ selective, $PI(3,5)P_2$-activated TPC channels? Increases in $PI(3,5)P_2$ will allow Na^+ to move down its concentration gradient, rapidly reducing and reversing (**Fig. 2.8D**) the endolysosomal potential, which is presumed to be luminal-side positive at rest (estimated to be + 30 to + 110 mV) (Dong et al., 2010b). In model membranes, it has been demonstrated that Na^+ and K^+ exhibit differential effects on membrane curvature (Kraayenhof et al., 1996). While oppositely-charged lipid bilayers tend to fuse (Anzai et al., 1993), Na^+ influx into the cytoplasm reportedly affects membrane fusion during exocytosis (Parnas et al., 2000). Thus, TPC-mediated Na^+ flux in response to a localized increase in $PI(3,5)P_2$ may rapidly depolarize endolysosomal membranes and promote fusion (**Fig. 2.8D**). Consistent with a previous study (Ruas et al., 2010), we found that TPC overexpression results in enlarged endolysosomes; this might be caused by enhanced endolysosomal fusion, decreased fission, or both. Finally, in addition to defining organelle specificity and determining the fusogenic potential of endolysosomes, the proposed cellular functions of $PI(3,5)P_2$ also include regulating endolysosomal ion homeostasis, especially H^+ homeostasis (Kerr et al., 2010; Shen et al., 2011). The proposed role of a putative monovalent cation (K^+ or Na^+) conductance in lysosomal acidification (Steinberg et al., 2010), together with our demonstration of a large Na^+ gradient across the endolysosomal membrane, suggest that $PI(3,5)P_2$-sensitive Na^+-permeable TPCs, but not K^+ release channels (see above), may participate in endolysosomal pH regulation in a transient and localized manner.

Experimental Procedures

Molecular biology and biochemistry

Full-length mouse and human *TPC1* and *TPC2* were cloned into the *EGFP-C2* vector (Clontech) or a similar vector allowing mCherry to be fused at the C terminus. TPC pore mutants were constructed using the Qiagen site-directed mutagenesis kit. All constructs were confirmed by sequencing, and protein expression was verified by Western blot and fluorescence imaging. COS-1 or HEK293T cells, used for all the heterologous expression experiments, were transfected using Lipofectamine 2000 (Invitrogen) with human *TPC1*, mouse *TPC1*, human *TPC2*, or mouse *TPC2* fused with either EGFP or mCherry. Confocal

images were taken using a Leica (TCS SP5) microscope and an Olympus Spinning-disk confocal system.

Targeted deletion of *TPC1* and *TPC2* in mice

Generation of *TPC1* and *TPC2* double knockout mice. Briefly, LoxP sites were introduced in the 5'UTR and the intron after the first exon encoding the translational start site (ATG) of *TPC1* and *TPC2*, separately. Heterozygotes were mated with *CRE* recombinase mice to generate mice with the region flanked by the LoxP sites deleted. The deletions are predicted to produce transcripts encoding channels lacking the first 69 amino acids (TPC1) or 49 amino acids (TPC2). Mouse and human *TPCs* truncated at corresponding positions do not generate functional channels when expressed in COS1 cells (**Fig. 2.10A**). The TRPML1 KO mouse was a kind gift from Dr. Susan Slaugenhaupt (Venugopal et al., 2007).

Endolysosomal electrophysiology

Endolysosomal electrophysiology was performed in isolated enlarged endolysosomes using a modified patch-clamp method (Dong et al., 2010a). Cells were treated with 1 μM vacuolin-1, a lipid-soluble polycyclic triazine that can selectively increase the size of endosomes and lysosomes (Huynh and Andrews, 2005), for at least 1h or up to 12h. Large vacuoles (up to 5μm; capacitance = 1.1 ± 0.1 pF, n= 29 vacuoles) were observed in most vacuolin-treated cells. Occasionally, enlarged vacuoles were also seen in non-treated cells; no significant difference in TPC channel properties were seen for enlarged vacuoles obtained with or without vacuolin-1 treatment. Whole-endolysosome recordings were performed on manually isolated enlarged endolysosomes (Dong et al., 2010a). In brief, a patch pipette was pressed against a cell and quickly pulled away to slice the cell membrane. Enlarged endolysosomes were released into a dish and identified by monitoring EGFP-TPC1/2, the mCherry-TPC1/2, or EGFP-Lamp1/mCherry-Lamp1 fluorescence. After formation of a gigaseal between the patch pipette and the enlarged endolysosome, capacitance transients were compensated. Voltage steps of several hundred mVs with ms duration were then applied to break into the vacuolar membrane (**Fig. 2.2**). The whole-endolysosome configuration was verified by the re-appearance of capacitance transients after break-in (**Fig. 2.2**).

Unless otherwise stated, bath (internal/cytoplasmic) solution contained (in mM) 140 K-gluconate, 4 NaCl, 1 EGTA, 2 $MgCl_2$, 0.39 $CaCl_2$, 20 HEPES (pH adjusted with KOH to

7.2; free $[Ca^{2+}]_i$ ~ 100 nM). In a subset of experiments, 2 mM Na_2-ATP and 0.1 mM GTP were added to the bath solution, and pH was re-adjusted. Pipette (luminal) solution was standard extracellular solution (modified Tyrode's; in mM): 145 NaCl, 5 KCl, 2 $CaCl_2$, 1 $MgCl_2$, 10 HEPES, 10 MES, 10 glucose (pH adjusted with NaOH to pH 4.6). In a subset of experiments, a low Cl^- pipette solution containing Na-gluconate replaced NaCl. All bath solutions were applied via a perfusion system that allowed us to achieve complete solution exchange within a few seconds. Data were collected using an Axopatch 2A patch clamp amplifier, Digidata 1440, and pClamp 10.2 software (Axon Instruments). Whole-endolysosome currents were digitized at 10 kHz and filtered at 2 kHz. All experiments were conducted at room temperature (21-23ºC), and all recordings were analyzed with pClamp 10.2, and Origin 8.0 (OriginLab, Northampton, MA). All PIPs were from A.G. Scientific; water-soluble diC8-PIPs, prepared in high-concentration stock solutions, were dissolved in the bath solutions, and delivered via the perfusion system at low concentrations (0.1-1 μM), and direct bath application at higher concentrations (10 μM).

Cationic Permeability of TPC Channels

The permeability to cations (relative to P_{Na}) was estimated according to Eqn. 1 (for monovalents) and Eqn. 2 (for Ca^{2+}) based on E_{rev} measurement under bi-ionic conditions (Lewis, 1979). The monovalent solutions contained 160 mM XCl (X=Na^+, K^+, Cs^+, or Li^+), 20 mM HEPES, 10 mM glucose, pH adjusted to pH 7.4 using XOH. Isotonic Ca^{2+} solution contained (in mM) 105 Ca^{2+}, 20 glucose, 20 HEPES (pH 7.4) or 20 MES (pH 4.6). The permeability ratios of cations were estimated from the following equations:

Equation 1

$$P_X/P_{Na} = \gamma_{Na}/\gamma_X \{ [Na^+]_{Luminal} / [X]_{Cytoplasmic} \} \{\exp(E_{rev}F/RT)\}$$

Equation 2

$$P_{Ca}/P_{Na} = \gamma_{Na}/\gamma_{Ca} \{4[Ca^{2+}]_{Luminal}/[Na^+]_{Cytoplasmic}\} \{\exp(E_{rev}F/RT)\} \{1 + \exp(E_{rev}F/RT)\}$$

where R, T, F, E_{rev}, and γ are, respectively, the gas constant, absolute temperature, Faraday constant, reversal potential, and activity coefficient. The liquid junction potentials were measured and corrected as described (Neher, 1992).

Lysosome isolation by subcellular fractionation

Lysosomes were isolated as described previously (Dong et al., 2010a; Graves et al., 2008). Briefly, cell lysates were obtained by Dounce homogenization in a homogenizing buffer (HM buffer; 0.25 M sucrose, 1 mM EDTA, 10 mM HEPES, and pH 7.0), and then centrifuged at 1900 *g* (4, 200 rpm) at 4°C for 10 min to remove the nuclei and intact cells. Post-nuclear supernatants then underwent ultracentrifugation through a Percoll density gradient using a Beckman L8-70 ultracentrifuge. An ultracentrifuge tube was layered with 2.5 M sucrose, 18% Percoll in HM buffer. Centrifugation speed was 67,200 *g* (14,000 rpm) at 4°C for 1 h using a Beckman Coulter 70.1 Ti Rotor. Samples were fractionated into light, medium, and heavy membrane fractions. Heavy membrane fractions contained concentrated bands of cellular organelles and were further layered over a discontinuous iodixonal gradient. The iodixonal gradient was generated by mixing iodixonal in the HM buffer with 2.5 M glucose (in v/v; 27%, 22.5%, 19%, 16%, 12%, and 8%); the osmolarity of all solutions was ~ 300 mOsm. After centrifugation at 4°C for 2.5 h, the sample was divided into 10 fractions (0.5 ml each) for biochemical and atomic absorption analyses. Note that the ionic composition of the lysosome was largely maintained due to the low rate of ion transport across the lysosomal membrane at 4°C. Antibodies used for Western blots: anti-Lamp1 (Iowa Hybridoma bank), 1:5000 dilution; anti-Annexin V (Abcam), 1:2000 dilution; anti-GM130 (Abcam), 1:2000 dilution; anti-EEA1 (Santa Cruz Biotechnology), 1:500 dilution; anti-Complex II (Abcam), 1:5000 dilution; anti-GFP (Covance), 1:5000 dilution.

Inductively Coupled Plasma Mass Spectrometry (ICP-MS)

Lysosomal fractions were prepared for atomic absorption by diluting the samples at a 1:1 ratio with concentrated nitric acid. After digestion (10min, 60ºC), the ionic composition was measured using a Thermo Scientific Finnigan Element inductively coupled with a plasma-high resolution mass spectrometer (ICP-HRMS)(Seby et al., 2003).

Lysosome Flow Cytometry

hTPC2-mCherry stable cell lines were homogenized and lysosomal fractions were kept in the HM buffer at 4°C, and loaded with Sodium Green (SG) tetraacetate (5 μM) for 30 min (Carrithers et al., 2007). After two washes at 14,000 rpm, the samples were re-suspended in the HM buffer and analyzed by a Flow Cytometer (Synergy, iCyt). The lysosome gate was

determined with 0.5 μm and 1 μm beads; 90% of the vesicles/sample were mCherry-positive. The samples were treated with DiC8-PI(3,5)P_2 or PI(4,5)P_2 (20 μM) for 5 min before FACS analysis. Total counts were > 10,000 events. Data were analyzed using the Winlist 3D software.

Preparation and culture of mouse macrophages

Murine bone marrow-derived macrophages were prepared and cultured as described previously (Link et al., 2010). Briefly, bone marrow cells from femurs and tibias were harvested and cultured in macrophage differentiation medium (RPMI-1640 medium with 10% FBS and 100 unit/ml recombinant colony stimulating factor from PeproTech). After 7d in culture at 37°C with 5% CO_2, the adherent cells (> 95% macrophages) were harvested for assays.

Data analysis.

Data are presented as the mean ± standard error of the mean (SEM). Statistical comparisons were made using analysis of variance (ANOVA). A *P* value < 0.05 was considered statistically significant.

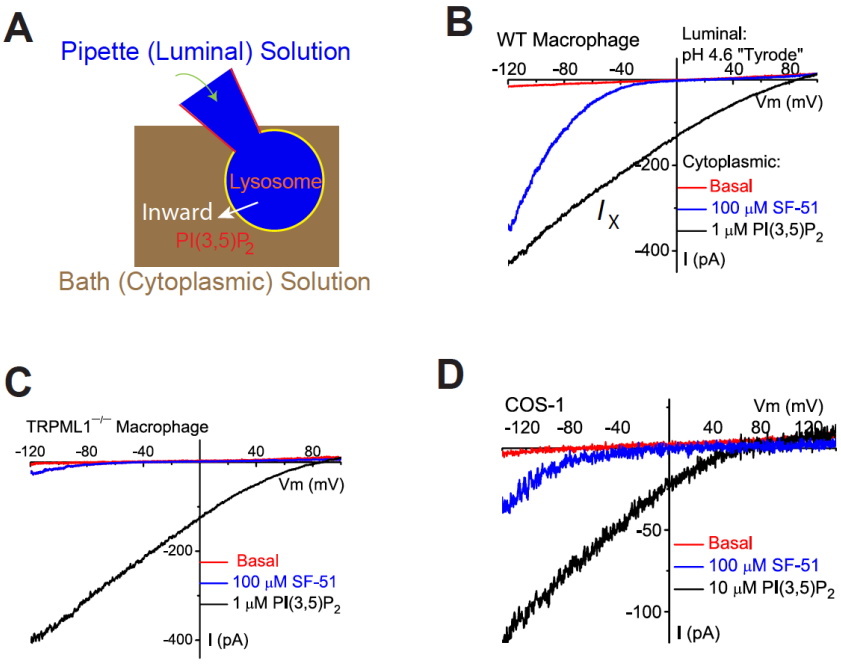

Figure 2.1. $PI(3,5)P_2$ activates endogenous TRPML1-independent inward currents in endolysosomes.

(A). Illustration of the whole-endolysosome recording configuration. Pipette (luminal) solution was a standard external (modified Tyrode's) solution adjusted to pH 4.6 to mimic the acidic environment of the lysosomal lumen. Bath (internal/cytoplasmic) solution was a K^+-based internal solution (140 mM K^+-gluconate). Note that the inward current indicates cations flowing out of the endolysosome (arrow). **(B).** Bath application of $PI(3,5)P_2$ (diC8, 1 μM) to the cytoplasmic side of enlarged endolysosome/vacuoles isolated from vacuolin-treated *WT* primary macrophage cells activated whole-endolysosome currents (296 ± 28pA/pF at -120mV, n = 24 vacuoles/endolysosomes) with positive E_{rev} (79 ± 2.4mV, n = 20). K^+-based cytoplasmic/bath solution contained (in mM) $140K^+/4Na^+/2Mg^{2+}$ (pH 7.2, free Ca^{2+} ~ 100 nM); luminal/pipette solution was a pH 4.6 modified Tyrode solution, which contained (in mM) $145Na^+/5K^+/1Mg^{2+}/2$ Ca^{2+} (pH 4.6); the equilibrium potential of Na^+ (E_{Na}) was estimated to be ~ +90mV. Inwardly rectifying TRPML-like currents ($I_{TRPML\text{-}L}$) with E_{rev} = 3.7 ± 1.7 mV (n = 20) were induced by a TRPML-specific small molecule agonist (SF-51) in the same vacuoles (blue trace). **(C).** $PI(3,5)P_2$ activated a current with a positive E_{rev} in an enlarged endolysosome/vacuole isolated from a $TRPML1^{-/-}$ primary macrophage cell. **(D).** $PI(3,5)P_2$ (10 μM) activated whole-endolysosome current (from 30 to 420 pA measured at -120 mV) with positive E_{rev} in enlarged endolysosome/vacuoles isolated from non-transfected COS-1 cells. Note the small $I_{TRPML\text{-}L}$ (E_{rev} ~ 0mV) activated by SF-51 in the same vacuoles.

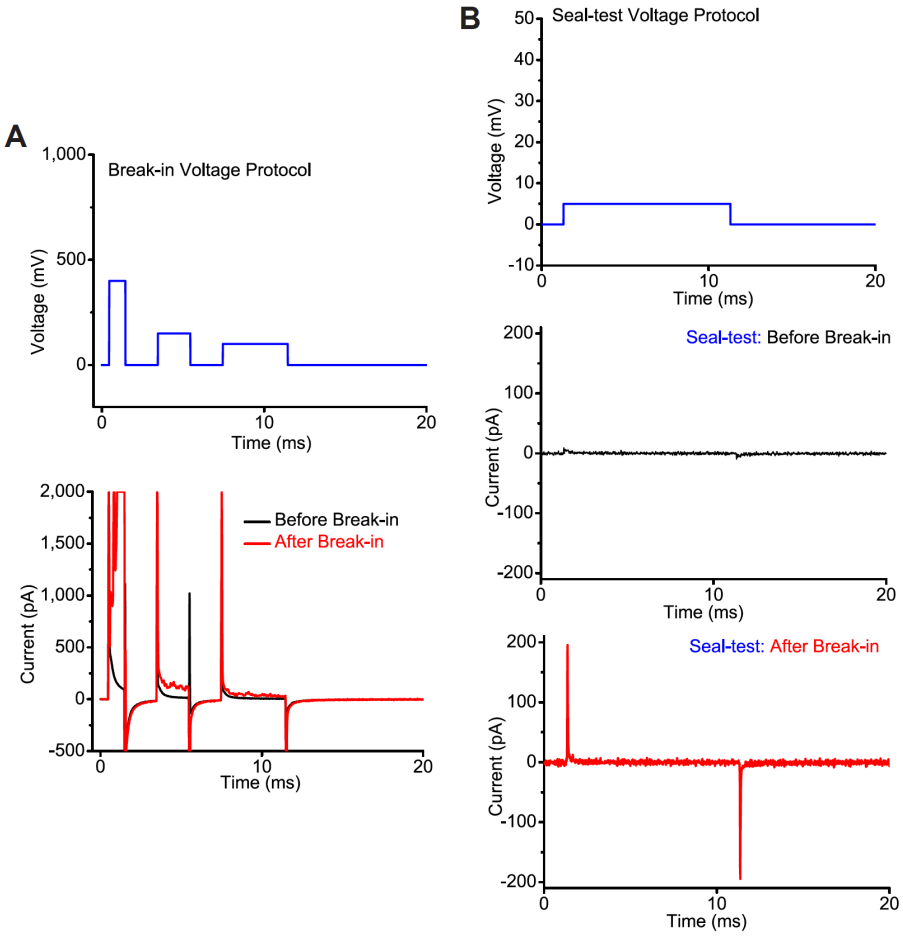

Figure 2.2. Experimental protocols for the whole-endolysosome patch-clamp technique

(A). Membrane test (the lower panel) before (black) and after (red) break-in using a voltage protocol (upper panel).

(B). Membrane test before (middle panel, black) and after (lower panel, red) break-in using a seal-test voltage protocol (upper panel).

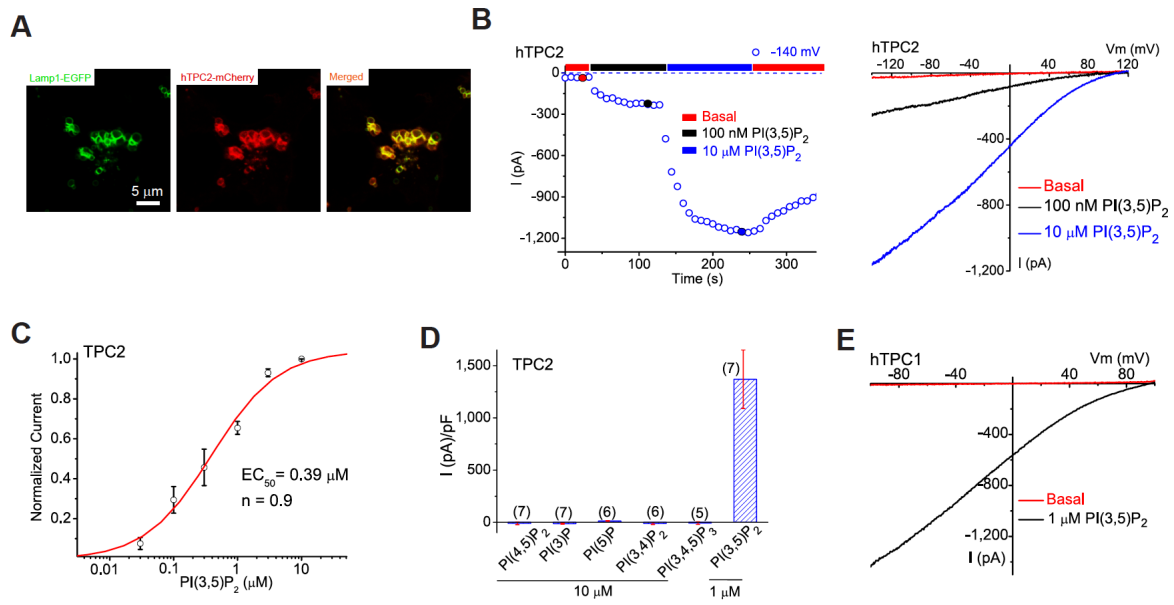

Figure 2.3. PI(3,5)P_2 activates recombinant TPCs in endolysosomes.

(A). TPC2 proteins are localized in Lamp1-positive late endosomes and lysosomes in COS-1 cells that were transfected with TPC2 and Lamp-1 fusion proteins and treated with vacuolin-1. **(B).** PI(3,5)P_2 activated a large whole-endolysosome current with E_{rev} > + 80mV in an EGFP (hTPC2)-positive endolysosome isolated from an *hTPC2-EGFP*-transfected COS-1 cell. Whole-endolysosome currents were elicited by repeated voltage ramps (-140 to +140 mV; 400 ms) with a 4s interval between ramps; current amplitudes measured at -140 mV were used to plot the time course of activation. The right panel shows representative I-V traces of hTPC2-mediated whole-endolysosome currents (I_{hTPC2}) before (red; -20 ± 4pA/pF at -120 mV, n = 9) and after (black and blue) PI(3,5)P_2 bath application at 3 different time points, as indicated in the left panel (red, blue and black circles). Only a portion of the voltage protocol is shown; holding potential (HP) = 0 mV. **(C).** Dose-dependence of PI(3,5)P_2-dependent activation (EC_{50} = 390 ± 94 nM, Hill slope (n) = 0.9, n= 13 vacuoles). **(D).** Specific activation of mTPC2 by PI(3,5)P_2 (in 1 µM), but not other PIPs (all in 10 µM). On average, I_{hTPC2} in the presence of 1 µM PI(3,5)P_2 was 1410 ± 360pA/pF at -120mV (n = 7). **(E).** Activation of I_{hTPC1} by 1 µM PI(3,5)P_2.

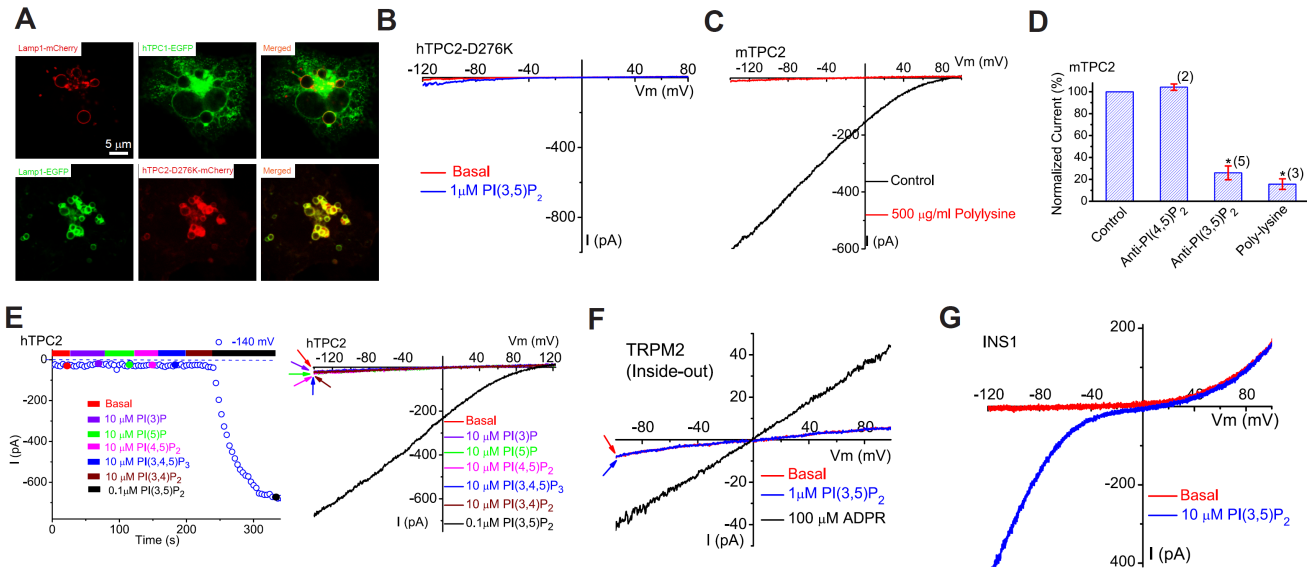

Figure 2.4. PI(3,5)P_2 specifically activates TPCs.

(A). Human TPC1 and TPC2 pore-mutant proteins were localized in endosomes and lysosomes. COS-1 cells were transfected with TPC and Lamp-1 fusion proteins and treated with vacuolin-1. **(B).** A mutation of a negatively-charged amino acid residue in the first putative pore region of TPC2 abolishes I_{hTPC2}. PI(3,5)P_2 (1 μM) activated a small TRPML-like current, but not I_{hTPC2}, in an enlarged endolysosome/vacuole isolated from an *hTPC2-D276K*-transfected COS-1 cell. **(C).** PI(3,5)P_2 –activated I_{mTPC2} was inhibited by bath (cytoplasmic) application of poly-L-lysine (500 μg/ml) to an enlarged endolysosome isolated from an mTPC2-EGFP-expressing COS-1 cell. **(D).** I_{mTPC2} (post PI(3,5)P_2 application) was inhibited by 80- 90% by bath application of poly-L-lysine (500 μg/ml) or anti-PI(3,5)P_2 antibody (5 μg/ml). The inhibition was irreversible (within several minutes), but I_{mTPC2} could be re-activated by PI(3,5)P_2 upon washout of poly-L-lysine or anti-PI(3,5)P_2 antibody. **(E).** Specific activation of hTPC2 by PI(3,5)P_2 (in 0.1 μM), but not other diC8 PIPs (all in 10 μM). The right panel shows representative traces of I_{hTPC2} with different PIPs applied at different time points, as shown in the left panel. **(F).** Bath application of ADPR (100 μM), but not PI(3,5)P_2 (1 μM), activated a current with a linear I-V in an inside-out patch excised from a TRPM2-transfected HEK293T cell. **(G).** PI(3,5)P_2 (10 μM) selectively activated the inward, but not the outward current, in an endolysosome isolated from an INS1 pancreatic β-cell.

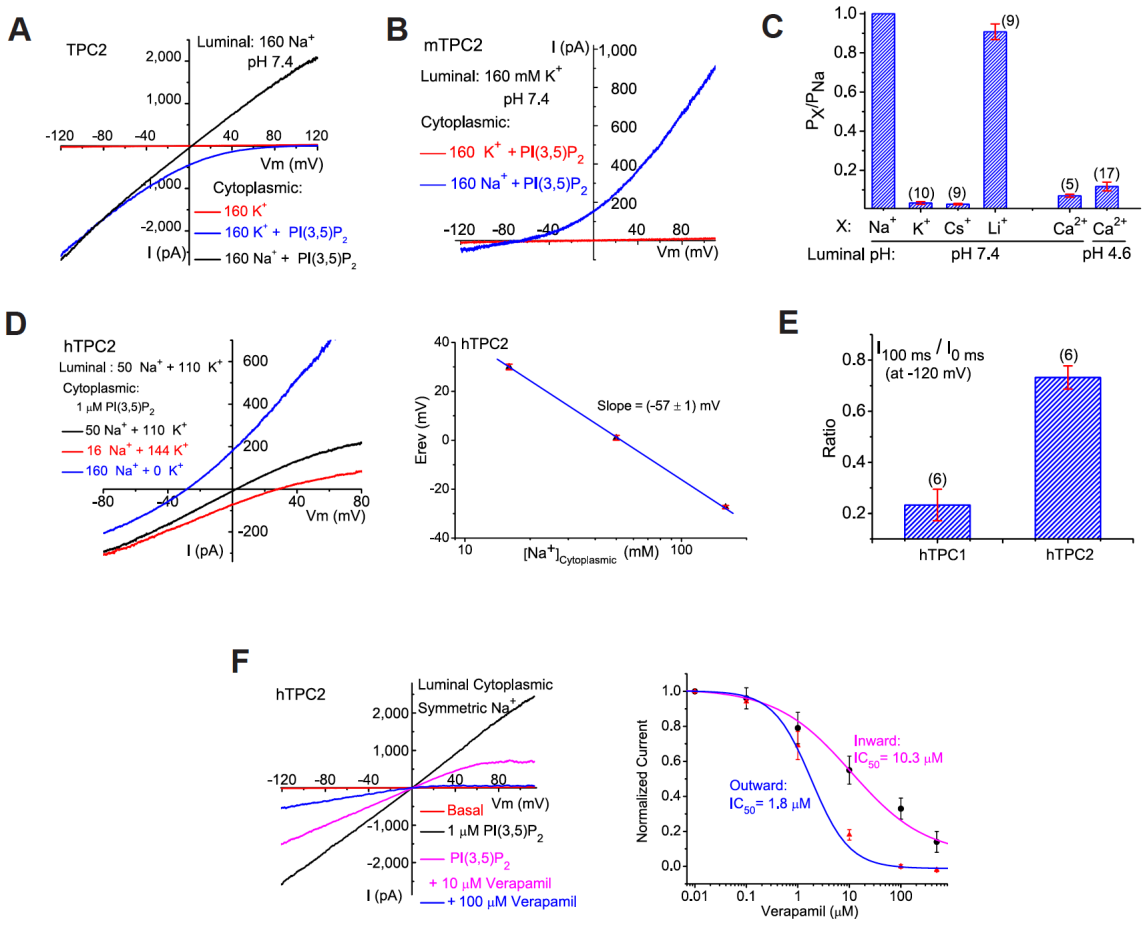

Figure 2.5. PI(3,5)P_2-activated TPC currents are Na^+-selective.

(A). PI(3,5)P_2-activated I_{TPC2} (E_{rev}= + 89 mV ± 5mV, n = 8) under bi-ionic conditions with luminal/pipette Na^+ and cytoplasmic/bath K^+. Large outward I_{hTPC2} was observed in cytoplasmic Na^+. **(B).** $I_{mTPC2,}$ E_{rev} (-68 ± 3mV, n = 5) under bi-ionic conditions with luminal K^+ and cytoplasmic Na^+. **(C).** Relative cationic permeability ratios of I_{hTPC2} based on E_{rev} measurement under bi-ionic conditions. **(D).** Na^+-dependence of I_{hTPC2} E_{rev}. The left panel shows I-V relations of I_{hTPC2} with cytoplasmic solutions containing various concentrations of Na^+ and K^+. **(E).** Distinct inactivation kinetics of I_{hTPC2} and I_{hTPC1} at -120 mV. **(F).** Verapamil inhibited outward and inward I_{hTPC2} with different dose-dependencies under luminal and cytoplasmic symmetric Na^+ (luminal pH 7.4).

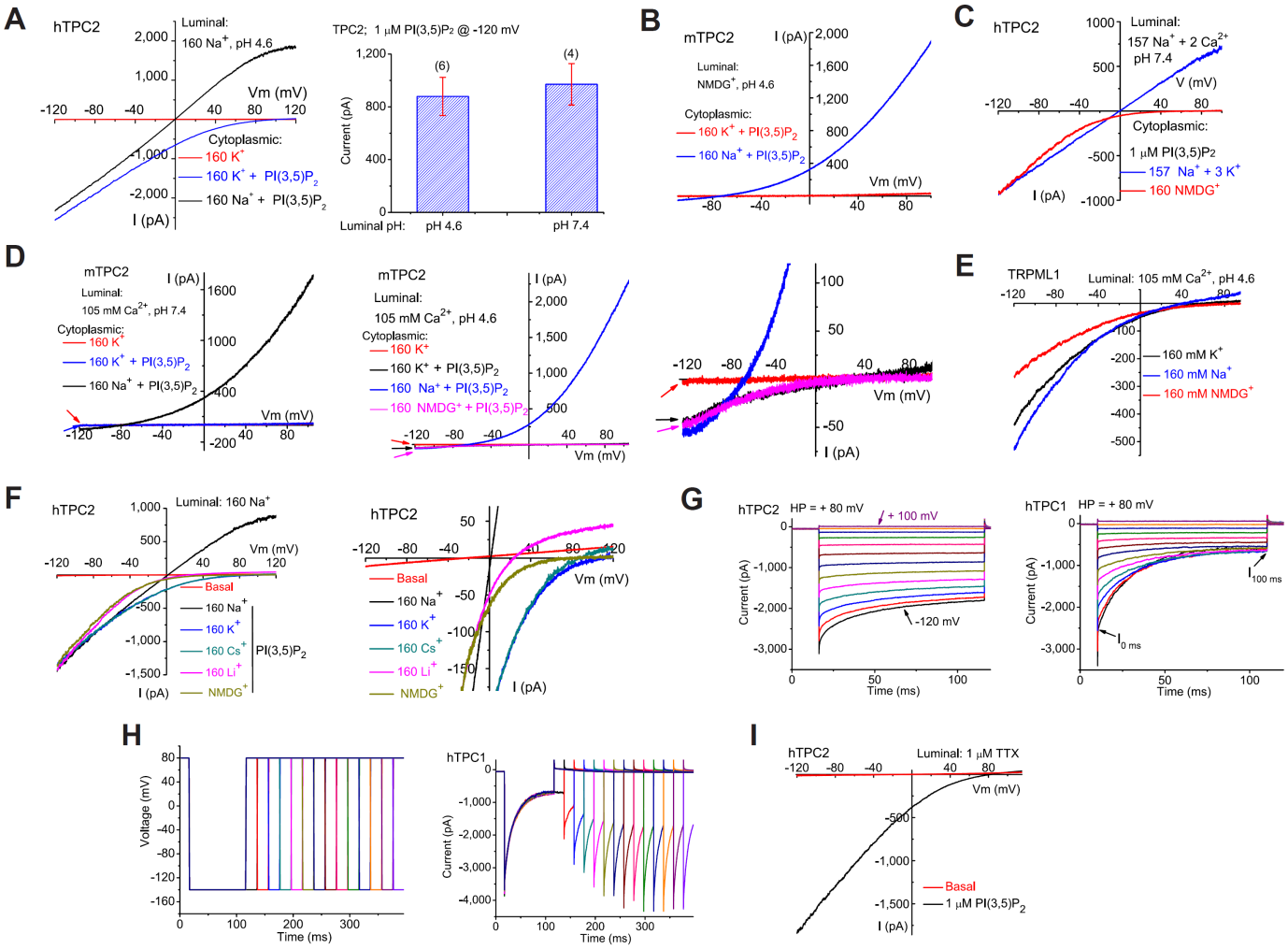

Figure 2.6. Whole-endolysosome I_{hTPC2} is selective for Na^+

(A). I_{TPC2} is selective for Na^+ over K^+ at both acidic and neutral luminal pH. Left panel: large outward I_{hTPC2} was seen with cytoplasmic Na^+, but not K^+, in the presence of luminal Na^+ at low pH (pH 4.6); Right panel: the current amplitudes of $PI(3,5)P_2$-activated I_{TPC2} were similar at neutral and acidic luminal pH. **(B).** I_{mTPC2} is impermeant to $NMDG^+$ or H^+; I_{mTPC2} exhibited no significant inward current in the presence of luminal $NMDG^+$ (150 mM; pH4.6), and cytoplasmic K^+ (160 mM) or Na^+ (160 mM). **(C).** Little or no effect of luminal Ca^{2+} on the inward current and E_{rev} of I_{hTPC2}. **(D).** I_{mTPC2} is selective for Na^+ over Ca^{2+} at acidic and neutral luminal pH. Left panel: in luminal isotonic Ca^{2+} (105 mM; pH 7.4) and cytoplasmic Na^+, E_{rev} for

I_{hTPC2} was < -60mV. Middle and right (an expanded view) panels: low I_{mTPC2} permeability to luminal Ca^{2+} under bi-ionic conditions (luminal isotonic Ca^{2+} versus cytoplasmic Na^{+}), the E_{rev} of I_{TPC2} was -68 ± 2mV (n = 12). **(E).** I_{TRPML1} is highly Ca^{2+}-permeable; I_{TRPML1} with luminal isotonic Ca^{2+} and cytoplasmic Na^{+} or K^{+} exhibited a positive E_{rev} (+ 47 ± 2mV, n = 3**). (F).** I_{hTPC2} is selectively permeable to Na^{+}, and to a lesser degree Li^{+}, but not K^{+} or Cs^{+}; I_{hTPC2} was recorded in the presence of cytoplasmic monovalent cations and luminal Na^{+}. Right panel shows an expanded view of E_{rev} in the presence of different cytoplasmic monovalent cations. **(G).** I_{hTPC2} and I_{hTPC1} elicited by a voltage-step protocol. HP = + 80 mV. **(H).** Time-dependent recovery of I_{TPC1} from inactivation at negative voltages. Removal of voltage-dependent inactivation (at -140 mV) by a short pre-pulse to positive membrane potential (+ 80 mV). Right panel shows the voltage protocol used to study the time-dependent recovery of I_{hTPC1} from inactivation. **(I).** Insensitivity of I_{hTPC2} to TTX (included in the luminal/pipette solution; pH 7.4).

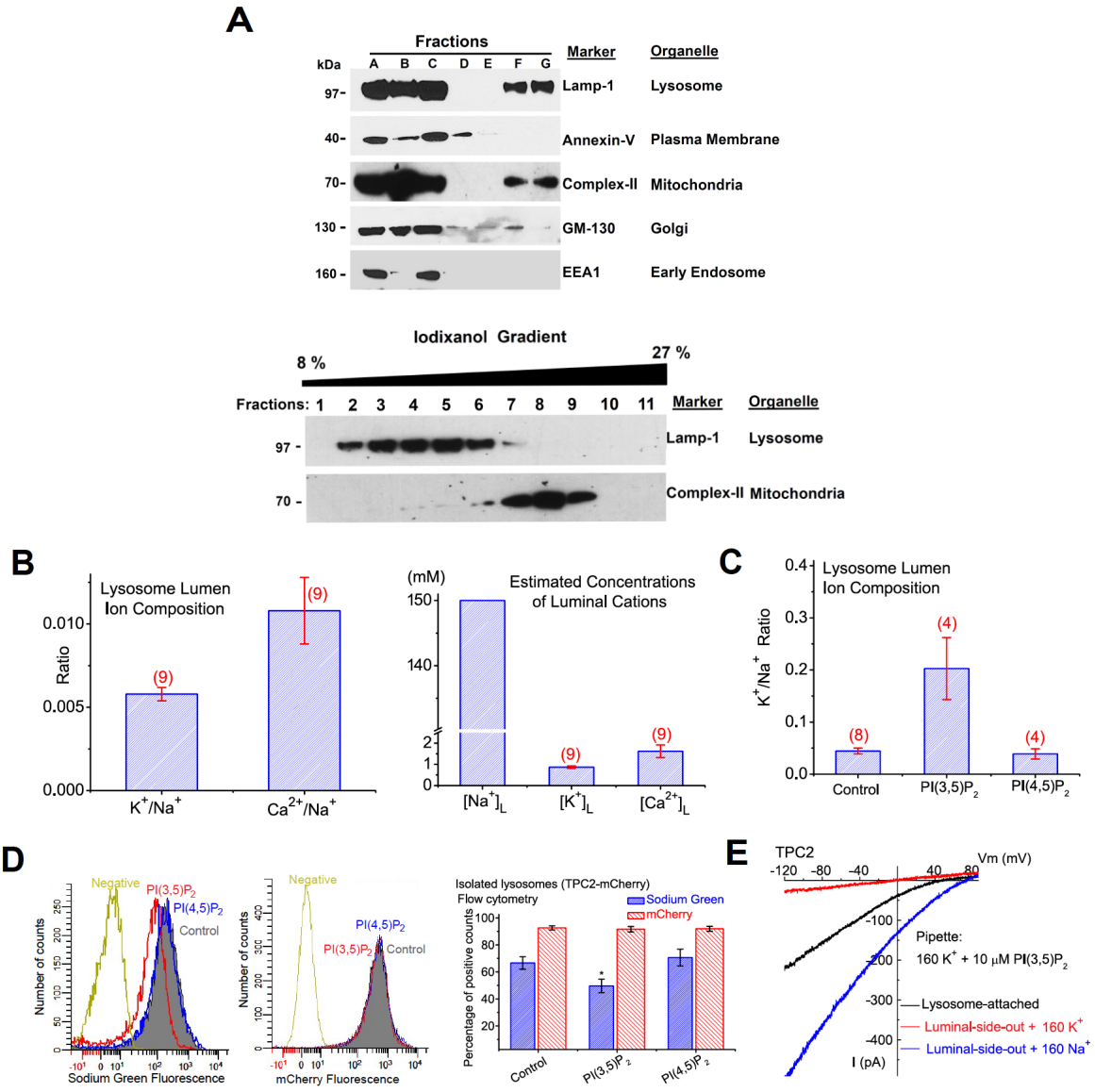
A
Fractions
kDa
A B C D E F G
Marker
Organelle
97-
Lamp-1
Lysosome
40-
Annexin-V
Plasma Membrane
70-
Complex-II
Mitochondria
130 -
GM-130
Golgi
160 -
EEA1
Early Endosome
Iodixanol Gradient
8 %
27 %
Fractions: 1 2 3 4 5 6 7 8 9 10 11
Marker
Organelle
97 -
Lamp-1
Lysosome
70 -
Complex-II
Mitochondria
B
Lysosome Lumen
Ion Composition
Ratio
0.010
0.005
0.000
(9)
(9)
K+/Na+
Ca2+/Na+
(mM)
Estimated Concentrations
of Luminal Cations
150
140
2
1
0
(9)
(9)
[Na+]L
[K+]L
[Ca2+]L
C
Lysosome Lumen
Ion Composition
K+/Na+ Ratio
0.4
0.3
0.2
0.1
0.0
(8)
(4)
(4)
Control
PI(3,5)P2
PI(4,5)P2
D
Negative
PI(3,5)P2
PI(4,5)P2
Control
Number of counts
Sodium Green Fluorescence
Negative
PI(4,5)P2
PI(3,5)P2
Control
Number of counts
mCherry Fluorescence
Isolated lysosomes (TPC2-mCherry)
Flow cytometry
Sodium Green
mCherry
Percentage of positive counts
100
80
60
40
20
*
Control
PI(3,5)P2
PI(4,5)P2
E
TPC2
-120 -80 -40
40 80
Vm (mV)
-100
-200
-300
-400
I (pA)
Pipette:
160 K+ + 10 μM PI(3,5)P2
Lysosome-attached
Luminal-side-out + 160 K+
Luminal-side-out + 160 Na+

Figure 2.7. Na^+ is the major cation in the lysosome.

(A). Western blotting was performed for each fraction (A-G) using various organelle markers: Lamp-1 for the lysosome; annexin-V for the plasma membrane; complex II for the mitochondria; GM-130 for the Golgi; EEA1 for the early endosome. Cellular fractionation protocol is described in **Fig. 2.8**. Centrifugation of cell homogenate (fraction A) of HEK293T cells resulted in a pellet (fraction B) and a supernatant (fraction C). The supernatant was then layered over a discontinued gradient containing a cushion of 2.5 M sucrose and 18% Percoll in the HM buffer. Further centrifugation of the gradient resulted in the light membrane fraction (fraction D), the medium membrane fraction (fraction E), and the heavy membrane fraction (fraction G). Lower panel: fraction G was then layered over a discontinuous iodixonal (8-27%) gradient (fractions 1-11); Western blotting was performed for each fraction using Anti-Lamp-1 and Anti-complex II. **(B).** Ionic composition (Na^+, K^+, and Ca^{2+}) in the lysosomal lumen of HEK293T cells determined by Inductively Coupled Plasma Mass Spectrometry (ICP-MS). Right panel: estimated concentrations of Na^+, K^+, and Ca^{2+} in the lysosome lumen; estimates were based on the assumptions that the lysosome lumen is iso-osmotic relative to the cytosol, and all the cations are osmotically-active. **(C).** Luminal K^+/Na^+ ratios were significantly increased for isolated lysosomes that were treated with $PI(3,5)P_2$ (20 μM), but not $PI(4,5)P_2$ (20 μM). **(D).** Left panel: application of $PI(3,5)P_2$ (red), but not $PI(4,5)P_2$ (blue) to isolated lysosomes decreased Sodium Green, but not mCherry fluorescence. Lysosomes were isolated from TPC2-mCherry-expressing HEK293 cells and loaded with Sodium Green dyes. "Control" and "Negative" indicate fluorescence levels in isolated lysosomes with and without Sodium Green dye loading, respectively. Right panel: decreased Sodium Green fluorescence intensity (reflecting luminal Na^+ concentration) from $PI(3,5)P_2$-treated lysosomes; data are presented as the percentage of lysosomes that were Sodium Green-positive. mCherry fluorescence remained constant upon $PI(3,5)P_2/PI(4,5)P_2$ application. **(E).** I_{TPC2} measured in lysosome-attached configuration. I_{TPC2} was activated in the lysosome-attached configuration with $PI(3,5)P_2$ (10 μM) in the K^+ pipette solution. I_{TPC2} was detected with luminal Na^+, but not K^+ upon excision into the luminal-side-out configuration. Note that the indicated voltages in the lysosome-attached configuration contained a contribution from the lysosomal membrane

potential, for which no accurate measurement is available. The smaller current amplitude seen in the lysosome-attached configuration might be due to luminal [Na^+] lower than 160 mM, relief from luminal inhibition, or both.

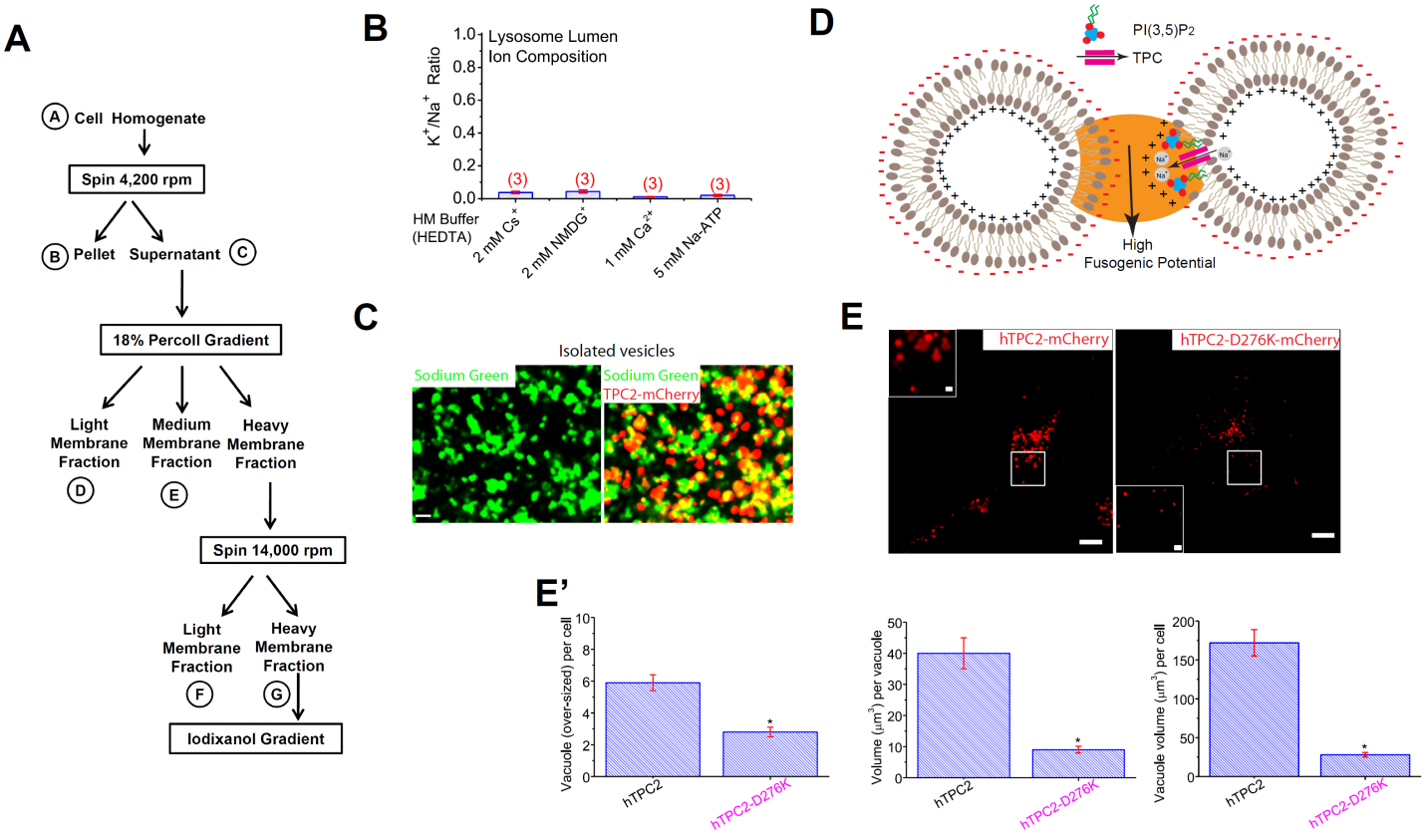

Figure 2.8. Ionic composition in the lysosomes of HEK293T cells isolated by cellular fractionation

(A). Centrifugation of cell homogenate (fraction A) of HEK293T cells resulted in a pellet (fraction B) and a supernatant (fraction C). The supernatant was then layered over a discontinued gradient containing a cushion of 2.5 M sucrose and 18% Percoll in the HM buffer. Further centrifugation of the gradient resulted in the light membrane fraction (fraction D), the medium membrane fraction (fraction E), and the heavy membrane fraction (fraction G). **(B).** Luminal K^+/Na^+ ratios under various homogenizing buffer conditions. **(C).** TPC2-mCherry-positive isolated vesicles/lysosomes were loaded with Sodium Green dye. Scale bar = 2 μm**. (D).** An electrostatic model for the potential role of TPC-mediated Na^+ flux in endolysosomal dynamics. Endolysosomes have a luminal-side positive transmembrane potential at rest (estimated to be +30 to +110 mV; see ref. (Dong et al., 2010b)). Charge repulsion may prevent docking and fusion of alike endolysosomes. Upon PIKfyve recruitment/activation, rapid and localized generation of $PI(3,5)P_2$ triggers TPC-mediated Na^+ efflux and subsequent depolarization of the endolysosomal membrane toward E_{Na}. This rapid and localized reversal of charge may permit the fusion of the $PI(3,5)P_2$-enriched microdomain. **(E).** Vacuole size measurement in COS1 cells transfected with either hTPC2-mCherry or hTPC2-D276K-mCherry constructs. Images were taken using an Olympus Spinning-Disk confocal with 0.2 μm Z-steps. Vacuole size was measured using the 4D viewer and object measurement functions of Metamorph (Olympus) software. Scale bar = 10 μm (2 μm for the inset). **(E').** Over-sized vacuoles (radius > 1 μm) were analyzed for number of vacuoles per cell, volume per vacuole, and total vacuole volume/cell. For each group, cells (n =49) were randomly selected from 3 independent transfections.

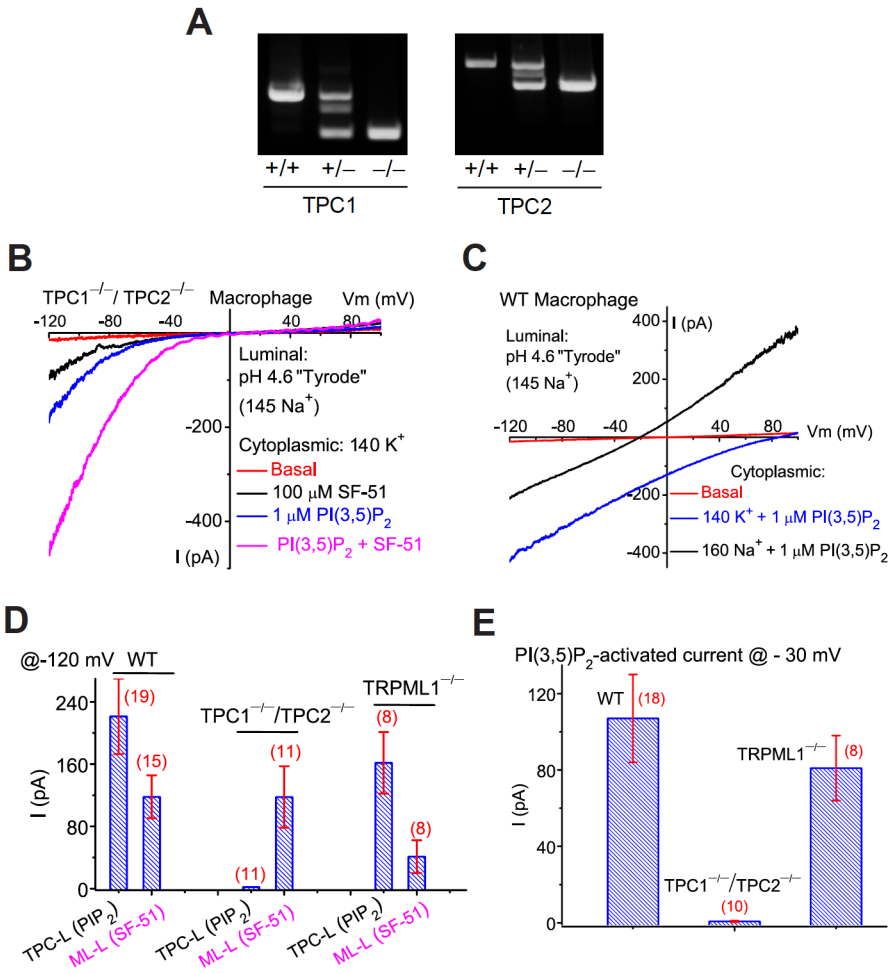

Figure 2.9. Genetic inactivation of TPC1 and TPC2 abolishes TPC currents in the endolysosome.

(A). PCR genotyping of *TPC1 KO (TPC1*$^{-/-}$*)* and *TPC2 KO (TPC2*$^{-/-}$*)* mice. **(B).** Lack of significant PI(3,5)P_2-activated TPC-like current ($I_{TPC\text{-}L}$) in vacuoles isolated from a *TPC1*$^{-/-}$*/ TPC2*$^{-/-}$ mouse macrophage. Instead, in 15/15 vacuoles, PI(3,5)P_2 activated $I_{TRPML\text{-}L}$ that was further potentiated by SF-51. **(C).** An endogenous $I_{TPC\text{-}L}$ activated by PI(3,5)P_2 (1 μM) in a vacuole isolated from a *WT* mouse macrophage cell. Switching the cytoplasmic solution from K^+ to Na^+ resulted in a leftward shift of E_{rev}, and an increase of the current at the outward direction. **(D).** Summary of $I_{TPC\text{-}L}$ and $I_{TRPML\text{-}L}$ in *WT, TPC1*$^{-/-}$*/ TPC2*$^{-/-}$, and *TRPML1*$^{-/-}$ macrophages. **(E).** Summary of PI(3,5)P_2-activated whole-endolysosome inward currents in *WT, TPC1*$^{-/-}$*/ TPC2*$^{-/-}$, and *TRPML1*$^{-/-}$

macrophages at -30mV. I_{PIP2} was 107 ± 23pA/pF (n= 18) and 0.7 ± 0.4pA/pF (n=10) for *WT* and *TPC1*$^{-/-}$/*TPC2*$^{-/-}$ macrophages, respectively.

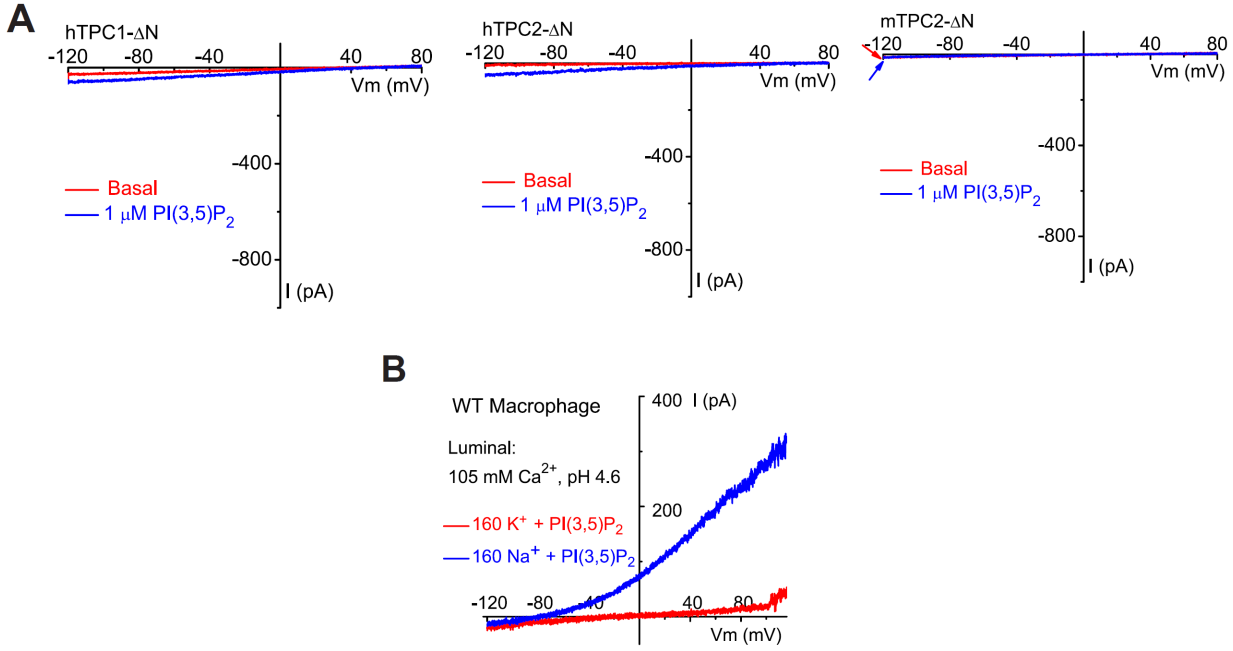

Figure 2.10. N-terminal truncations of TPC1 and TPC2 abolish TPC currents in the endolysosome

(A). N terminal truncations in hTPC1, hTPC2, and mTPC2 abolished I_{TPC}. $PI(3,5)P_2$ (1 μM) activated small currents in enlarged vacuoles isolated from hTPC1-ΔN (the left panel), hTPC2-ΔN (the middle panel), or mTPC2-ΔN (the right panel) -transfected COS-1 cells**. (B).** $PI(3,5)P_2$ –activated whole-endolysosome currents in macrophages are Na^+ selective over Ca^{2+}. E_{rev} was negative for an endogenous whole-endolysosome $PI(3,5)P_2$-activated current of a macrophage in the presence of luminal isotonic Ca^{2+} and cytoplasmic Na^+.

CHAPTER 3

Two-pore channels are not NAADP receptors

Abstract

Nicotinic acid adenine dinucleotide phosphate (NAADP) is the most potent intracellular Ca^{2+} mobilizing messenger. NAADP triggers Ca^{2+} release from lysosome-related acidic stores in many cell types, although the molecular identities for NAADP receptors are still controversial. Two-pore channels (TPCs) have recently been reported to underlie the NAADP-induced Ca^{2+} release, however, a direct demonstration that NAADP activates TPC channels is not established. In chapter 2, we have discovered that TPC proteins form a Na^{+}-selective ion channels activated by $PI(3,5)P_2$. Here using whole-endolysosome patch clamp recordings, we surprisingly find that TPCs are not activated by NAADP. The calcium imaging results also show that NAADP-induced Ca^{2+} signaling is intact in TPCs-knockout cells. Taken together, our results suggest that TPCs are unlikely to be NAADP receptors.

Introduction

Ca^{2+} mobilization from intracellular stores induced by second messengers upon extracellular stimuli represents an important mechanism for Ca^{2+} signaling. Inositol trisphosphate (IP_3) and cyclic ADP-ribose (cADPR) are known to cause Ca^{2+} release from the Sacro/Endoplasmic Reticulum (S/ER) store by activations of IP_3 receptors (IP_3Rs) and ryanodine receptors (RyRs), respectively (Berridge et al., 2000). Nicotinic acid adenine dinucleotide phosphate (NAADP) is another intracellular messenger (Lee and Aarhus, 1995) mobilizing Ca^{2+} from acidic compartments (lysosomes) (Churchill et al., 2002; Morgan et al., 2011). NAADP is shown to induce lysosomal Ca^{2+} release initially, and then trigger further Ca^{2+} release from ER, a process referred to as Ca^{2+}-induced Ca^{2+} release (CICR) (Cancela et al., 1999; Guse and Lee, 2008). NAADP signaling has been linked with a variety of physiological processes, including insulin secretion in pancreatic β cells (Arredouani et al., 2010; Masgrau et al., 2003), digestive enzyme release in pancreatic acinar cells (Yamasaki et al., 2005), cardiac (Macgregor et al., 2007) and smooth muscle contraction (Boittin et al., 2002; Kinnear et al., 2004), neurotransmitter release, and neurite outgrowth (Brailoiu et al., 2006; Brailoiu et al., 2003). However, the molecular mechanism underlying NAADP-induced Ca^{2+} signaling remains unclear.

Two-pore channel (TPC) proteins are newly cloned members of the voltage-gated cation channel superfamily, which include voltage-gated Na^+ and Ca^{2+} (Na_V and Ca_V) channels. Na_V and Ca_V channels are expressed at the plasma membrane of excitable cells, and are very well characterized. In contrast, TPC proteins are localized in intracellular endosomes and lysosomes, and their functions have remained enigmatic. A number of recent studies suggested that TPCs may be the NAADP receptors, mediating lysosomal Ca^{2+} release triggered by NAADP (Brailoiu et al., 2009; Calcraft et al., 2009; Zong et al., 2009), although the direct measurements of TPC channel activities evoked by NAADP are not clear (Brailoiu et al., 2010; Pitt et al., 2010; Schieder et al., 2010). Previously we discovered that TPC proteins form Na^+-selective ion channels in endosomes and lysosomes, activated by an endolysosome-specific phosphoinositide $PI(3,5)P_2$. Here by direct patch-clamping of the endolysosomal membrane, we surprisingly find that NAADP can not activate TPC channels in either heterologous expression or endogenous systems, neither does NAADP modulate $PI(3,5)P_2$-activated TPC currents. In pancreatic β cell lines, NAADP-induced Ca^{2+} signaling is present, but endogenous TPC currents are absent. Finally, we show that the NAADP-evoked Ca^{2+} response is largely intact in TPCs-knockout islets. Since TPCs are NAADP-insensitive Na^+-selective channels, and loss of TPCs has little

effects on NAADP-Ca^{2+} signaling, TPCs are unlikely to be the NAADP receptors.

Results

TPCs are not activated by NAADP.

Since TPC1 and TPC2 were reportedly activated by NAADP in endolysosomes (Calcraft et al., 2009; Morgan et al., 2011; Ruas et al., 2010; Zong et al., 2009), we measured endolysosomal currents after direct application of NAADP. Surprisingly, in TPC2-positive enlarged vacuoles, no significant current activation was seen with varying concentrations of NAADP (**Fig. 3.1A; Fig. 3.2A**). In contrast, $PI(3,5)P_2$ (10 μM) reliably (> 90%) and robustly activated I_{TPC2} in the same vacuoles. NAADP (1-10μM) also failed to modulate or desensitize I_{TPC2} that was activated by a low concentration of $PI(3,5)P_2$ (100 nM; **Fig. 3.1B**). Similar results were seen with two NAADP analogs (4-methyl NAADP and 5-methyl NAADP) that induce Ca^{2+} release from sea urchin egg homogenates (Jain et al., 2010). I_{TPC1} was also insensitive to NAADP (**Fig. 3.2A**). To exclude the possibility that NAADP responsiveness was impaired in vacuolin-enlarged endolysosomes, we also tested NAADP on surface-expressed mutant hTPC2 channels (i.e. hTPC2-$L^{11}L^{12}$/AA; see ref. (Brailoiu et al., 2010)). However, plasma membrane I_{TPC2}, which exhibited no notable difference in channel properties to lysosomal I_{TPC2}, was also insensitive to NAADP in inside-out patches and in the whole-cell configuration (**Fig. 3.1C, D**). In contrast, NAADP (100 μM) activated the NAADP-sensitive plasma membrane I_{TRPM2} (see ref. (Toth and Csanady, 2010)) (**Fig. 3.2B, C**), demonstrating that NAADP was active.

Pancreatic β-cells exhibit robust NAADP-mediated Ca^{2+} responses and have been commonly used as a cellular model to study endogenous NAADP signaling (Morgan et al., 2011). In INS1 pancreatic β-cell lines, intracellular perfusion with 100 nM NAADP in the whole-cell current-clamp configuration induced membrane depolarization and spike generation (**Fig. 3.3A**). It has been reported that Ned-19, a membrane-permeable inhibitor of the NAADP receptor, completely inhibits NAADP- or glucose-induced Ca^{2+} responses at high μM concentrations (Naylor et al., 2009b). However, Ned-19 had only a weak inhibitory effect on I_{hTPC2}, even at very high concentrations (1 mM; **Fig. 3.2D**). Together with the fact that TPCs have limited Ca^{2+} permeability, these results suggest that TPCs do not contribute directly to NAADP-induced endolysosomal Ca^{2+} release.

TPC currents are absent in pancreatic β-cell lines that exhibit NAADP-induced lysosomal Ca^{2+} release.

Consistent with the results obtained from the pipette dialysis experiments (**Fig. 3.3A**), cell-permeant NAADP-AM (1-100 μM) (Parkesh et al., 2007) induced Ca^{2+} transients in INS1 (**Fig.3.3B, C**; **Fig. 3.4A, B**) and MIN6 (**Fig. 3.4D**) pancreatic β-cell lines, in the absence or presence of external Ca^{2+}. NAADP-AM-induced Ca^{2+} responses in INS-1 cells were abolished by the NAADP receptor blocker, Ned-19 (**Fig. 3.3B, C** & **Fig. 3.4A**), or by pretreatment with Bafilomycin A1, which inhibits the V-ATPase to deplete acidic Ca^{2+} stores (Morgan et al., 2011) (**Fig. 3.3C**; **Fig. 3.4C**). These results suggest that, consistent with previous studies, NAADP induces Ca^{2+} release from lysosomal stores. Surprisingly, no measurable NAADP-activated whole-endolysosomal current was seen in INS1 (**Fig. 3.3D; Fig. 3.4E**) or MIN6 (**Fig. 3.4F**) cells. Furthermore, $PI(3,5)P_2$ (10 μM) activated $I_{TRPML\text{-}L}$ in 14/14 vacuoles, but I_X or $I_{TPC\text{-}L}$ were not detected (**Fig. 3.3D & Fig. 3.4E, F**). Collectively, NAADP-mediated responses appeared to be distinct from $I_{TPC\text{-}L}$ in pancreatic β-cell lines, suggesting that TPCs do not contribute to the NAADP-mediated response.

TPC1 and TPC2 are not required for NAADP- or glucose- induced Ca^{2+} responses in pancreatic islets.

Glucose induces robust Ca^{2+} responses in pancreatic β-cells mediated via NAADP and its receptor localized in the endolysosome (Morgan et al., 2011). However, in WT primary pancreatic β-cells, we did not observe significant whole-endolysosome $I_{TPC\text{-}L}$ (**Fig. 3.5A**). Glucose (5, 8, and 15 mM) induced significant increases of intracellular [Ca^{2+}] (measured with Fura-2 Ca^{2+}-sensitive dyes) in pancreatic islets (**Fig. 3.5B,C**), which was dramatically inhibited by Ned-19 (100 μM; **Fig. 3.5D**), but the glucose-induced Ca^{2+} response was still largely intact in *TPC1*$^{-/-}$*/TPC2*$^{-/-}$ islets (**Fig. 3.5B-D**). Finally, the NAADP-AM-induced Ca^{2+} response was not significantly reduced in *TPC1*$^{-/-}$*/TPC2*$^{-/-}$ pancreatic islets (**Fig. 3.5E**). These results demonstrate that TPCs are not essential for NAADP- and glucose-induced Ca^{2+} responses in pancreatic β-cells.

Discussion

TPCs have been reported to serve as the receptors (Brailoiu et al., 2009; Calcraft et al., 2009; Ruas et al., 2010; Zong et al., 2009) or co-receptors (Lin-Moshier et al., 2012) for NAADP.

NAADP-activated TPC currents have been shown to be K^+-permeable (Pitt et al., 2010), Cs^+-permeable (Brailoiu et al., 2010), or Ca^{2+}-selective (Schieder et al., 2010). Those studies contrast drastically with our direct measurements of TPCs as NAADP-insensitive $PI(3,5)P_2$-activated Na^+ selective channels using whole-endolysosome patch-clamp recordings. Because NAADP-induced Ca^{2+} responses are robust in cells that lack $I_{TPC\text{-}L}$ and are largely intact in *TPC1*$^{-/-}$/*TPC2*$^{-/-}$ cells, and because our direct measurements of TPCs show that they are insensitive to NAADP, it should be clear that TPCs are not the NAADP receptor. Supporting this argument, recent studies using photoaffinity labeled NAADP suggested that TPCs are unlikely to be the genuine NAADP binding sites (Lin-Moshier et al., 2012) (More discussion in Chapter 6, 6.2 and 6.3)

Experimental procedures

Molecular biology and biochemistry.

The TPC constructs were generated as stated in Chapter 2. HEK293T cells were transfected using Lipofectamine 2000 (Invitrogen). Confocal images were taken using a Leica (TCS SP5) microscope and an Olympus Spinning-disk confocal system.

Targeted deletion of *TPC1* and *TPC2* in mice

TPC1 and *TPC2* double knockout mice were generated as described in Chapter 2.

Endolysosomal electrophysiology.

Endolysosomal electrophysiology was performed as described in Chapter 2.

Pancreatic β-cell lines and mouse islets.

Mouse pancreatic islets were isolated from the pancreas (Li et al., 2009) and cultured in RPMI-1640 medium (10 mM glucose) for 3d before Ca^{2+} imaging experiments (Zhang et al., 2003). INS1 cells were cultured in RPMI-1640 medium (11 mM glucose) supplemented with 10% FBS and 50 μM β-mercaptoethanol (Colombo et al., 2008). MIN6 cells were cultured in Dulbecco's modified Eagle's medium (25 mM glucose) supplemented with 10% FBS and 140 μM β-mercaptoethanol (Yamasaki et al., 2004). 1-4h before Ca^{2+} imaging and electrophysiology experiments, cells were placed in a low-glucose (5.5 mM) Dulbecco's modified Eagle's medium.

Pancreatic β-cell electrophysiology.

Current-clamp recordings were performed in INS1 pancreatic β-cells in the whole-cell configuration. The bath solution was a standard extracellular solution (Tyrode's; mM) 145 NaCl, 5 KCl, 2 $CaCl_2$, 1 $MgCl_2$, 10 HEPES, 10 glucose (pH adjusted to pH 7.4 with NaOH). Pipette solution contained (in mM):140 KCl, 2 $MgCl_2$, 2 Na_2-ATP, 0.05 EGTA, 10 HEPES (pH adjusted with KOH to 7.2). NAADP was dissolved in the pipette solution and applied through patch electrodes.

Ca^{2+} imaging

INS1, MIN6, and primary pancreatic β-cells were loaded with 5 μM Fura-2-AM in culture medium at 37^{o}C for 60 min. Cells were then washed in a low-glucose modified Tyrode's solution (in mM; 140 NaCl, 4.75 KCl, 5 $NaHCO_3$, 2.54 $CaCl_2$, 1.2 $MgSO_4$, 1.18 KH_2PO4, 2.8 glucose, and 20 HEPES) for 10–30 min. 'Zero' Ca^{2+} low-glucose solution contained 1 mM EGTA with no added (nominal) $CaCl_2$. Ca^{2+} imaging of pancreatic islets was performed using the perfusion medium containing (in mM): NaCl 120, KCl 4.8, $CaCl_2$ 2.5, $MgCl_2$ 1.2, $NaHCO_3$ 24, BSA 1mg/ml, gassed with O_2/CO_2 (95:5). Fluorescence at different excitation wavelengths was recorded using an EasyRatioPro system (PTI). Fura-2 ratios (F_{340}/F_{380} ; the ratio of fluorescence intensity following excitation at 340 and 380 nm) recorded changes in intracellular [Ca^{2+}] upon stimulation. GPN (Glycyl-L-phenylalanine 2-naphthylamide; 200 μM, a lysosome-disrupting agent) and Bafilomycin A1 (500 nM, a V-ATPase inhibitor) were used as positive controls to induce Ca^{2+} release from lysosome stores and acidic stores, respectively (Calcraft et al., 2009). Ionomycin (1 μM) was added at the conclusion of all experiments to induce a maximal response for comparison. NAADP-AM was synthesized according to ref (Parkesh et al., 2007).

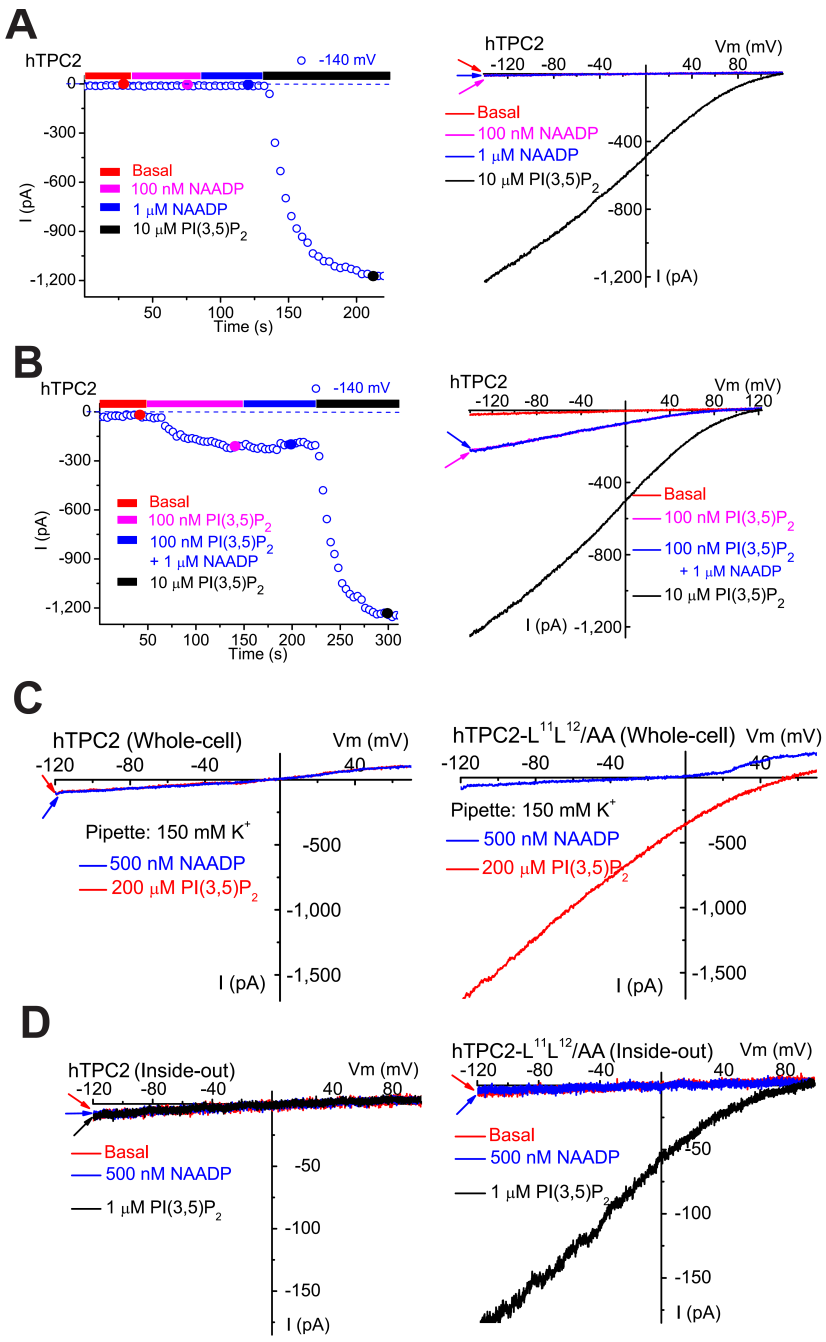
A
hTPC2
-140 mV
Basal
100 nM NAADP
1 μM NAADP
10 μM PI(3,5)P2
I (pA)
Time (s)
hTPC2
Vm (mV)
Basal
100 nM NAADP
1 μM NAADP
10 μM PI(3,5)P2
I (pA)
B
hTPC2
-140 mV
Basal
100 nM PI(3,5)P2
100 nM PI(3,5)P2
+ 1 μM NAADP
10 μM PI(3,5)P2
I (pA)
Time (s)
hTPC2
Vm (mV)
Basal
100 nM PI(3,5)P2
100 nM PI(3,5)P2
+ 1 μM NAADP
10 μM PI(3,5)P2
I (pA)
C
hTPC2 (Whole-cell)
Vm (mV)
Pipette: 150 mM K+
500 nM NAADP
200 μM PI(3,5)P2
I (pA)
hTPC2-L11L12/AA (Whole-cell)
Vm (mV)
Pipette: 150 mM K+
500 nM NAADP
200 μM PI(3,5)P2
I (pA)
D
hTPC2 (Inside-out)
Vm (mV)
Basal
500 nM NAADP
1 μM PI(3,5)P2
I (pA)
hTPC2-L11L12/AA (Inside-out)
Vm (mV)
Basal
500 nM NAADP
1 μM PI(3,5)P2
I (pA)

Figure 3.1. NAADP does not activate TPCs.

(A). NAADP (100 nM or 1 μM) failed to activate whole-endolysosome I_{hTPC2}. In contrast, $PI(3,5)P_2$ robustly activated I_{hTPC2} in the same vacuole. The right panel shows representative I-V traces of whole-endolysosome currents at 4 different time points (indicated by color-coded circles) shown in the left panel. **(B).** NAADP (1 μM) failed to modulate $PI(3,5)P_2$–activated I_{hTPC2}. **(C).** Pipette dialysis of $PI(3,5)P_2$ (200 μM) or NAADP (500 nM) failed to elicit whole-cell current in HEK293T cells transfected with WT hTPC2. In contrast, pipette dialysis of $PI(3,5)P_2$ (200 μM), but not NAADP (500 nM) activated whole-cell I_{TPC2} in HEK293T cells transfected with mutant (hTPC2-$L^{11}L^{12}$/AA). **(D).** $PI(3,5)P_2$, but not NAADP, activated $I_{TPC2\text{-}LL\text{-}AA}$ in inside-out macro-patches isolated from hTPC2-$L^{11}L^{12}$/AA -transfected HEK293T cells.

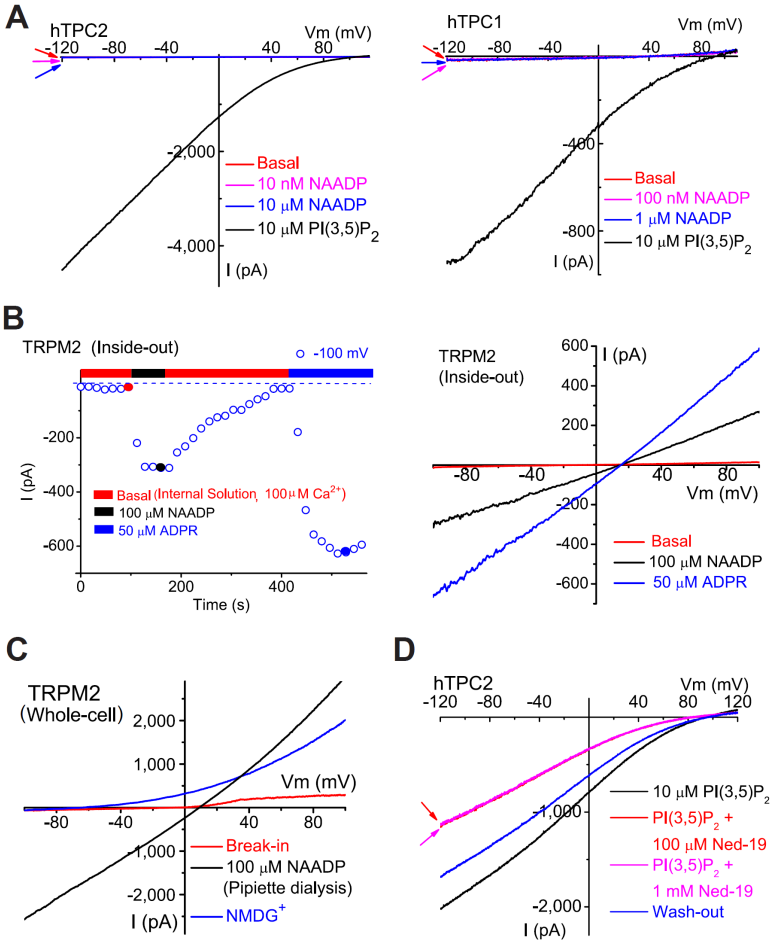

Figure 3.2. NAADP activates TRPM2, but not TPC1 or TPC2.

(A). NAADP (10 nM or 10 μM) failed to activate whole-endolysosome I_{hTPC2}. In contrast, $PI(3,5)P_2$ robustly activated I_{hTPC2} in the same vacuole. Likewise, NAADP (100 nM or 1 μM) failed to activate whole-endolysosome I_{hTPC1}. In contrast, $PI(3,5)P_2$ robustly activated I_{hTPC1} in the same vacuole. **(B).** NAADP (100 μM) or ADPR (50 μM) activated a current with a linear I-V in an inside-out patch excised from a TRPM2-transfected HEK293T cell. **(C).** Activation of whole-cell I_{TRPM2} by pipette dialysis of NAADP. Inclusion of NAADP (100 μM) into the pipette solution under the whole-cell configuration induced I_{TRPM2} in a TRPM2-transfected HEK293T cell. **(D).** I_{hTPC2} was relatively insensitive to Ned-19, a blocker of the endogenous NAADP receptor; $PI(3,5)P_2$-activated I_{hTPC2} was weakly inhibited by Ned-19 (100 μM or 1mM).

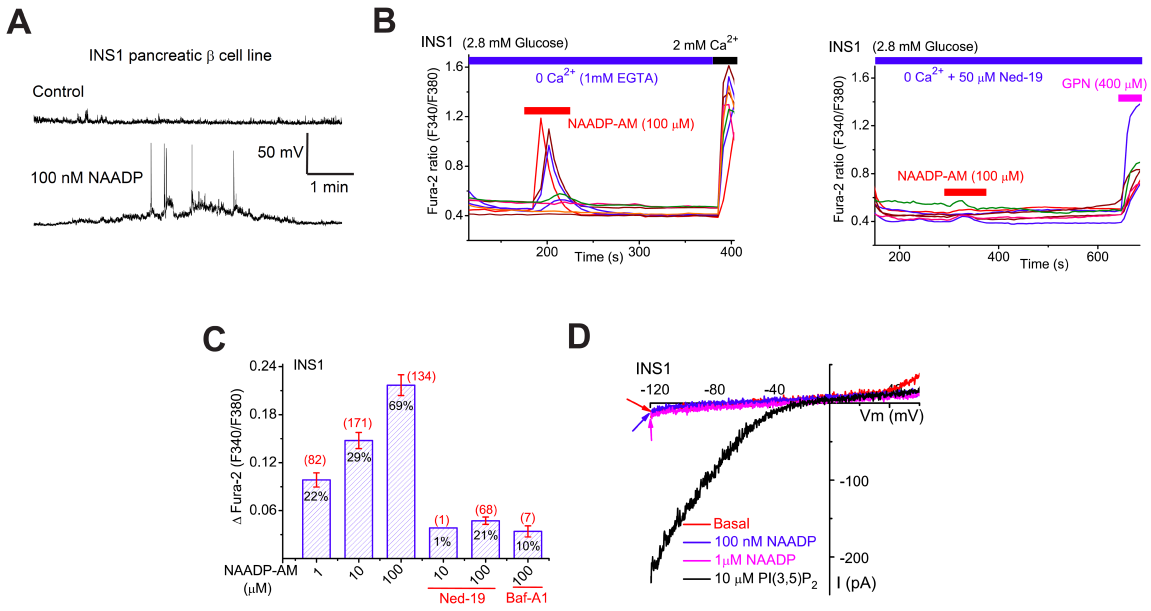

Figure 3.3. NAADP induces lysosomal Ca^{2+} release in pancreatic β-cell line that lack TPC currents.

(A). Pipette dialysis of NAADP (100 nM) induced membrane depolarization and spike generation in an INS1 pancreatic b-cell line under the whole-cell current-clamp configuration. **(B).** In the absence of external Ca^{2+} (free [Ca^{2+}] < 10 nM), NAADP-AM (100 μM) induced Ca^{2+} release measured with Fura-2 (F_{340}/F_{380}) ratios from intracellular stores in INS1 cells; Ned-19 (50 μM) abolished the majority of the NAADP-induced response. **(C).** Average peak Ca^{2+} responses induced by NAADP-AM (1, 10, 100 μM) with and without Ned-19 and Baf-A1 (500 nM). Percentage (% from a total of 100-400 cells) of responding (**D**Fura-2> 0.02) cells; the number of the responding cells are indicated.

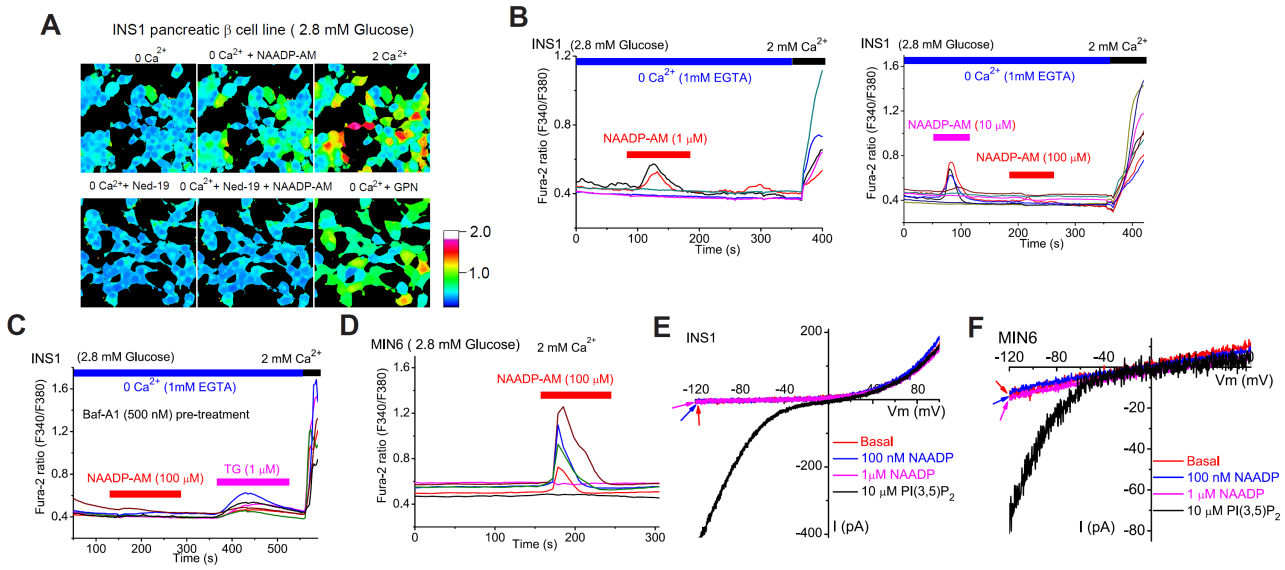

Figure 3.4. Pancreatic β-cell lines exhibit NAADP-induced lysosomal Ca^{2+} release but lack TPC currents.

(A). In the absence of external Ca^{2+} (free [Ca^{2+}] < 10 nM), NAADP-AM (100 μM) induced Ca^{2+} release measured with Fura-2 (F_{340}/F_{380}) ratios from intracellular stores in INS1 cells. Ned-19 (50 μM) abolished the majority of the response. **(B)**. NAADP-AM (1 μM) induced small Ca^{2+} transients in a subset of INS1 cells in the absence of external Ca^{2+} ('0' Ca^{2+}); NAADP-AM (10 μM) induced and desensitized Ca^{2+} release in INS1 cells. After NAADP-AM (10 μM) induced small Ca^{2+} transients in a subset of INS1 cells in the absence of external Ca^{2+} ('0' Ca^{2+}), a higher concentration of NAADP-AM (100 μM) failed to further induce Ca^{2+} responses in the same cells. **(C)**. Bafilomycin A1 pretreatment abolished NAADP-induced Ca^{2+} release in INS1 cells; thapsigargin (TG; 1 μM) induced Ca^{2+} responses in the same cells. **(D)**. NAADP-AM (100 μM) induced small Ca^{2+} transients in MIN6 pancreatic β-cell. **(E)**. NAADP (100 nM or 10 μM) failed to elicit whole-endolysosome current in INS1 cells. In contrast, $PI(3,5)P_2$ activated TRPML-like currents in the same vacuole. Note that the outward current present in this vacuole was insensitive to $PI(3,5)P_2$. **(F)**. $PI(3,5)P_2$ activated predominantly TRPML-like inward currents in MIN6 cells. NAADP (100 nM or 1 μM) failed to elicit any measureable whole-endolysosome.

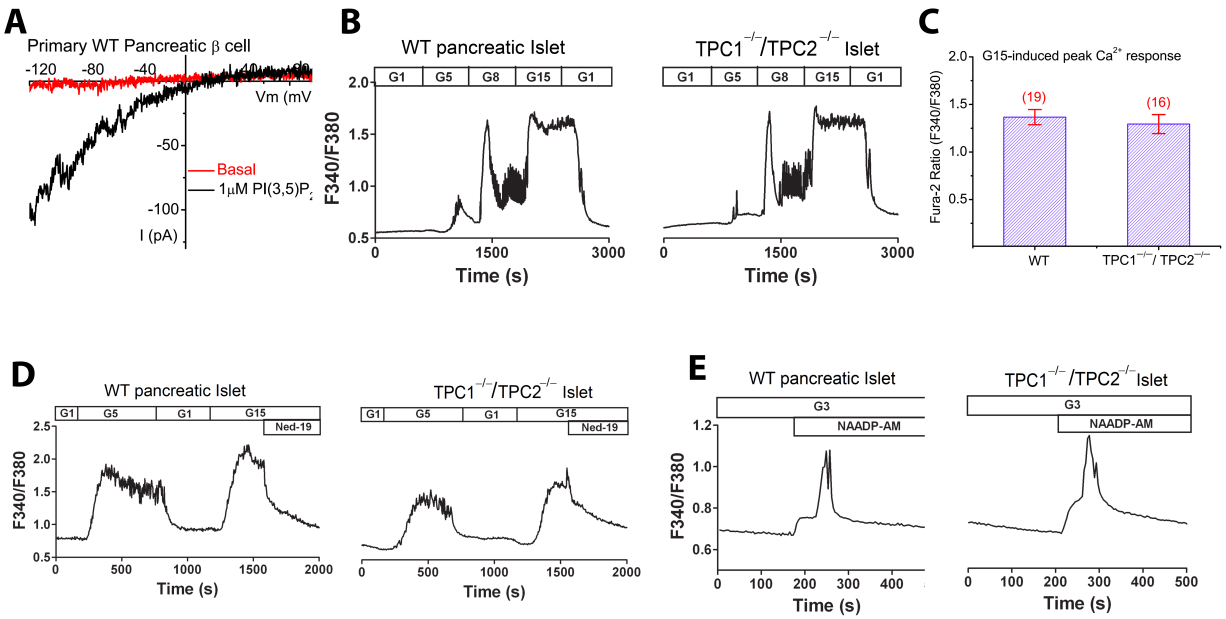

Figure 3.5. TPCs are not required for NAADP-Ca^{2+} responses

(A). $PI(3,5)P_2$ activated $I_{TRPML-L}$ in a vacuole from a *WT* primary pancreatic b-cell. **(B).** *TPC1*$^{-/-}$/ *TPC2*$^{-/-}$ primary pancreatic islets exhibit normal concentration-dependent glucose-induced Ca^{2+} responses. Cytosolic [Ca^{2+}] increased significantly in both *WT* and *TPC1*$^{-/-}$/ *TPC2*$^{-/-}$ pancreatic islets in response to elevations of the glucose concentration (in mM; 1, 5, 8, 15; G1, G5, G8, and G15) in the perfusion solution (2.5 mM Ca^{2+}). The traces shown are representatives from 19 *WT* and 16 *TPC1*$^{-/-}$/ *TPC2*$^{-/-}$ islets, respectively. **(C).** shows the average peak of Ca^{2+} responses induced by 15 mM glucose (G15) in *WT* and *TPC1*$^{-/-}$/ *TPC2*$^{-/-}$ pancreatic islets. **(D).** Glucose-induced Ca^{2+} responses in *WT* and *TPC1*$^{-/-}$/ *TPC2*$^{-/-}$ pancreatic islets were inhibited by Ned-19 (100 μM). The traces shown are representative of the results obtained in 7 *WT* and 7 *TPC1*$^{-/-}$/ *TPC2*$^{-/-}$ islets, respectively. **(E).** NAADP-AM (200 μM) induced bi-phasic Ca^{2+} increases in the presence of 3 mM glucose (Yamasaki et al., 2004) in both *WT* and *TPC1*$^{-/-}$/ *TPC2*$^{-/-}$ islets. Traces shown are representatives of the results obtained in 2 *WT* and 3 *TPC1*$^{-/-}$/ *TPC2*$^{-/-}$ islets, respectively.

CHAPTER 4

$PI(3,5)P_2$ controls membrane trafficking by direct activation of mucolipin Ca^{2+} release channels in the endolysosome

Abstract

Ca^{2+} is a key regulator of synaptic vesicle fusion during neurotransmission. Similarly, Ca^{2+} is thought to regulate other, more general membrane trafficking pathways. However, in these cases, the source of Ca^{2+} is unknown. For these general pathways, it has been postulated that Ca^{2+} is released through unidentified Ca^{2+} channels from the lumen of vesicles and organelles. Mucolipin transient receptor potential channels (TRPMLs) are a family of Ca^{2+}-permeable cation channels in endolysosomes. Mutations in the human *TRPML1* gene cause Mucolipidosis type IV (ML4) neurodegenerative disease. Cells lacking TRPML1 exhibit defects in membrane traffic in the late endocytic pathway. Intracellular traffic also requires phosphoinositides, but their mode of action is poorly understood. $PI(3,5)P_2$ is an endolysosome-specific phosphoinositide; human mutations in $PI(3,5)P_2$-metabolizing enzymes cause a variety of neurodegenerative diseases. Here we show by direct patch-clamping of the endolysosomal membrane, that $PI(3,5)P_2$ binds and activates TRPMLs with specificity and potency. Furthermore the enlarged vacuole phenotype observed in $PI(3,5)P_2$-deficient mouse fibroblasts , is suppressed by overexpression of TRPML1. We propose that TRPMLs regulate membrane trafficking by transducing information about $PI(3,5)P_2$ levels into changes in juxtaorganellar Ca^{2+}, thereby triggering membrane fusion/ fission events.

Introduction

Membrane fusion and fission in intracellular trafficking is controlled by both intraluminal Ca^{2+} release (Hay, 2007; Luzio et al., 2007a) and phosphoinositide (PIP) signaling (Di Paolo and De Camilli, 2006). Cells that lack TRPML1 exhibit enlarged endolysosomes and trafficking defects in the late endocytic pathway (reviewed in Refs. (Cheng et al., 2010; Puertollano and Kiselyov, 2009)). Notably, these phenotypes are similar to those observed in $PI(3,5)P_2$-deficient cells (reviewed in Ref. (Poccia and Larijani, 2009)). Therefore, we hypothesized that TRPML1 may act as an endolysosomal Ca^{2+}-release channel that is regulated by $PI(3,5)P_2$.

Results

Activation of endolysosomal TRPML channels by $PI(3,5)P_2$

TRPML1 is primarily localized on membranes of late endosomes and lysosomes (LELs) (Cheng et al., 2010; Pryor et al., 2006; Puertollano and Kiselyov, 2009), which are inaccessible to conventional electrophysiological approaches. Using our recently established modified patch-clamp method (Dong et al., 2008; Dong et al., 2009), we performed recordings directly on native LEL membranes. Cos-1 cells were transfected with either EGFP-TRPML1 alone, or co-transfected with mCherry-TRPML1 and EGFP-Lamp1 (a marker for LEL). Whole-endolysosome recordings were performed on enlarged vacuoles manually isolated from cells pre-treated with vacuolin-1 (Dong et al., 2008), which caused an increase in the diameter of the vacuoles from < 0.5 μm to up to 5 μm (mean capacitance = 0.68 ± 0.05 pF, N = 44 vacuoles) (**Fig. 4.1A**). The majority (> 85%) of mCherry-TRPML1-positive vacuoles were also EGFP-Lamp1-positive, confirming that the TRPML1-positive vacuoles were enlarged LELs (Dong et al., 2008). In the TRPML1-positive enlarged LELs, small basal inwardly rectifying currents (72 ± 12 pA/pF at -140 mV, N = 65 vacuoles) were seen under the whole-endolysosome configuration (**Fig. 4.1B,C**). Bath application of 100 nM $PI(3,5)P_2$ in a water-soluble diC8 form, rapidly and dramatically activated TRPML1-mediated current (I_{TRPML1}; t = 15 ± 4 s at -140 mV, N = 8 vacuoles; 18.3 ± 2.7-fold increase over basal activity, N = 20 vacuoles) (**Fig. 4.1B,C**). $PI(3,5)P_2$ activation was dose-dependent (EC_{50}= 48 ± 14 nM, hill slope (n) = 1.9, N = 7 vacuoles). On average, I_{TRPML1} in the presence of 100 nM diC8 $PI(3,5)P_2$ was 982 ± 150 pA/pF at -140 mV (N = 23 vacuoles) (**Fig. 4.1D**).

In yeast, $PI(3,5)P_2$ is exclusively produced from PI(3)P by the PIKfyve/Fab1 PI 5-kinase (Bonangelino et al., 2002; Cooke et al., 1998; Gary et al., 1998). $PI(3,5)P_2$ can be quickly

metabolized into PI(3)P by Fig4, or to PI(5)P by MTMR-family phosphatases (Dove et al., 2009; Duex et al., 2006a; Rudge et al., 2004; Shen et al., 2009). Neither PI(3)P (1 μM; **Fig. 4.1E**) nor PI(5)P (1 μM) activated I_{TRPML1}. PI(3)P and PI(3,5)P_2 are localized in the endolysosome system. Other PIPs such as PI(3,4)P_2, PI(4,5)P_2, and PI(3,4,5)P_3, are localized in the plasma membrane, or in other intracellular organelles, and are sequestered from endolysosomes (Poccia and Larijani, 2009). I_{TRPML1} was not activated by these other PIPs (**Fig. 4.1E**). TRPML2 and TRPML3 are also localized in the endolysosome (Cheng et al., 2010). PI(3,5)P_2, but not PI(3)P, activated whole-endolysosome I_{TRPML2} and I_{TRPML3} (data not shown). Thus, PI(3,5)P_2 activated TRPMLs with a striking specificity. Since PI(3,5)P_2 and TRPMLs are both primarily localized in the LEL, (Cheng et al., 2010; Dove et al., 2009; Pryor et al., 2006; Puertollano and Kiselyov, 2009), the insensitivity of I_{TRPML1} to PI(3)P or PI(5)P, and its robust activation by PI(3,5)P_2 suggested that TRPML1 might be acutely regulated by the activities of PIKfyve/Fab1, or by Fig4 or MTMR phosphatases in the LEL.

Suppression of I_{TRPML1} by a decrease in PI(3,5)P_2

To test that PI(3,5)P_2 is an endogenous activator of TRPML1, we recorded basal I_{TRPML1} after depleting the PI(3,5)P_2 level by overexpressing MTM1, a PI-3 phosphatase that can convert PI(3,5)P_2 and PI(3)P into PI(5)P and PI, respectively (Dove et al., 2009; Poccia and Larijani, 2009). A Rapamycin-dependent heterodimerization system was used to recruit the otherwise cytosolic MTM1 (Zoncu et al., 2009) (see **Fig. 4.2A)**. In cells expressing both RFP-FRB-MTM1 and EGFP-2*FKBP-Rab7, Rapamycin induced a rapid recruitment of MTM1 to Rab7-positive LEL membranes (**Fig. 4.2B)**. We noticed that the basal $I_{TRPML1}$was consistently larger for vacuoles isolated from Cos-1 cells with longer (> 5h) pretreatment of vacuolin-1 (data not shown). Following recruitment of MTM1, but not the inactive mutant (C375S) MTM1, a large suppression of basal whole-endolysosome I_{TRPML1} was seen (**Fig. 4.2C-F**). Collectively, these results suggested that PI(3,5)P_2 levels were the primary determinant of TRPML1 channel activity in the endolysosome.

Binding of PI(3,5)P_2 to the N terminus of TRPML1 *in vitro*.

Phosphoinositides are known to bind with high affinity to PI-binding modules such as PH or FYVE domain, or to a poly-basic region with unstructured clusters of positively-charged amino acid residues, such as Arg and Lys, in an electrostatic manner (Suh and Hille, 2008). PI(4,5)P_2

can bind directly to the intracellular N- and C- termini of several plasma membrane TRPs (Kwon et al., 2007; Nilius et al., 2008). Notably, the intracellular N terminus of TRPML1 has a predicted PH-like domain (Nilius et al., 2008) (**Fig. 4.2A**). To test whether $PI(3,5)P_2$ binds directly to TRPML1, we fused GST to the entire N-terminus of mouse TRPML1, up to residue 69 (membrane topology, **Fig. 4.3A**). The protein, GST-ML1-N, was used to probe phosphoinositides immobilized on a nitrocellulose membrane (Kwon et al., 2007; Nilius et al., 2008; Suh and Hille, 2008). GST-ML1-N, but not GST alone, bound to PIP_3 and PIP_2s, but not to other PIPs or phospholipids (**Fig. 4.3B**), suggesting that $PI(3,5)P_2$ bound directly *in vitro* to the cytoplasmic N-terminus of TRPML1.

To further map the $PI(3,5)P_2$-binding sites, we systematically replaced positively charged amino-acid residues (Arg and Lys) within and adjacent to the poly-basic region with non-charged Gln residues and assayed Gln-substituted, purified GST fusion proteins for $PI(3,5)P_2$ binding. We also tested whether $PI(3,5)P_2$ activated Gln-substituted TRPML1 channels using whole-endolysosome recordings. A dramatic decrease in $PI(3,5)P_2$ binding and activation (**Fig. 4.3C,D**) was observed in a 7Q mutant, with seven substitutions (R42Q/R43Q/R44Q/ K55Q/R57Q/R61Q/K62Q; **Fig. 4.3A**). In contrast to GST-ML1-N, GST-ML1-7Q-N failed to bind significantly to $PI(3,5)P_2$ or to other PIPs in the PIP strip (**Fig. 4.3B**). Considering the specificity of $PI(3,5)P_2$ for TRPML1 activation, one plausible explanation for the apparent discrepancy between our biochemical assays (see **Fig. 4.3B**) and electrophysiological measurements is that the purified GST-ML1-N protein fragment did not recapitulate the specificity of PIP binding of full-length TRPML1 in the endolysosomal membrane. Nevertheless, the binding affinity of ML1-N to $PI(3,5)P_2$ was dramatically reduced by removing the charges with the 7Q mutations (**Fig. 4.3B**), suggesting that multiple positively charged amino-acid residues are critical for $PI(3,5)P_2$ binding.

Compared with WT TRPML1, TRPML1-7Q was only weakly activated by high concentrations of $PI(3,5)P_2$, with a maximal response (efficacy) that was approximately 20% of I_{TRPML1} (EC50 = 2.2 ± 2 μM, Hill slope (n) = 0.8, N = 6 vacuoles) (**Fig. 4.3C,D**). Similar to $TRPML1^{Va}$, $TRPML1^{Va\text{-}7Q}$ also exhibited large basal currents (**Fig. 4.3E**), suggesting a relatively specific effect of 7Q mutations on $PI(3,5)P_2$-dependent activation. Collectively, our results suggest that $PI(3,5)P_2$ bound directly to the cytoplasmic N terminus of TRPML1, resulting in conformational changes that favor the opening of TRPML1.

TRPML1 and PI(3,5)P_2 in endolysosomal trafficking

The data presented here suggest that TRPMLs might be activated down- stream of the PI(3,5)P_2 increase to trigger membrane fusion and fission. If this hypothesis is correct, expression of TRPML1, which often exhibits substantial basal activity in heterologous systems (Cheng et al., 2010), might alleviate trafficking defects in PI(3,5)P_2-deficient cells. In cultured Vac14$^{-/-}$ fibroblast cells, the trafficking defects from PI(3,5)P_2 deficiency were reflected by enlarged vacuoles/LELs (> 3 up to 12 μm in diameter) in 79 ± 7% of cells (N = 3 experiments with > 100 cells) (**Fig. 4.4A**; (Zhang et al., 2007a)). Only approximately 5-10% of WT cells were vacuolated (< 4 μm; data not shown). Transfection of a WT Vac14 construct was sufficient to restrict vacuoles to 15 ± 2% of cells (N = 3 experiments; **Fig. 4.4A**). Interestingly, we were able to rescue the vacuolar phenotype by transfection of TRPML1, which showed vacuolation in 18 ± 1% cells (N = 6), but not pore-mutant TRPML1 (ML1-KK) with 69 ± 6% vacuolation (N = 3), or the PI(3,5)P_2-insensitive mutant TRPML1 (ML1-7Q) with 75 ± 7% vacuolation (N = 3) (**Fig. 4.4A-D**). Although ML1-7Q still localized to Lamp1-positive compartments (**Fig. 4.4B,E**), large vacuoles were seen in the majority of ML1-7Q-transfected Vac14$^{-/-}$ fibroblasts (**Fig. 4.4A-D**). Collectively, these results suggested that TRPML1 channel activity and PI(3,5)P_2 sensitivity had important roles in controlling vacuole size.

Discussion

Using biochemistry and whole-endolysosomal patch-clamp recordings, we showed that PI(3,5)P_2 directly binds and activates TRPML1 in the endolysosome with potency and specificity. Moreover we showed that overexpression of WT, but not the PIP_2-insensitive variant of TRPML1, was sufficient to rescue the trafficking defects in PI(3,5)P_2-deficient mammalian cells, as demonstrated by observation of enlarged vacuoles. Our identification of an endolysosome-localizing Ca^{2+} channel that is activated by the endolysosome-specific PI(3,5)P_2 provides a previously unknown link between these two important regulators of intracellular membrane trafficking.

Similar trafficking defects are seen in both TRPML1$^{-/-}$, and PI(3,5)P_2-deficient cells. For example, LEL-to-Golgi retrograde trafficking, a process requiring membrane fission, is defective in both TRPML1$^{-/-}$ cells (Chen et al., 1998; Cheng et al., 2010; Pryor et al., 2006; Puertollano and Kiselyov, 2009; Thompson et al., 2007) and in PI(3,5)P_2-deficient cells (Botelho et al., 2008; Dove et al., 2009; Duex et al., 2006a; Duex et al., 2006b; Poccia and Larijani, 2009; Zhang et al.,

2007a). Furthermore, both TRPML1 and PI(3,5)P_2-metabolizing enzymes are implicated in membrane-fusion processes like exocytosis (Dong et al., 2009; Dove et al., 2009; Poccia and Larijani, 2009) and lysosomal fusion with autophagosomes (Dove et al., 2009; Ferguson et al., 2009; Puertollano and Kiselyov, 2009). Thus, both TRPML1 and PI(3,5)P_2 play active roles in membrane fission and fusion. However, the cellular defects of PI(3,5)P_2-deficient cells are generally more severe than TRPML1$^{-/-}$ cells. Activation of TRPML1 might define a subset of the multiple functions of PI(3,5)P_2. Such activation, however, may provide an essential spatial and temporal regulation of endolysosomal dynamics. Membrane fusion and fission are highly coordinated processes requiring an array of cytosolic and membrane-bound proteins and factors. A local increase in PI(3,5)P_2 likely recruits protein complexes required to generate the membrane curvature necessary for membrane fusion and fission (Poccia and Larijani, 2009). A local increase in PI(3,5)P_2 could also activate TRPML1 to elevate juxtaorganellar Ca^{2+}, which binds to a putative Ca^{2+} sensor protein such as Syt/CaM (Luzio et al., 2007a) or ALG-2 (Vergarajauregui et al., 2009), to exert effects on SNARE proteins or lipid bilayer fusion (Poccia and Larijani, 2009; Roth, 2004).

The remarkable specificity of PI(3,5)P_2 in activating TRPML1 is consistent with the role of Ca^{2+} in controlling the direction and specificity of membrane traffic (Hay, 2007; Luzio et al., 2007a). Although we identified several positively charged amino acid residues as potential PI(3,5)P_2 binding sites, electrostatic interaction alone is unlikely to provide a high affinity PI(3,5)P_2 binding pocket (Nilius et al., 2008; Suh and Hille, 2008). Thus, additional structural determinants such as hydrophobic amino acid residues must also contribute to specificity, by interacting with the lipid portion of PI(3,5)P_2. Because of the low abundance of PI(3,5)P_2 (Dove et al., 2009), such specificity might be a pre-requisite for PI(3,5)P_2 and TRPML1 to control the trafficking direction in the late-endocytic pathway. In other organelles, however, other PIPs and intracellular Ca^{2+} channels are likely to provide machinery necessary for Ca^{2+}-dependent membrane fission and fusion. Within LELs, membrane fusion and fission are likely to occur in sub-organellar compartments that are enriched for both TRPMLs and PIKfyve. While TRPML-mediated juxtaorganellar Ca^{2+} transients might be captured using real-time live-imaging methods, these seemingly “spontaneous” events may correlate with membrane fusion and fission events that can be simultaneously monitored with fluorescence-imaging approaches.

Experimental procedure

Molecular biology and biochemistry.

Full-length mouse TRPML1, 2, and 3 were cloned into the EGFP-C2 (Clontech) or mCherry vector as described previously (Dong et al., 2008; Dong et al., 2009; Xu et al., 2007). TRPML1 non-conducting pore mutant (D471K/D472K; abbreviated TRPML1-KK) and PIP_2-insensitive mutant (R42Q/R43Q/R44Q/K55Q/R57Q/R61Q/K62Q; abbreviated TRPML1-7Q) were constructed using a site-directed mutagenesis kit (Qiagen). For glutathione S-transferase (GST) fusion constructs, DNA fragments corresponding to the N- (amino acid residues 1-69) terminal regions of mouse TRPML1 were generated by PCR amplification and cloned into the Eco*RI* and Xho*I* site of pGEX4T1, in frame to generate GST-fusion protein plasmids (pGEX-ML1-N). FKBP*2 fragment was PCR-amplified from eGFP-FKBP12-Rab5 and inserted into the HindIII and XhoI site of EGFP-Rab7 vector. RFP-FRB-MTM1 and EGFP-FKBP*2-Rab5 were kind gift from Dr.Banasfe Larijani. All constructs were confirmed by sequencing, and protein expression was verified by Western blot. Cos-1, or mouse primary fibroblast cells were transiently transfected with TRPML1-3 and the TRPML1 mutants for electrophysiology, biochemistry, live-cell imaging, and confocal imaging. TRPML1 Western blot analyses were performed with an anti-GFP monoclonal antibody (Covance).

Endolysosomal electrophysiology.

Endolysosomal electrophysiology was performed as described previously (Dong et al., 2008; Dong et al., 2009). Briefly, Cos-1 cells were transfected using Lipofectamine 2000 (Invitrogen) with TRPML1 or mutants fused to GFP or mCherry. LEL size is usually < 0.5 μm, which is suboptimal for patch clamping. We therefore treated cells with 1 μM vacuolin-1, a small chemical known to selectively increase the size of endosomes and lysosomes, for ~1h (Huynh and Andrews, 2005). Large vacuoles (up to 5 μm; capacitance = 0.68 ± 0.05 pF, N = 44 vacuoles) were observed in most vacuolin-treated cells. Occasionally, enlarged LELs were obtained from TRPML1-transfected cells without vacuolin-1 treatment. No significant difference in TRPML channel properties were seen for enlarged LELs obtained with or without vacuolin-1 treatment. Vacuoles positive for both mCherry-TRPML1 and EGFP-Lamp1 were considered enlarged LELs. Whole-endolysosome recordings were performed on isolated enlarged LELs. In brief, a patch pipette (electrode) was pressed against a cell and quickly pulled away to slice the cell membrane. Enlarged LELs were released into a dish and identified by monitoring

EGFP-TRPML1, the mCherry-TRPML1 or EGFP-Lamp1 fluorescence. Unless otherwise stated, bath (internal/cytoplasmic) solution contained 140 mM K-Gluconate, 4 mM NaCl, 1 mM EGTA, 2 mM Na_2-ATP, 2 mM $MgCl_2$, 0.39 mM $CaCl_2$, 0.1 mM GTP, 10 mM HEPES (pH adjusted with KOH to 7.2; free $[Ca^{2+}]_i$ approximately 100 nM). Pipette (luminal) solution was pH 4.6 standard extracellular solution (modified Tyrode's) with 145 mM NaCl, 5 mM KCl, 2 mM $CaCl_2$, 1 mM $MgCl_2$, 20 mM HEPES, 10 mM glucose (pH adjusted with NaOH). All bath solutions were applied via a fast perfusion system to achieve a complete solution exchange within a few seconds. Data were collected using an Axopatch 2A patch clamp amplifier, Digidata 1440, and pClamp 10.0 software (Axon Instruments). Whole-endolysosome currents were digitized at 10 kHz and filtered at 2 kHz. All experiments were conducted at room temperature (21-23ºC), and all recordings were analyzed with pCLAMP10 (Axon Instruments, Union City, CA), and Origin 8.0 (OriginLab, Northampton, MA). All PIPs are from A.G. Scientific, Inc.

GST fusion proteins.

To purify GST-tagged proteins, *Escherchia coli* BL21DE3 was transformed with empty pGEX vectors, pGEX-ML1-N, and pGEX-ML1-C. After growth to approximately OD_{600} = 0.6 in SuperBroth media supplemented with ampicillin, expression was induced with IPTG (1 M) for 7 h at 37°C. Cells were collected and resuspended in 30 ml of ice-cold PBS supplemented with protease inhibitor cocktail, 0.5 mM EDTA, and deoxytibonuclease, and lysed with a French press. Cell lysates in 1% Triton-X100 were incubated with 2 mL mixed glutathione Sepharose (GE Healthcare) for 1 h at 4°C. After three washes with 30 mL PBS, proteins were eluted with 7 mL elution buffer (10 mM Glutathinone, 50 mM Tris, pH 8).

Lipid Strip Binding Assay.

Lipid binding analysis of GST-ML1-N and GST-ML1-7Q-N fusion proteins was conducted using PIP Strips (Echelon Biosciences Inc.), with each spot containing 100 pmol active lipids. Membranes were blocked with PBST solution (supplemented with 3% fatty acid-free BSA) for 1 h at room temperature, and incubated with 0.5-3 μg GST-fusion protein in blocking buffer overnight. After six washes, the membranes were incubated with a mouse anti-GST antibody (1:5000, Sigma) for 1 h at room temperature, and secondary antibody HRP-labeled goat anti-mouse (1:5000) was added before detection by enhanced chemiluminescence.

Mouse fibroblast vacuole assay.

Vac14$^{-/-}$ mouse fibroblast cells were isolated and cultured as described previously (Zhang et al., 2007a). Briefly, fibroblasts were transiently transfected by electroporation (260 V, 950 μF) with 100 μg of the following expression constructs: mCit, mCit-Vac14, GFP-ML1, GFP-ML1-KK, or GFP-ML1-7Q. Cells were grown on 100-mm plates to 90% confluence and distributed to six 35-mm plates after electroporation. Cells were fixed with 4% PFA 24 h after electroporation. Fibroblasts were considered to be vacuolated if they had at least one enlarged (> 3 μm) cytoplasmic vacuole.

Cellular fractionation.

Lysosomal fractionation studies were performed as described previously (Kim et al., 2009). Briefly, cell lysates were obtained by dounce homogenization in a homogenizing buffer (0.25 M sucrose, 1 mM Na_2EDTA, 10 mM HEPES, pH 7.0). Lysates were centrifuged at 1900 x *g* at 4°C for 10 min to remove the nuclei and intact cells. Post-nuclear supernatants underwent ultracentrifugation through a Percoll density gradient using a Beckman L8-70 ultracentrifuge. An ultracentrifuge tube was layered with 2.5 M sucrose, 18% Percoll in homogenizing buffer, and the post-nuclear supernatant on top. Centrifugation was 67,200 x *g* at 4°C for 1.5 h in a Beckman Coulter 70.1 Ti Rotor. Samples were fractionated into 16 samples of unequal volume. Top fractions contained minimal cellular components; bottom fractions contained concentrated bands of cellular organelles and were separated into smaller fraction volumes.

Confocal imaging.

All images were taken using a Leica (TCS SP5) confocal microscope. Lamp1 antibody was from the Iowa Hybridoma Bank.

Data analysis.

Data are presented as the mean ± standard error of the mean (SEM). Statistical comparisons were made using analysis of variance (ANOVA). A P value < 0.05 was considered statistically significant.

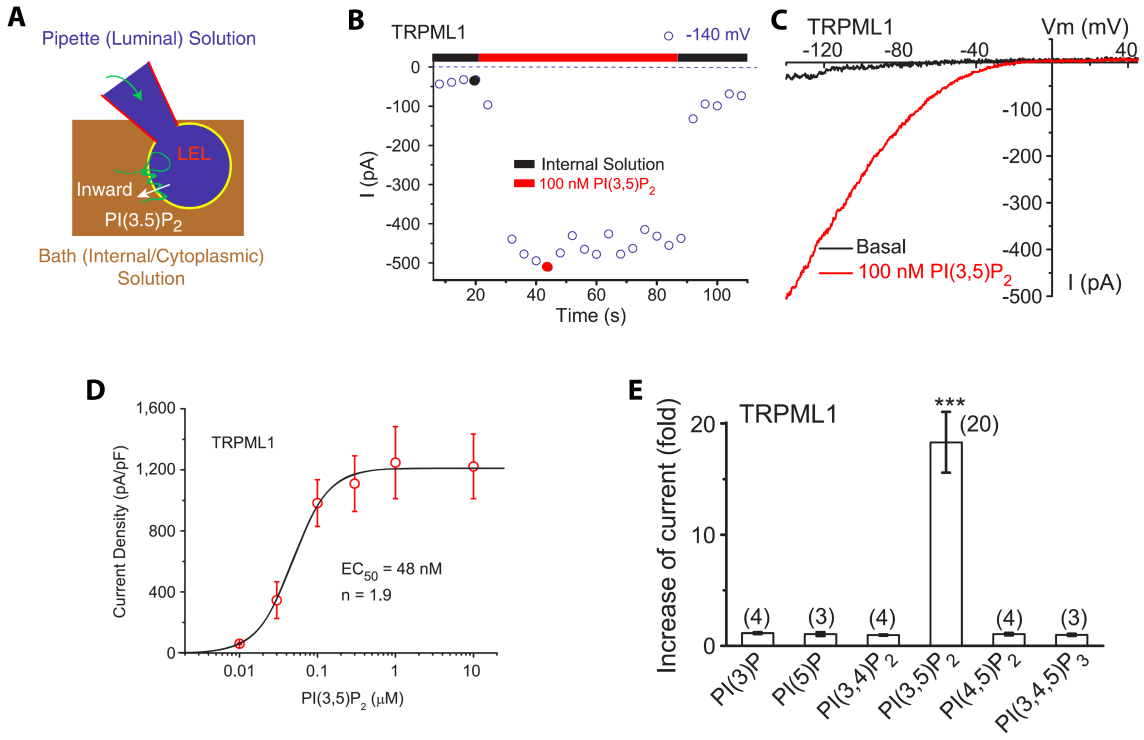

Figure 4.1. $PI(3,5)P_2$ activates TRPML channels in the endolysosomal membranes. (Contributed by Dr. Xianping Dong)

(A.) Illustration of a whole-endolysosome recording configuration. Pipette (luminal) solution was a standard external (Tyrode's) solution adjusted to pH 4.6 to mimic the acidic environment of the lysosome lumen. Bath (internal/cytoplasmic) solution was a K^+-based solution (140 mM K^+-gluconate). Note that the inward current indicates cations flowing out of the endolysosome. **(B).** Bath application of $PI(3,5)P_2$ (diC8, 100 nM) activated inwardly rectifying whole-endolysosome TRPML1-mediated current (I_{TRPML1}) in an enlarged endolysosome/vacuole from a TRPML1-EGFP-expressing Cos-1 cell that was pre-treated with vacuolin-1. $I_{TRPML1}$was elicited by repeated voltage ramps (-140 to +140 mV; 400 ms) with a 4-s interval between ramps. I_{TRPML1} exhibited a small basal current prior to $PI(3,5)P_2$ application; bath application of $PI(3,5)P_2$ to the cytoplasmic side of the endolysosome resulted in maximal activation of 18-fold over baseline within a minute, measured at -140 mV of I_{TRPML1}. **(C).** Representative traces of I_{TRPML1} before (black) and after (red) $PI(3,5)P_2$ at two time points, as shown in a (black and red circles). Only a portion of the voltage protocol is shown; holding potential = 0 mV. **(D).** Dose-dependence of $PI(3,5)P_2$ activation (EC_{50} = 48 nM, n = 1.9). **(E).** Specific activation of TRPML1 by $PI(3,5)P_2$, but not other PIPs in diC8.

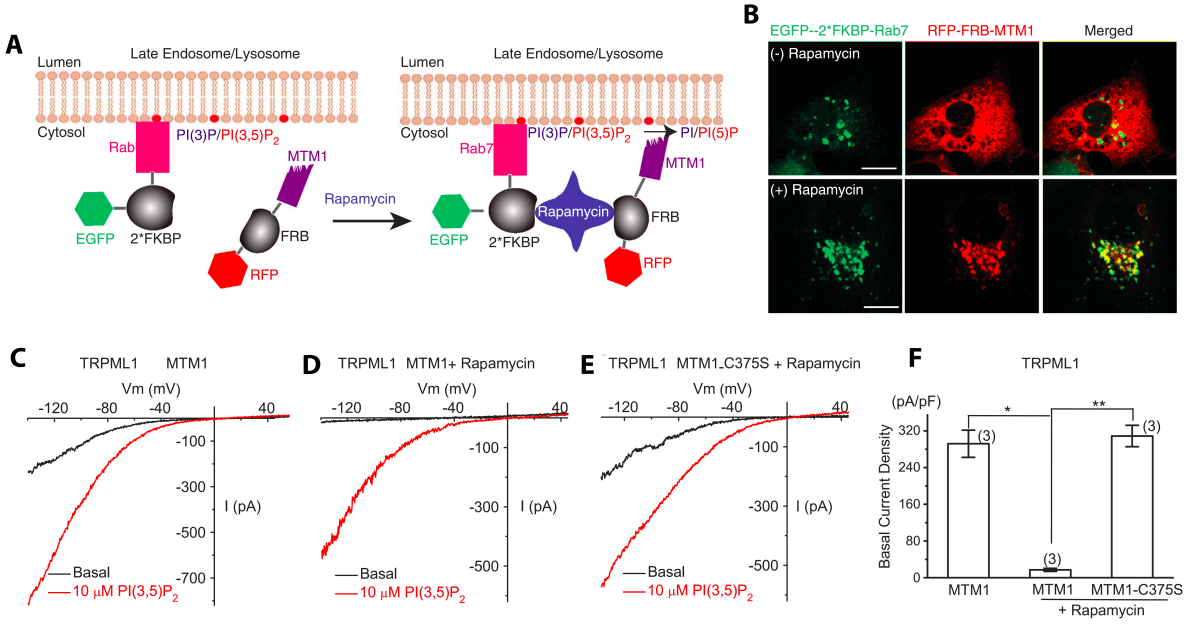

Figure 4.2. A decrease in PI(3,5)P_2 suppresses TRPML1 channel activity in the endolysosomal membrane.

(A). Recruitment of MTM1 to endolysosomal membranes by rapamycin-dependent heterodimerization of RFP-FRB-MTM1 and EGFP-2*FKBP-Rab7. Rab7 is a LEL-specific Rab protein. MTM1 is a PI-3 phosphatase that can convert PI(3,5)P_2 and PI(3)P into PI(5)P and PI, respectively. **(B).** Rapamycin-dependent heterodimerization of RFP-FRB-MTM1 and EGFP-2*FKBP-Rab7 alters subcellular localization of MTM1. Cos-1 cells were transfected with both RFP-FRB-MTM1 and EGFP-2*FKBP-Rab7. Rapamycin (500 nM; 20 min) treatment promotes co-localization of MTM1-RFP with Rab7-EGFP. Scale Bar = 10 μm. **(C-F).** The effects of MTM1 on I_{TRPML1}. Cos-1 cells were co-transfected with human TRPML1-myc, RFP-FRB-MTM1 or RFP-FRB-MTM1-C375S, and EGFP-2*FKBP-Rab7. MTM1 was recruited to LEL membranes by rapamycin (500 nM)-dependent heterodimerization of RFP-FRB-MTM1 and EGFP-2*FKBP-Rab7. **(C).** I_{TRPML1} in MTM1-transfected cells before rapamycin treatment. **(D).** I_{TRPML1} in MTM1-transfected cells after rapamycin treatment. **(E).** I_{TRPML1} in MTM1-C357S-transfected cells after rapamycin treatment. **(F).** Differential effects of WT and inactive mutant (C375S) MTM1 on basal whole-endolysosome I_{TRPML1}. Data are presented as the mean ± s.e.m.; the *n* numbers are in parentheses. Statistical comparisons were made using analysis of variance: $*P < 0.05$; $**P < 0.01$.

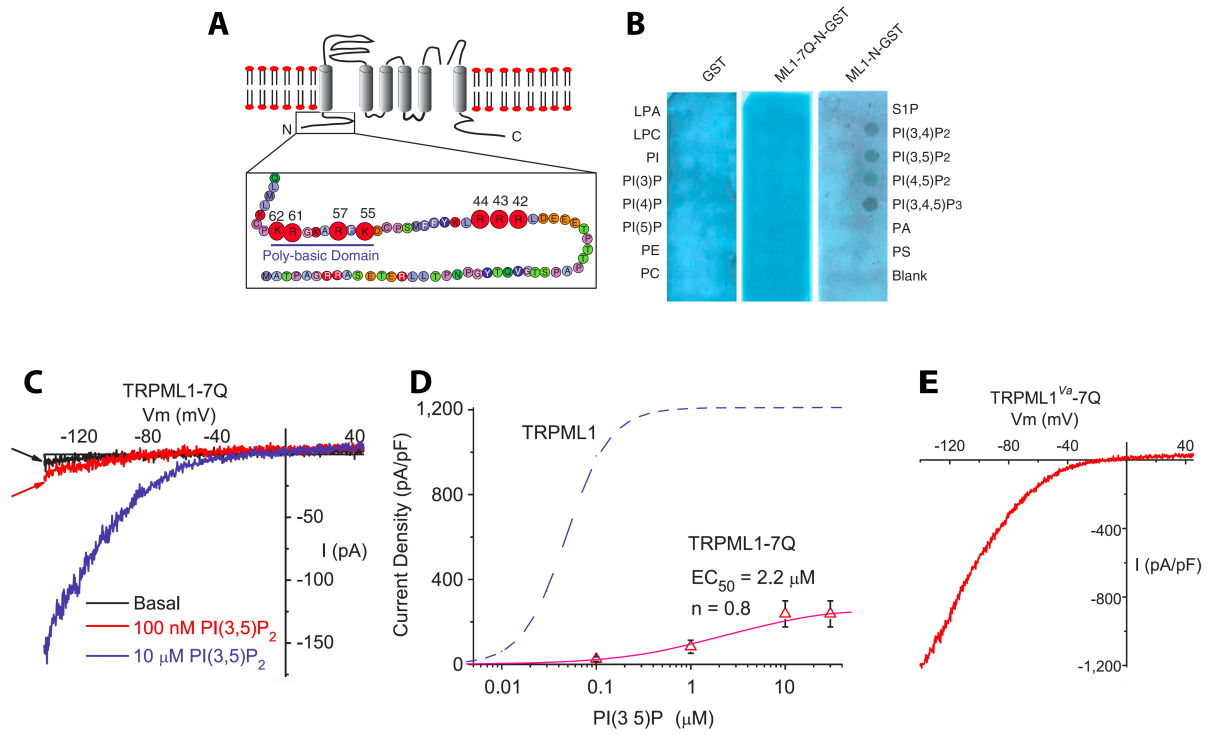

Figure 4.3. Direct binding of PI(3,5)P_2 to the TRPML1 N terminus requires multiple positively charged amino-acid residues.

(A). The cytoplasmic N terminus of TRPML1 contains a poly-basic region and clusters of positively charged amino-acid residues as potential PI(3,5)P_2-binding sites. The positively charged amino-acid residues (Arg and Lys) that were mutated into neutral amino acids Gln (Q) in this study are shown with enlarged circles and their amino-acid residue numbers. **(B).** Protein-lipid overlays. The strip contained 15 different types of lipids. PA, phosphatidic acid; S1P, sphingosine-1-phosphate. Three purified proteins were used to probe the strip: GST alone (left panel), GST-fused to the N-terminal fragment of TRPML1 (ML1-NGST; right panel), and Gln-substituted mutant of ML1-N-GST (ML1-7Q-N-GST; middle). Proteins were detected with anti-GST antibodies. **(C).** Whole-endolysosome $I_{TRPML1\text{-}7Q}$ was weakly activated by high concentrations of PI(3,5)P_2. **(D).** PI(3,5)P_2 dose dependence of $I_{TRPML1\text{-}7Q}$. Dotted line indicates the dose dependence of I_{TRPML1} (replotted from **Fig. 4.1.D**). **(E).** Large basal whole-endolysosome $I_{TRPML1\text{-}Va\text{-}7Q}$. Charge-removing Gln substitutions (7Q) were introduced into the gain-of-function *Va* background. Data are presented as the mean ± s.e.m.; the n numbers are in parentheses. Statistical comparisons were made using analysis of variance: * * * $P < 0.001$.

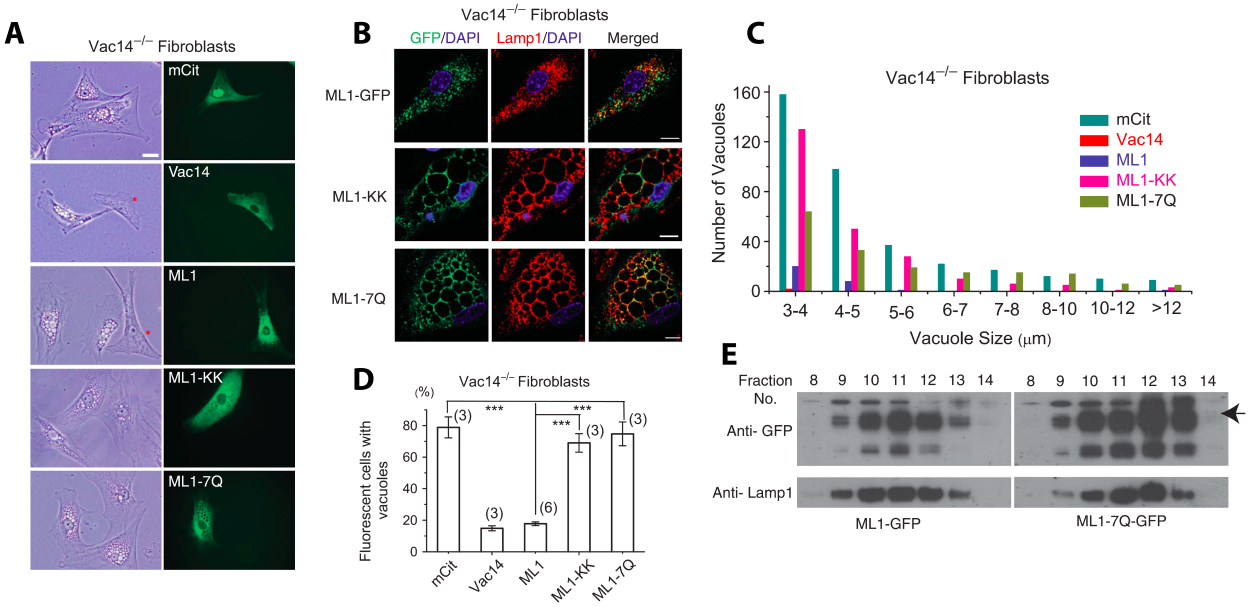

Figure 4.4. Overexpression of TRPML1 rescues the enlarged endolysosome phenotype of PI(3,5)P_2-deficient mouse fibroblasts.

(A,B). The effects of overexpression of WT TRPML1 and pore (ML1-KK) or PI(3,5)P_2-insensitive (ML1-7Q) mutant TRPML1 on the number and size of the vacuoles in Vac14$^{-/-}$ fibroblasts. Cultured Vac14$^{-/-}$ mouse fibroblast cells exhibited variable numbers (1-20) of large (> 3 μm) vacuoles / endolysosomes. Left, differential interference contrast image, right epifluorescence. Green fluorescence, mCit (vector only), mCit-Vac14, GFP-ML1, GFP-ML1-KK, GFP-ML1-7Q. Non-vacuolated cells are indicated by asterisk. Scale bar, 20 μm. **(B).** TRPML1, ML1-KK and ML1-7Q proteins were co-localized in Lamp1-positive compartments of Vac14$^{-/-}$ fibroblast cells. **(C).** Histogram analysis of the vacuole size/number in Vac14$^{-/-}$ fibroblasts transfected with indicated constructs. **(D).** Large vacuoles in 75 % of vector (mCit)-transfected Vac14$^{-/-}$ fibroblast cells. Overexpression of Vac14-mCit or EGFP-ML1 reduced the percentage (of enlarged vacuoles) to approximately 15%, whereas the 75% of EGFP-ML1-KK or EGFP-ML1-7Q-transfected cells contained enlarged vacuoles. Data are presented as the mean ± s.e.m.; the n numbers are in parentheses. Statistical comparisons were made using analysis of variance: * * * $P < 0.001$. **(E).** Cellular organelle fractionation analysis reveals co-localization of TRPML1 and TRPML1-7Q with Lamp-1. Gradient cellular fractionations were obtained using ultracentrifugation. Both TRPML1 and TRPML1-7Q proteins were concentrated in Lamp1-rich fractionations. Arrow shows full-length TRPML1-EGFP.

CHAPTER 5

The role of TRPML1 in Ca^{2+}-dependent lysosomal exocytosis

Abstract

Lysosomes undergo exocytosis in response to an increase of intracellular Ca^{2+}. This process has important roles in a variety of cellular functions, including phagocytosis and plasma membrane repair. Lysosomes are considered to provide Ca^{2+} required for the exocytosis, however, the molecular identity mediating the Ca^{2+} release remains elusive. The mucolipin-1 (TRPML1) is a Ca^{2+}-permeable channel primarily localized in late endosomes and lysosomes. Here we identified several gain-of function mutations of TRPML1 with constitutive Ca^{2+} permeability. Cells expressing these gain-of-function mutants of TRPML1 have dramatically increased lysosomal exocytosis. Particle binding in macrophages is a physiological stimulus to evoke lysosomal exocytosis. Upon particle binding, lysosomal exocytosis is shown to be required to provide membrane supplies to engulf particles to facilitate phagosome formation. By direct patch-clamping of phagosomal membranes and whole-cell recordings, we found that upon particle binding, TRPML1-associated lysosomes are delivered to the newly-formed phagosomes via lysosomal exocytosis in a Ca^{2+}-dependent manner, suggesting a role of TRPML1 in lysosomal exocytosis and phagosome formation.

Introduction

TRPML1 belongs to the mucolipin subfamily of transient receptor potential (TRPML) proteins, which contain three members (TRPML1-3). TRPML1 is primarily localized on the late endosome and lysosome (Cheng et al., 2010). Human mutations of *TRPML1* cause Mucolipidosis type IV (ML4), a childhood neurodegenerative disorder (Bargal et al., 2000; Bassi et al., 2000; Cheng et al., 2010; Puertollano and Kiselyov, 2009; Sun et al., 2000). Cells that lack TRPML1 exhibit enlarged endolysosomes and trafficking defects in the late endocytic pathway (Cheng et al., 2010). Previous work form our lab has demonstrated that TRPML1 is a major Ca^{2+}-permeable channel in lysosomes (Dong et al., 2008; Dong et al., 2010a; Dong et al., 2009) and is specifically activated by $PI(3,5)P_2$ (Dong et al., 2010a). Spontaneous mutations in the mouse *TRPML3 (A419P)* result in the *varitint-waddler (Va)* phenotype (Cuajungco and Samie, 2008; Puertollano and Kiselyov, 2009). Compared with wild-type TRPML3, much larger TRPML3-mediated currents are seen in cells expressing $TRPML3^{A419P}$ ($TRPML3^{Va}$). The $TRPML3^{Va}$ channel exhibits similar pore properties as wild-type TRPML3, but with altered gating behavior, suggesting that *Va* is a channel gain-of-function mutation (Cuajungco and Samie, 2008; Grimm et al., 2007; Kim et al., 2007; Martina et al., 2009; Nagata et al., 2008; Puertollano and Kiselyov, 2009; Xu et al., 2007). Furthermore, because proline introductions into a transmembrane α-helix often cause kinks, hinges, or swivels (Tieleman et al., 2001), the "helix-breaking effect" of proline was proposed to lock the $TRPML3^{Va}$ channel in an unregulated and "open" state (Cuajungco and Samie, 2008). Similarly, the proline substitution at the homologous positions in *TRPML1* (*V432P* or $TRPML1^{Va}$) leads to large inwardly rectifying whole-cell currents (Dong et al., 2008), although it's unclear how the *Va* mutation causes the surface expression of TRPML1.

Accumulated evidence has shown that lysosomes undergo exocytosis in response to an increase of intracellular Ca^{2+} in most, if not all cell types (Andrews, 2000; Coorssen et al., 1996; Ninomiya et al., 1996; Rodriguez et al., 1999; Rodriguez et al., 1997). Lysosomal exocytosis plays important roles in numerous physiological processes, including phagocytosis (Czibener et al., 2006), plasma membrane repair (Andrews, 2005; Reddy et al., 2001), bone resorption (Zhao et al., 2008), neurite outgrowth (Arantes and Andrews, 2006), neurotransmitter release (Chen et al., 2005; Dou et al., 2012; Liu et al., 2011; Zhang et al., 2007b), axonal remyelination (Chen et al., 2012) and cellular clearance (Medina et al., 2011). The critical trigger for lysosomal exocytosis is the proximal Ca^{2+} increase, presumably from lysosomal Ca^{2+} release under

physiological conditions (Czibener et al., 2006; Liu et al., 2011; Tapper et al., 2002). However, definitive evidence to support this hypothesis is still lacking, and more essentially, the ion channel(s) responsible for Ca^{2+} release from lysosomes remains elusive. TRPML1 represents a natural candidate for the Ca^{2+} release channel in the endolysosome.

In macrophages, phagocytosis of large extracellular particles such as apoptotic bodies is required for cellular clearance and tissue remodeling (Flannagan et al., 2012). Particle binding to the plasma membrane triggers a localized signaling cascade to orchestrate focal cytoskeleton reorganization and delivery of membranes from intracellular pools, resulting in the formation of plasmalemmal pseudopods. The lysosome is a major source of intracellular membranes required for particle ingestion, and is delivered to phagocytic cups via Ca^{2+}-dependent lysosomal exocytosis (Braun et al., 2004; Czibener et al., 2006; Huynh et al., 2007). The process of particle uptake has provided an opportunity to study lysosomal exocytosis in physiological conditions.

In the current study, firstly, to understand the mechanisms of the *Va* mutation in TRPML1, we performed systemic proline substitutions and obtained several gain-of function mutations of TRPML1 with constitutive Ca^{2+} permeability. These gain-of-function mutants of TRPML1 lead to dramatically increased lysosomal exocytosis. We further tested the role of TRPML1 in lysosomal exocytosis-mediated particle uptake in macrophages. By direct patch-clamping of phagosomal membranes, we found that TRPML1 is rapidly recruited to nascent phagosomes upon particle binding. Using whole-cell recordings, we detected the plasma membrane insertion of TRPML1 in a Ca^{2+}-dependent manner during particle uptake, suggesting TRPML1-associated lysosomes are delivered to nascent phagosomes via TRPML1-mediated lysosomal exocytosis.

Results

Va-like gain-of-function mutations

To identify additional *Va*-like mutations in TRPML1 that lead to measurable whole-cell currents, we constructed 20 Pro substitutions near the *Va* locus in the S4-S5 linker and the bottom half of TM5 (transmembrane 5) (**Fig. 5.1A**). This region was previously implicated in the channel gating of various 6TM channels, including TRP channels (Cuajungco and Samie, 2008; Long et al., 2005). Proline-substituted TRPML1 channels were then transiently expressed in HEK-293T cell lines. To monitor expression, TRPML1 was fused to enhanced green fluorescent protein (EGFP) at its N-terminus (Dong et al., 2008; Xu et al., 2007). Cells transfected with $TRPML1^{Va}$

or TRPML3^{Va} exhibit elevated intracellular Ca^{2+} levels, i.e., Ca^{2+} overload (Grimm et al., 2007; Xu et al., 2007). Therefore, our initial screening of Pro substitutions was conducted using Fura-2-based Ca^{2+} imaging. The expressions of TRPML1 and the Pro mutations were confirmed by measuring EGFP fluorescence (F470; **Fig. 5.1B**).

The basal intracellular Ca^{2+} ($[Ca^{2+}]_i$) levels of WT TRPML1-transfected HEK293T cells were similar to those of non-transfected cells (**Fig. 51B,E**). In contrast, elevated $[Ca^{2+}]_i$ levels were seen in most TRPML1^{Va}-transfected cells (**Fig. 5.1C,F**) in the standard extracellular Tyrode solution (2 mM Ca^{2+}). Removal of Ca^{2+} from the bath (0 mM Ca^{2+}) rapidly decreased the Fura-2 ratios in most TRPML1^{Va}-transfected cells. However, in a subpopulation of TRPML1^{Va}-transfected cells with high basal $[Ca^{2+}]_i$ levels (fura-2 ratio> 2), Ca^{2+} removal only slightly decreased the Fura-2 ratios (**Fig. 5.1F**). These cells might have entered an irreversible apoptotic program that was triggered by Ca^{2+} overload (Grimm et al., 2007; Nagata et al., 2008; Xu et al., 2007). Nevertheless, even with TRPML1^{Va}-transfected cells with low basal $[Ca^{2+}]_i$ levels (Fura-2 ratio < 2), Fura-2 ratios never dropped to nontransfected cell levels upon Ca^{2+} removal. These results suggest that TRPML1^{Va} might also have increased basal $[Ca^{2+}]_i$ levels by mobilizing intracellular Ca^{2+} stores. High basal $[Ca^{2+}]_i$ levels were also seen in two other TRPML1 Pro substitutions, TRPML1^{C430P} and TRPML1^{C431P} (**Fig. 5.1H**). Intermediate $[Ca^{2+}]_i$ levels were observed in another proline substitution, TRPML1^{R427P} (**Fig. 5.1D,G**). In contrast, no significant alterations in the basal $[Ca^{2+}]_i$ levels were observed in other Pro substitutions (**Fig. 5.1H)**. Thus, the *Va* locus and its vicinity at the cytosolic side may be the only areas susceptible to Pro substitutions. Together, these results indicate that TRPML1^{R427P}, TRPML1^{C430P}, and TRPML1^{C431P} were also TRPML1^{Va}-like GOF mutations. These GOF mutations were also shown to result in large whole-cell inwardly-rectifying currents (**Fig 5.2**).

GOF mutations lead to increased lysosomal exocytosis

One possible route by which the GOF mutations could get to the plasma membrane is by enhanced fusion of lysosomes with these mutant TRPML1 channels, i.e. increased lysosomal exocytosis. To probe this possibility, we used Lamp-1 surface staining to monitor lysosomal exocytosis (Reddy et al., 2001). Non-transfected or TRPML1-transfected cells did not exhibit significant Lamp-1 surface staining (**Fig. 5.3A**), suggesting a low rate of lysosomal exocytosis. However, in cells transfected GOF Pro mutants, evident punctuate Lamp-1 staining was seen in most transfected cells (**Fig. 5.3B-E**). TRPML1^{R427P} exhibited an intermediate level of Lamp-1

surface staining (**Fig. 5.3B,H**). The Lamp-1 staining appeared to be in the cell surface based on its colocalization with a plasma membrane marker DilC18 (**Fig. 5.3F**). Pro substitutions increased both whole cell and whole lysosome currents, resulting in increases of both intralysosomal Ca^{2+} release and Ca^{2+} entry (data not shown). To separate these two potential distinct effects on lysosomal exocytosis, we performed the experiments under Ca^{2+}-free conditions by removing external Ca^{2+} in the culture medium. Under this condition, the global Ca^{2+} level of TRPML1^{Va}-transfected cells was only slightly above the resting Ca^{2+} level of non-transfected cells (**Fig. 5.3G**). Interestingly, Lamp-1 surface staining in TRPML1^{V432P}-transfected cells was even enhanced under Ca^{2+}-free conditions (**Fig. 5.3H**). These results indicate that GOF Pro mutations induce a high level of lysosomal exocytosis via a mechanism that is dependent on lysosomal Ca^{2+} release, and suggest that TRPML1-mediated Ca^{2+} release may trigger lysosomal exocytosis.

Particle binding induces lysosomal exocytosis in a Ca^{2+}- and TRPML1-dependent manner

To probe the role of TRPML1 under physiological condition, we tested the involvement of TRPML1 in the process of particle uptake in macrophages. Particle uptake requires the Ca^{2+}-dependent lysosome fusion with the plasma membrane to provide the additional membrane. We hypothesized that particle binding triggers TRPML1-mediated lysosomal Ca^{2+} release, rapidly delivering TRPML1-resident lysosomal membranes to nascent phagosomes via lysosomal exocytosis. To study particle uptake/ingestion, we isolated bone marrow macrophages (BMMs) (Chow et al., 2004) from wild-type (WT) and TRPML1 knockout (KO) (Venugopal et al., 2007) mice, and exposed BMMs to IgG-opsonized sheep red blood cells (IgG-RBCs) (all about 5 μm in size). We first investigated the insertion of TRPML1 onto the plasma membrane during particle uptake. Because current antibodies are inadequate for detecting endogenous TRPML1 proteins, we developed a whole-cell patch-clamp method to "detect" the plasma membrane insertion of TRPML1 during particle uptake. This electrophysiology-based "exocytosis assay" provides temporal resolution far superior to other exocytosis/secretion assays. In order to facilitate detection (by decreasing the turnover time of TRPML1 at the plasma membrane), we used a cell-permeable dynamin inhibitor, dynasore (Macia et al., 2006), to block endocytosis that is presumed to be coupled with focal exocytosis (Lee et al., 2007; Tam et al., 2010). TRPML1-specific activator ML-SA1 (Shen et al., 2012) induced large whole-cell TRPML1-like currents upon exposure of WT BMMs to IgG-RBCs for 10 min in the presence of

dynasore (**Fig. 5.4 B,D**). In contrast, no significant ML-SA1-induced whole-cell currents were observed in RBC-treated TRPML1 KO BMMs, or WT BMMs treated with dynasore alone (**Fig. 5.4 A,C,D**). IgG-RBC-induced whole-cell I_{TRPML1} was completely inhibited by BAPTA-AM pretreatment (**Fig. 5.4D**), suggesting that membrane insertion during phagocytosis is a Ca^{2+}-dependent process.

TRPML1 is rapidly recruited to nascent phagosomes.

To further determine whether TRPML1-associated lysosomes contribute to the phagosome formation via lysosomal exocytosis, we developed a patch-clamp method to directly record from phagosomal membranes (**Fig. 5.5A,B**). Phagosomes were isolated from Lamp1-GFP or TRPML1-GFP-transfected RAW 264.7 cells (macrophage cell lines) after exposure to IgG-RBCs or beads for 5 min. In Lamp1-GFP-transfected RAW cells, bath application of $PI(3,5)P_2$ (100 nM) or ML-SA1 (25 μM) readily activated endogenous whole-phagosome TRPML1-like currents (**Fig. 5.5C**); much larger whole-phagosome ML-SA1-activated currents were seen in TRPML1-GFP-transfected RAW cells. In WT BMMs, whole-phagosome I_{ML1} was activated by ML-SA1, but inhibited by TRPML1 antagonist ML-SI1 (**Fig. 5.5D**); no significant whole-phagosome I_{TRPML1} was seen in TRPML1 KO BMMs (**Fig. 5.5D**). In contrast, $PI(3,5)P_2$-activated I_{TPC} (see chapter 2) was present in both WT and TRPML1 KO BMMs (**Fig. 5.5D**). These results have thus provided functional evidence that TRPML1 is recruited to nascent phagosomes. Taken together, our functional analysis has provided definite evidence for that upon particle binding, TRPML1-associated lysosomes are delivered to the newly-formed phagosomes via lysosomal exocytosis, and has suggested a role of TRPML1 in lysosomal exocytosis and phagosome formation.

Discussion

In this study, by performing systemic Pro substitution on 20 amino acids residues around the *Va* spot, we obtained several additional GOF *Va*-like mutations that displayed constitutive Ca^{2+} permeability and increased surface expression reflected by their large whole-cell currents. Consistent with the role of TRPML1 in a Ca^{2+}-dependent lysosomal exocytosis, Lamp-1 surface staining was dramatically increased in cells expressing GOF TRPML1 channels. Thus the simplest model is that GOF channel activities cause TRPML1-mediated lysosomal Ca^{2+} release, and lead to the appearance of TRPML1 and Lamp-1 at the plasma membrane via lysosomal

exocytosis. The helix-breaking effect of Pro introduction may have interfered the conformational changes that normally occurred during channel activation gating. GOF Pro substitutions could have locked the TRPML1 channel in an unregulated and open state. Such mechanisms have been demonstrated in several other 6TM cation channels (Cuajungco and Samie, 2008; Grimm et al., 2007; Zhao et al., 2004). All GOF Pro substitutions are located in the cytoplasmic face of TM5. Thus, it is possible that unidentified cellular mechanisms may activate wt TRPML1 via a conformational change in this S4-S5 linker region, which has been previously implicated in the gating of various 6TM cation channels (Cuajungco and Samie, 2008; Long et al., 2005).

Lysosomes containing TRPML1 channels with constitutive Ca^{2+} permeability may undergo un-regulated exocytosis. Although intralysosomal Ca^{2+} release is the proposed initiative step, the triggering mechanism for lysosomal Ca^{2+} release remains unknown. A previous study suggested TRPML1 may be involved in lysosomal exocytosis (LaPlante et al., 2006), and our results further indicated that activating mutant of TRPML1 causes increased lysosomal exocytosis. It is hypothesized that upon unidentified cellular stimulus, TRPML1 mediates intralysosomal Ca^{2+} release to trigger lysosomal exocytosis. Lysosomal exocytosis is well studied in plasma membrane repair (Idone et al., 2008), however, during this process, the extracellular Ca^{2+} entry from the wounded areas is proposed to trigger lysosomal exocytosis, which may mask the role of TRPML1-mediated lysosomal Ca^{2+} release. To study TRPML1-mediated lysosomal exocytosis under physiological stimuli, we employed the process of the particle binding in macrophages, in which intralysosomal Ca^{2+} is indicated to be involved (Czibener et al., 2006). Using whole-cell recordings and phagosome-recordings, we have demonstrated that upon particle binding, TRPML1-associated lysosomes are delivered to the plasma membrane via lysosomal exocytosis and then subsequently recruited into nascent phagosomes. It's worth mentioning that the phagosome recording developed in this study has provided a nice assay to study functions of TRPML1 and other ion channels (such as Hv1) (El Chemaly and Demaurex, 2012) on the phagosomes. Furthermore, recent identification of TRPML1 activators (Grimm et al., 2010; Shen et al., 2012) and inhibitors (Samie et al., unpublished), combined with lysosomal Ca^{2+} imaging and live imaging, would greatly facilitate the study to dissect the role of TRPML1 in lysosomal exocytosis (Samie et al., unpublished).

TRPML1-dependnet lysosomal exocytosis is implicated to promote cellular waste clearance. TFEB, a transcription factor that regulates lysosomal genes, is reported to reduce the lysosomal pathological storage in several lysosomal storage diseases. The rescue effects were

proposed to be caused by induction of lysosomal exocytosis in a TRPML1-dependent manner. Consistent with this result, our lab has previously shown that increasing TRPML1 activity by small activator ML-SA1 alleviated the lysosomal lipid storage in Niemann-pick C disease cells (Shen et al., 2012), possibly also through promoting lysosomal exocytosis. Thus TRPML1 may serve as an important therapeutic target for disorders associated with intracellular storage, including Lysosomal Storage diseases (LSDs) and other commonly-acquired neurodegeneration diseases, such as Alzheimer's disease, Parkinson's disease and Huntington's disease.

Experimental procedure

Molecular biology, biochemistry, and histocytochemistry.

Full length mouse TRPML1 was cloned into the EGFP-C2 vector (Clontech) or mCherry as described previously (Dong et al., 2008; Xu et al., 2007). Proline mutations were constructed using a site-directed mutagenesis kit (Qiagen). All constructs were confirmed by sequencing analysis, and protein expression was verified by Western blotting. HEK293T cells were transiently transfected with WT TRPML1 or Pro-substituted TRPML1 channels for electrophysiology, Ca^{2+} imaging. The Lamp-1 antibody was from the Iowa Hybridoma Bank. The surface expression of Lamp-1 was detected using a mouse monoclonal antibody (H4A3) against the luminal epitope of human Lamp-1 on non-permeabilized cells (Reddy et al., 2001).

Ca^{2+} imaging.

HEK293T cells were loaded with 5 μM Fura-2 AM (Molecular Probes) in culture medium at 37^{o}C for 60 min. Cells were washed in Tyrode solution for 10-30 min and the fluorescence intensities at 340 nm (F340) and 380 nm (F380) were recorded on an EasyRatioPro system (Photon Technology International, Birmingham, NJ). Fura-2 ratios (F340/F380) were used to determine $[Ca^{2+}]_i$. The EGFP-positive cells were identified by monitoring fluorescence intensity at 470 nm (F470).

Mouse lines.

The generation and characterization of TRPML1 (Venugopal, Browning et al. 2007) has been described previously. Animals were used under approved animal protocols and Institutional Animal Care Guidelines at the University of Michigan.

Macrophage cell culture.

Murine BMMs were prepared and cultured as described previously (Link et al., 2010). Briefly, bone marrow cells from femurs and tibias were harvested and cultured in macrophage differentiation medium (RPMI-1640 medium with 10% fetal bovine serum (FBS) and 100 unit/ml recombinant colony stimulating factor (PeproTech, Rocky Hill, NJ). After 7 days in culture at 37 °C with 5% CO_2, the adherent cells (> 95% are expected to be macrophages) were harvested for assays. RAW 264.7 cells are cultured in DMEM/F12 media supplemented with 10% FBS at 37°C and 5% CO_2.

Whole-phagosome electrophysiology.

RAW macrophages and BMMs were transfected with Lamp1-GFP or ML1-GFP using Neon transfection system (Invitrogen, MPK 5000). IgG-RBCs were first incubated with macrophages at 4°C for 20 min to synchronize the binding of IgG-RBCs to cells. Phagocytosis does not happen at this temperature. After several gentle washes, cells were placed at 37°C and 5% CO2 for 5 min to initiate the phagocytosis, and then transferred to room temperature to slow down the phagocytosis (Holevinsky and Nelson, 1998). Since the duration of phagocytosis is only 5 min, the phagosomes formed at this stage were not fused with endo-lysosomes (Vieira et al., 2002), and were considered as newly-formed or nascent phagosomes. Because the majority of RBC-containing phagosomes (~5 μm, roughly as the size of RBCs) were also Lamp1-GFP or ML1-GFP-positive (see **Fig. 5.5A,B**), the GFP-positive vesicles (~ 5 μm) were identified as nascent phagosomes. To isolate phagosomes, a patch pipette was used to open the cell by slicing the cell membrane. Then phagosomes were released into the dish and recognized by GFP fluorescence. The bath (cytoplasmic) solution contained 140 mM K-gluconate, 4 mM NaCl, 1 mM EGTA, 2 mM $MgCl_2$, 0.39 mM $CaCl_2$, and 10 mM HEPES (pH adjusted with KOH to 7.2; free [Ca2+] ~100 nM). The pipette (luminal) solution contained 145 mM NaCl, 5 mM KCl, 2 mM $CaCl_2$, 1 mM $MgCl_2$, 10 mM HEPES, 10 mM MES, and 10 mM glucose (pH 6.5, adjusted with NaOH).

Whole-cell electrophysiology.

Whole-cell recordings were performed as described previously (Dong et al., 2008; Dong et al., 2009). The pipette solution contained 147 mM Cs^+, 120 mM methane-sulfonate, 4 mM NaCl, 10 mM EGTA, 2 mM Na_2-ATP, 2 mM $MgCl_2$, and 20 mM HEPES (pH 7.2; free $[Ca^{2+}]_i$< 10 nM).

The standard extracellular bath solution (modified Tyrode's solution) contained 153 mM NaCl, 5 mM KCl, 2 mM $CaCl_2$, 1 mM $MgCl_2$, 20 mM HEPES, and 10 mM glucose (pH 7.4). BMMs were incubated with IgG-RBCs at 4 °C for 20 min and then were placed at 37°C and 5% CO_2 for 5~10 min before whole-cell recordings. Dynasore (100 μM) was added when the RBCs were applied to BMMs.

Data analysis

Data are presented as the mean ± SEM. Statistical comparisons were made using analysis of variance (ANOVA). A P value < 0.05 was considered statistically significant.

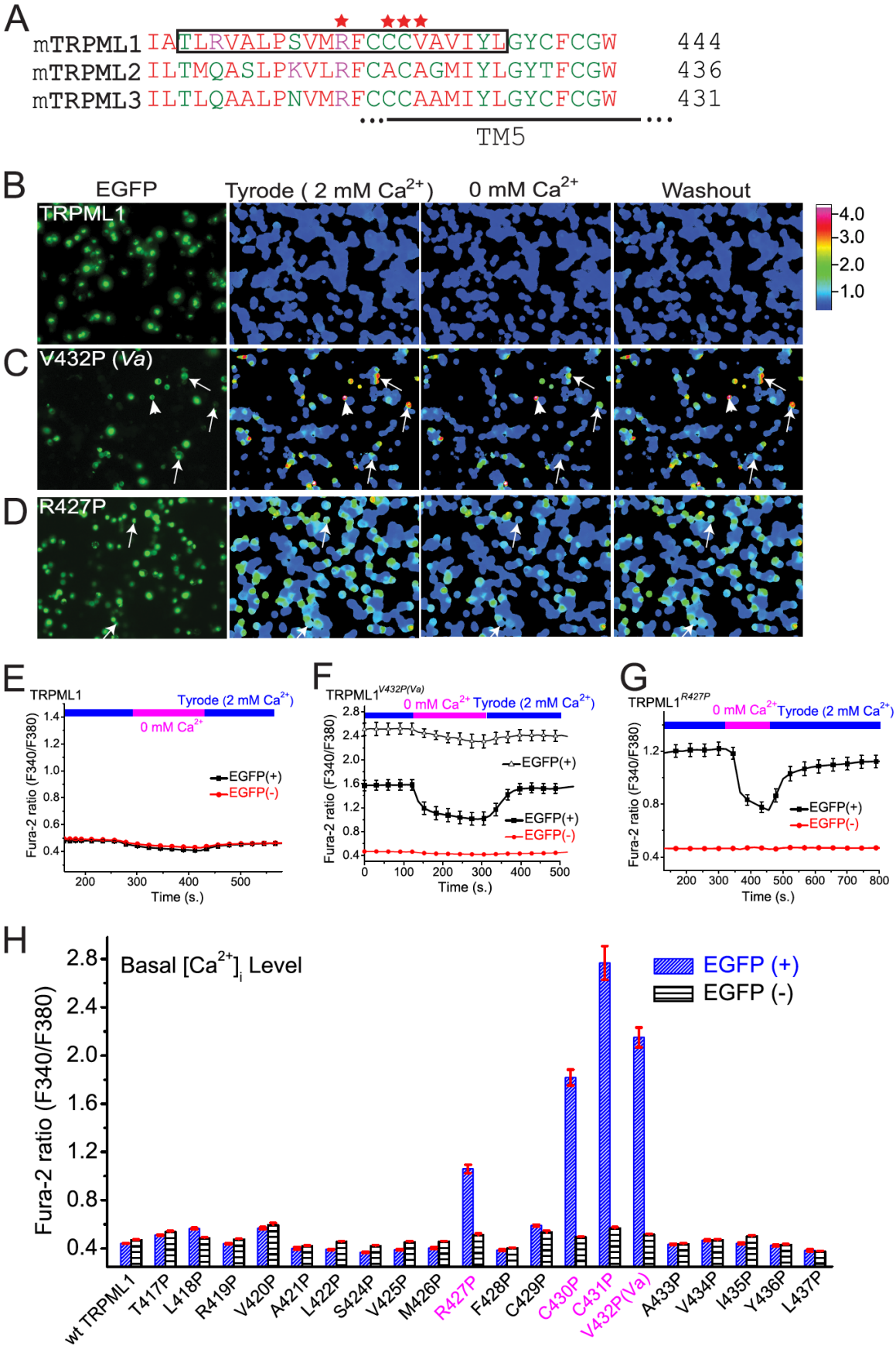
A
mTRPML1 IATLRVALPSVMRFCCCVAVIYLGYCFCGW 444
mTRPML2 ILTMQASLPKVLRFCACAGMIYLGYTFCGW 436
mTRPML3 ILTLQAALPNVMRFCCCAAMIYLGYCFCGW 431
TM5
B
EGFP
Tyrode (2 mM Ca2+)
0 mM Ca2+
Washout
TRPML1
4.0
3.0
2.0
1.0
C
V432P (Va)
D
R427P
E
TRPML1
Tyrode (2 mM Ca2+)
0 mM Ca2+
EGFP(+)
EGFP(-)
Fura-2 ratio (F340/F380)
Time (s.)
F
TRPML1V432P(Va)
0 mM Ca2+ Tyrode (2 mM Ca2+)
G
TRPML1R427P
0 mM Ca2+Tyrode (2 mM Ca2+)
H
Basal [Ca2+]i Level
EGFP (+)
EGFP (-)
Fura-2 ratio (F340/F380)
wt TRPML1
T417P
L418P
R419P
V420P
A421P
L422P
S424P
V425P
M426P
R427P
F428P
C429P
C430P
C431P
V432P(Va)
A433P
V434P
I435P
Y436P
L437P

Figure 5.1. Elevated intracellular Ca^{2+} in HEK293T cells expressing several Pro substitutions of TRPML1 channels.

(A). Alignment of TRPML (TRPML1, TRPML2, and TRPML3) protein sequences in the S4-S5 linker and the bottom half of the TM5. Stars (red) indicate the locations of the amino acids that, when mutated into Pro, resulted in gain-of-function (GOF) channel activity. TM5 (S5), putative transmembrane domain 5. **(B-D).** Elevated intracellular [Ca^{2+}] ($[Ca^{2+}]_i$) in two Pro substitutions of TRPML1. The effect of extracellular Ca^{2+} ($[Ca^{2+}]_o$, 2 mM) on $[Ca^{2+}]_i$ was investigated in HEK293T cells transfected with EGFP-tagged wild-type (WT) TRPML1 and two Pro substitutions (V432P, TRPML1^{V432P}; R427P, TRPML1^{R427P}). TRPML1 protein expression was monitored by the presence of an EGFP signal measured at an excitation of 470 nm (F470). $[Ca^{2+}]_i$ was monitored with Fura2 ratios (F340/F380). Basal $[Ca^{2+}]_i$ in WT TRPML1-transfected cells was similar to nontransfected cells (**B**). In contrast, $[Ca^{2+}]_i$ was significantly elevated in TRPML1^{V432P} (**C**)- and TRPML1^{R427P} (**D**)- transfected cells in the presence of 2 mM extracellular Ca^{2+}. Results are representative of several (n = 4-8) independent experiments. Arrows indicate the representative cells. **(E-G).** In TRPML1^{V432P}- and TRPML1^{R427P}- transfected cells (**F&G**), the Fura-2 ratios dropped significantly when $[Ca^{2+}]_o$ was reduced from 2 mM (Tyrode) to 0 mM (nominal Ca^{2+} plus 1 mM EGTA), and gradually recovered with addition of 2 mM Ca^{2+} (Tyrode; washout). The Fura-2 ratios for WT TRPML1 (**E**) did not change significantly after extracellular Ca^{2+} was removed. Note that for TRPML1^{V432P}, cells with Fura-2 ratios >2 (in empty triangle) and < 2 (in solid square) were plotted separately. **(H).** Average basal $[Ca^{2+}]_i$ in cells transfected with TRPML1 and 20 Pro substitutions in the S4-S5 linker and the bottom half of TM5. Data represent the averaged responses of total 40-120 cells from 3-5 independent experiments.

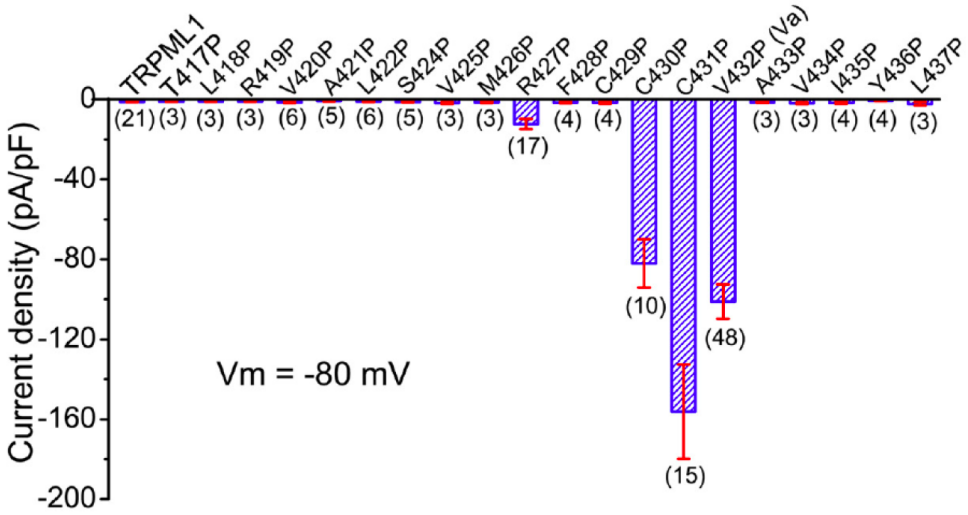

Figure 5.2. Gain-of-function Pro substitutions of TRPML1 channels generated inwardly rectifying whole-cell currents (Contributed by Dr. Xianping Dong).

Average current densities (pA/pF) of 20 Pro substitutions of TRPML1 channels. Only 4 ($I_{TRPML1\text{-}R427P}$, $I_{TRPML1\text{-}C430P}$, $I_{TRPML1\text{-}C431P}$, and $I_{TRPML1\text{-}V432P}$) were significantly larger than I_{TRPML1}, which was not significantly different from the nontransfected cell currents. Currents were measured at -80 mV in the standard extracellular (Tyrode) bath solution and normalized to the size of the cells (capacitance; pF). The number of cells for each Pro substitution is shown in parenthesis.

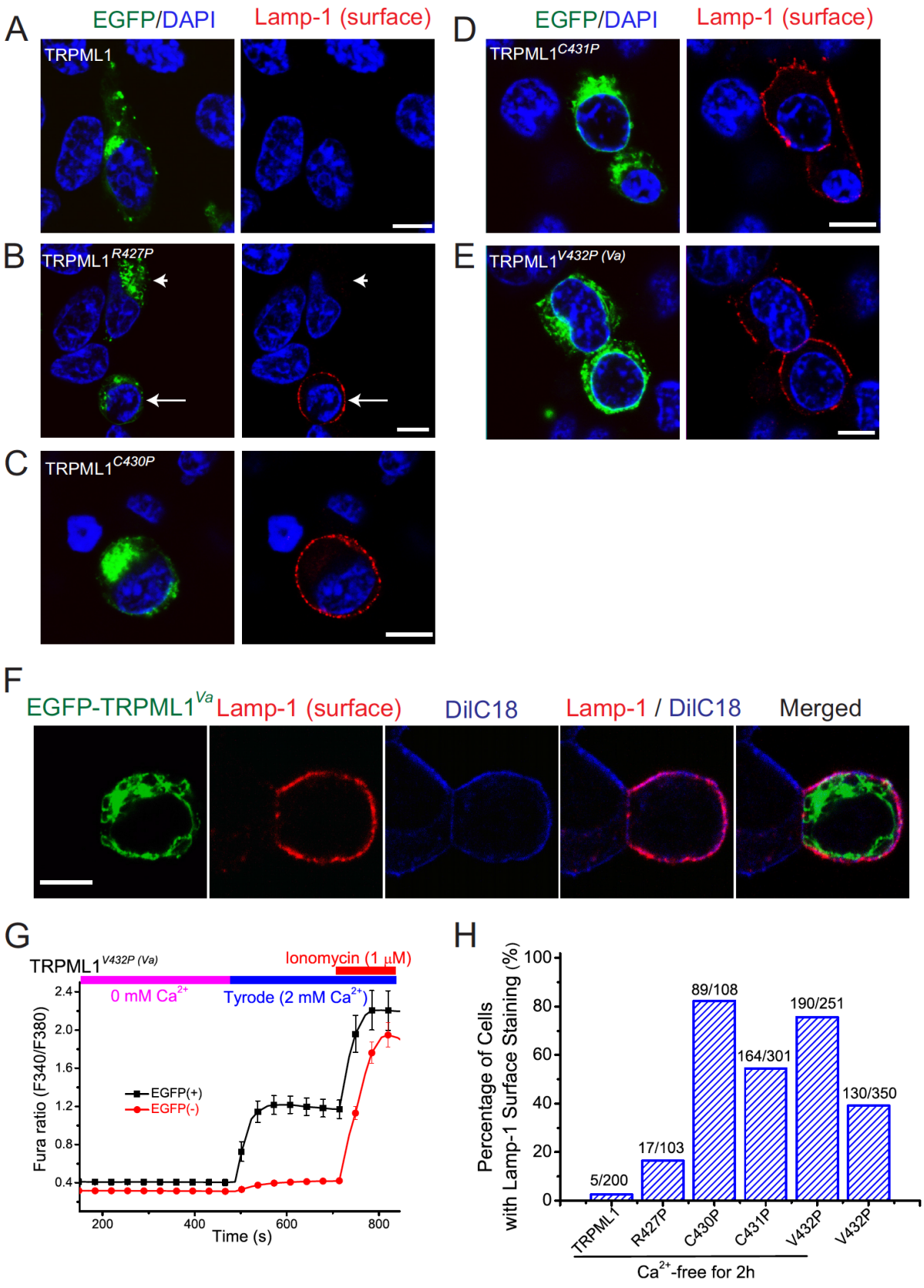
A
EGFP/DAPI
Lamp-1 (surface)
TRPML1
B
TRPML1R427P
C
TRPML1C430P
D
EGFP/DAPI
Lamp-1 (surface)
TRPML1C431P
E
TRPML1V432P (Va)
F
EGFP-TRPML1Va
Lamp-1 (surface)
DilC18
Lamp-1 / DilC18
Merged
G
TRPML1V432P (Va)
Ionomycin (1 μM)
0 mM Ca2+
Tyrode (2 mM Ca2+)
Fura ratio (F340/F380)
EGFP(+)
EGFP(-)
Time (s)
H
Percentage of Cells with Lamp-1 Surface Staining (%)
5/200
17/103
89/108
164/301
190/251
130/350
TRPML1
R427P
C430P
C431P
V432P
V432P
Ca2+-free for 2h

Figure 5.3. High levels of lysosomal exocytosis in HEK cells expressing GOF Pro substitutions of TRPML1.

(A-E). TRPML1 and Pro substitutions were transiently transfected in HEK293T cells. To reduce the cellular toxicity of GOF mutations due to Ca^{2+} overload, these experiments were performed 17–20 h after transfection. Before immunostaining analysis, cells were kept inCa^{2+}-free medium (nominal 0 mM Ca^{2+}, 1 mM EGTA) for 2-6 h. The exocytosis of lysosomal content (lysosomal exocytosis) was monitored by immunostaining of Lamp-1 in non-permeabilized cells using a Lamp-1 antibody whose epitope is located on the luminal side. **(A).** No significant Lamp-1 staining was seen in TRPML1-trasnfected cells. **(B)**. For TRPML1^{R427P}-transfected cells, some exhibited significant Lamp-1 surface staining (see *arrows* for examples), whereas others didn't (see *arrowheads* for examples). Lamp-1 staining in cells transfected with TRPML1^{C430P} **(C)**, TRPML1^{C431P} **(D)**, and TRPML1^{V432P} **(E)**. **(F).** Lamp-1 surface staining in TRPML1^{V432P}-transfected cells was colocalized with the plasma membrane marker DilC18. **(G).** Slightly elevated $[Ca^{2+}]_i$ in TRPML1^{V432P}-transfected cells that were preincubated in Ca^{2+}-free medium for 2-6 h. **(H).** Percentage of EGFP-positive cells with Lamp-1 surface staining under standard (2 mM external Ca^{2+}) and Ca^{2+}-free conditions.

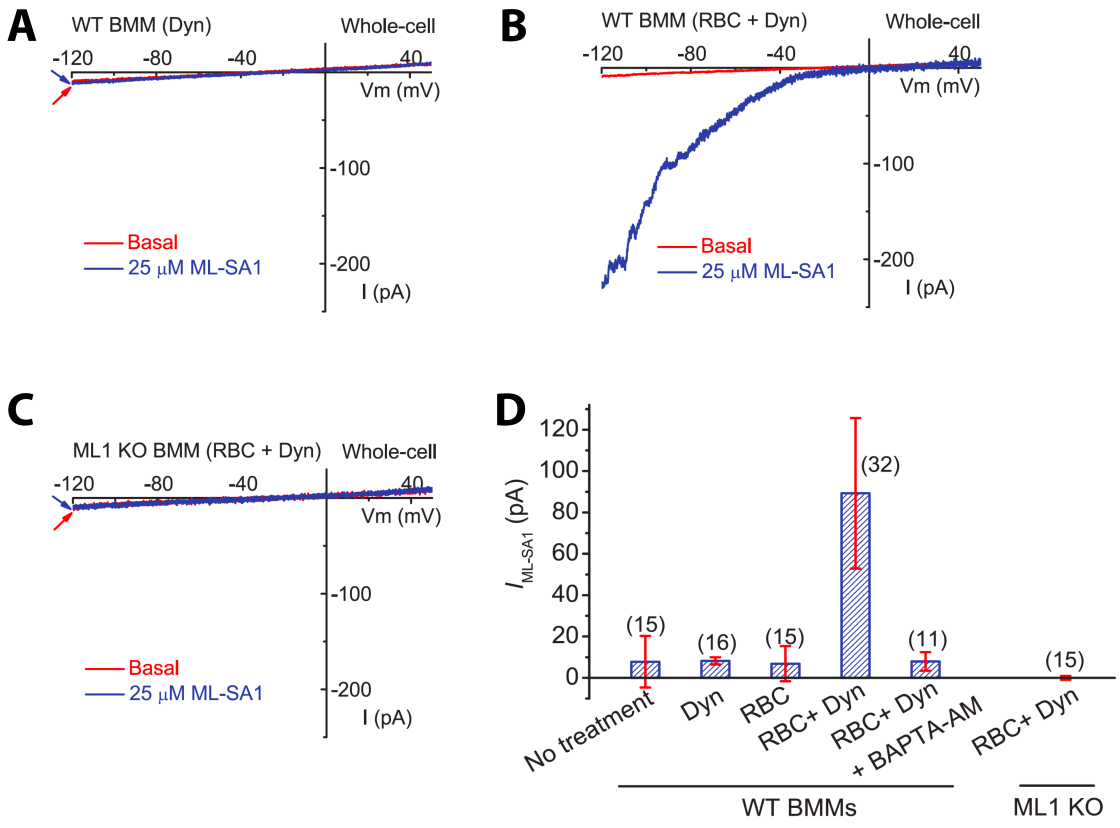

Figure 5.4. Particle binding induces TRPML1-dependent lysosomal exocytosis in macrophages.

(**A-C**). Whole-cell TRPML1-like currents in WT BMMs that were exposed to IgG-RBCs for 10 min. Dynasore (Dyn, 100 μM) was used to block Dynamin-dependent endocytosis to facilitate the detection of whole-cell I_{TRPML1}. No significant whole-cell $I_{TRP\mathrm{ML1}}$ was detected in TRPML1 KO BMMs (IgG-RBCs for 10 min). (**D**) Summary of whole-cell $I_{TRP\mathrm{ML1}}$ under different experimental conditions.

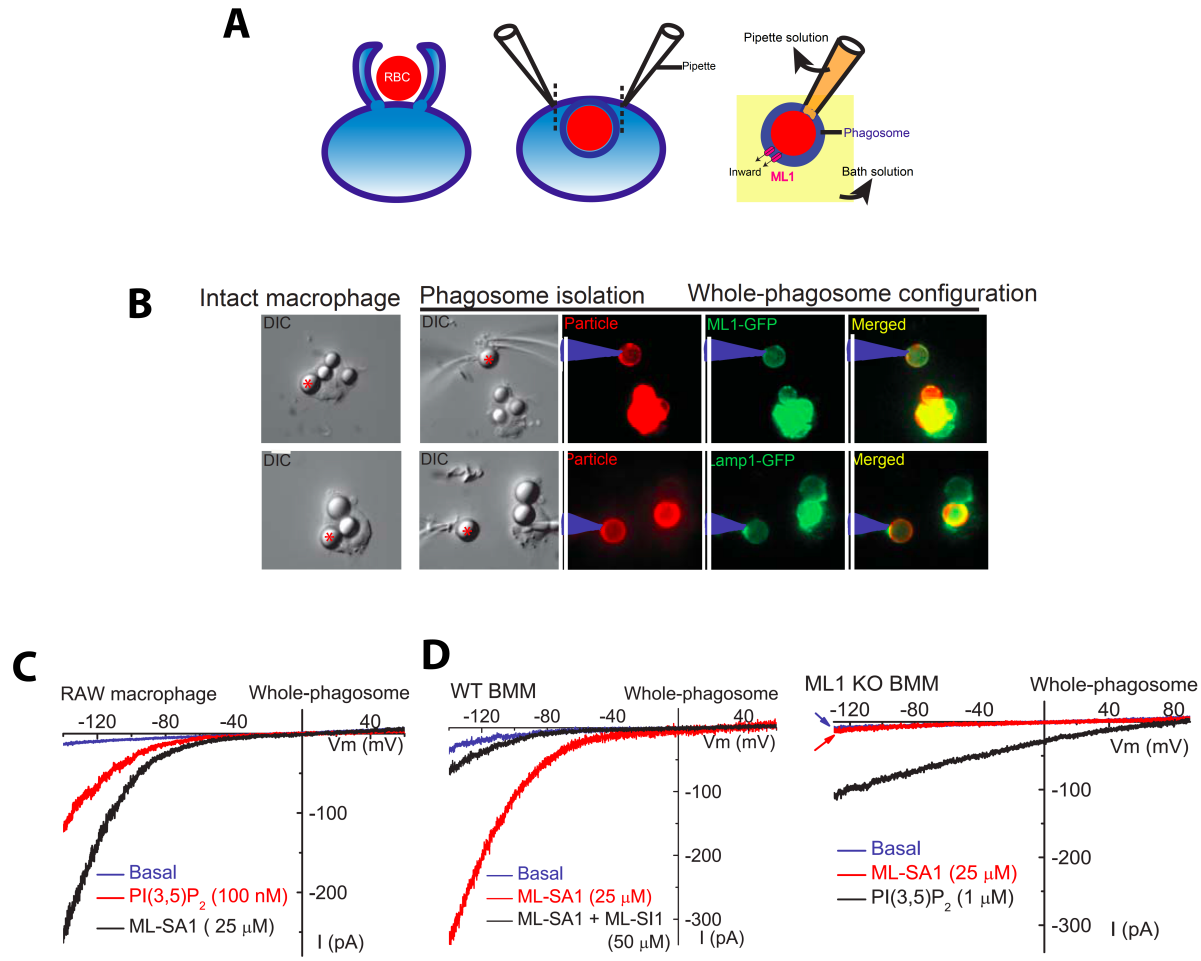

Figure 5.5. Particle binding to macrophages rapidly recruits TRPML1 to the nascent phagosomes.

(A-B). An illustration of whole-phagosome configuration. Cells were transfected with Lamp-1-GFP or TRPML1-GFP and then exposed to IgG-coated beads on ice for 20 min; after phagocytosis was induced by transferring the cells to 37°C for 5 min, the newly formed phagosomes were isolated for electrophysiology. **(C).** ML-SA1- or $PI(3,5)P_2$-activated endogenous whole-phagosome TRPML-like currents in RAW 246.7 cells.

(D). Whole-phagosome I_{TRPML1} in WT, but not TRPML1 KO BMMs. ML-SA1 (25 μM) -activated I_{TRPML1} was inhibited by ML-SI1 (50 μM) in WT phagosomes (left panel). No ML-SA1- activated I_{TRPML1} was seen in TRPML1 KO phagosomes, in which $PI(3,5)P_2$ (1 μM) robustly activated I_{TPC}.

CHAPTER 6

Discussion

6.1 Summary

Lysosomes are intracellular organelles primarily serving as the cell's "garbage disposal and recycling center". Recent compelling evidence has revealed that lysosomes have a range of functions, including membrane trafficking, signal transduction, plasma membrane repair and phagocytosis. Dysfunction of lysosomes contributes to more than 50 types of Lysosomal Storage Diseases (LSD), as well as amyotrophic lateral sclerosis (ALS), Charcot-Marie-Tooth (CMT) disease, and common neurodegenerative diseases, such as Alzheimer's disease, Huntington's disease and Parkinson's disease (Settembre et al., 2013).

Lysosomes are newly recognized ion stores enriched with H^+, Ca^{2+}, and Na^+, and it is established that lysosomal ion homeostasis is essential for the proper functioning of lysosomes. However, until recently the functions of ion transporters and channels residing on lysosomal membranes were barely understood, largely due to the lack of a reliable functional assay for the intracellularly-localized membrane channels, as the conventional patch-clamp technique that has been extensively employed for ion channel studies is mostly limited to the plasma membrane channels. Recently our lab established a modified patch-clamp method (Dong et al., 2008), which allows us to perform electrophysiological recordings directly on native lysosomal membranes. This technique, referred to as lysosome patch-clamp, has opened a new avenue for the study of ion channels/transporters in the lysosome.

My dissertation research has taken advantage of both conventional and lysosomal patch-clamp techniques to study ion channels in the lysosome. Using an integrative approach by combining electrophysiology with molecular biology, Ca^{2+} imaging, immunochemistry, confocal microscopy, and mouse genetics, my goal was to understand how lysosomal channels are regulated by phospholipid signaling, and how this regulation contributes to the function of lysosomes under physiological and pathological conditions. Using lysosome patch-clamp, I have discovered and characterized two novel lysosomal Na^+-selective channels (Two-Pore channels TPC1 and TPC2), and demonstrated that the channels are activated by $PI(3,5)P_2$, an endolysosome-specific phosphoinositide of low-abundance. In collaboration with my colleagues, we have also identified $PI(3,5)P_2$ as the endogenous activator of a Ca^{2+} release channel in the lysosome (mucolipin-1, TRPML1). $PI(3,5)P_2$ signaling is essential for the normal function of the

lysosome, and human mutations in $PI(3,5)P_2$-metabolizing enzymes cause various neurodegenerative diseases, including ALS and CMT diseases (Chow et al., 2007). My results showed that increasing TRPML1 activity alleviated the cellular defects in $PI(3,5)P_2$ deficient cells, which may help develop therapeutic approaches for various neurological diseases associated with the impaired signaling of $PI(3,5)P_2$. Overall, my thesis work has characterized two important channels (TPCs and TRPMLs) in the lysosome, and successfully bridged two separate fields: membrane traffick/ lipid signaling and ion channels (two areas rarely studied together).

TPC proteins form phosphoinositide-activated sodium-selective ion channels in endosomes and lysosomes (Chapter 2 and Chapter 3)

Mammalian Two-Pore Channel proteins (TPC1 and TPC2) are newly cloned members of the voltage-gated cation channel superfamily, which include voltage-gated Na^+ and Ca^{2+} (Na_V and Ca_V) channels. Na_V and Ca_V channels are expressed at the plasma membrane of excitable cells (i.e., muscle cells and neurons), and are very well characterized. In contrast, TPC proteins are localized in the intracellular endosomes and lysosomes, and their functions have remained enigmatic. A number of recent studies suggest that TPCs might mediate lysosomal Ca^{2+} release triggered by the second messenger nicotinic acid adenine dinucleotide phosphate (NAADP) (Calcraft et al., 2009). By directly recording TPCs in endolysosomes from wild-type and TPC double knockout mice, I found that, in contrast to previous studies, TPCs are in fact Na^+-selective channels. Moreover, TPCs are not activated by NAADP, but specifically activated by $PI(3,5)P_2$, an endolysosome-specific phosphoinositide that regulates lysosomal ion homeostasis and membrane potential (See **Fig. 6.1; Fig. 6.2**). Additionally, by combining the lysosomal fractionation and atomic absorption, my colleagues and I found that the primary endolysosomal ion is Na^+, not K^+, as had been previously assumed (Steinberg et al., 2010). The significance of my discovery is multifaceted. First, I have identified TPCs as the first intracellular Na^+-selective channels. Second, it has provided important corrections to the ion channel field. Third, it has revealed a novel mechanism to regulate membrane trafficking: membranous lipids directly regulate ion flux, causing rapid changes in the membrane potential and the fusogenic potential of intracellular organelles.

$PI(3,5)P_2$ controls membrane trafficking by regulating TRPML Ca^{2+} release channels (Chapter 4).

Membrane fusion and fission events in lysosomal membrane trafficking are controlled by both intraluminal Ca^{2+} release and phospholipids, such as $PI(3,5)P_2$. However, the molecular identities of the Ca^{2+} release channels and the target proteins of $PI(3,5)P_2$ are elusive (**See Fig. 6.2**). Using lysosomal recordings, my colleagues and I demonstrated that TRPML1 is the principle Ca^{2+} channel in late endosomes and lysosomes (Dong et al., 2008; Dong et al., 2009). Human mutations in *TRPML1* result in type IV Mucolipidosis (ML4) neurodegenerative diseases, and at the cellular level, lysosomal trafficking defects and lysosome storage. Similar trafficking defects and lysosome storage are also seen in $PI(3,5)P_2$-deficient cells, (for example, cells from amyotrophic lateral sclerosis (ALS) patients carrying mutations in the $PI(3,5)P_2$-synthesizing enzyme complex, i.e. *Fig4* gene (Chow et al., 2007)). Using the patch-clamp technique, my colleagues and I found that $PI(3,5)P_2$ directly activates TRPML1 channels (**Fig. 6.2**). Importantly, I found that the introduction of TRPML1 into fibroblasts with impaired $PI(3,5)P_2$ signaling (from mouse models of ALS) is able to rescue the enlarged vacuole phenotype associated with $PI(3,5)P_2$-deficiency. This work has established a link between $PI(3,5)P_2$ signaling, TRPML1-mediated Ca^{2+} release, and lysosomal membrane trafficking (see **Fig. 1.1**). A novel concept can be developed: lysosome enhancement by stimulating TRPML1's channel activity to speed membrane trafficking may break the vicious cycle between membrane trafficking defects and lysosomal storage, providing a new therapeutic approach for $PI(3,5)P_2$-deficient diseases and many other Lysosomal Storage diseases.

TRPML1-mediated lysosomal Ca^{2+} release induces lysosomal exocytosis (Chapter 5)

The contents of lysosomes undergo exocytosis (lysosomal exocytosis) in response to an increase of intracellular Ca^{2+} (See **Fig. 1.1**). Lysosomal exocytosis has been implicated in a variety of cell biological functions, including neurotransmitter release and plasma membrane repair. The source of Ca^{2+} required in these processes, however, is unclear. By performing mutagenesis screening, I have identified several gain-of-function mutants of TRPML1 that exhibit constitutive Ca^{2+} permeability. Interestingly, using a lysosome protein (Lamp-1) cell surface-staining assay, I found that lysosomal exocytosis is dramatically increased in cells expressing gain-of-function mutants of TRPML1, indicating that TRPML1-mediated Ca^{2+} release may trigger lysosomal exocytosis (Dong et al., 2009). Particle binding in macrophages is a physiological stimulus to

evoke lysosomal exocytosis. Upon particle binding, lysosomal exocytosis is necessary to provide the membrane supplies to engulf particles and facilitate phagosome formation. By whole-phagosome recordings and whole-cell recordings, I found that upon particle binding, TRPML1-associated lysosomes are delivered to the newly-formed phagosomes via lysosomal exocytosis in a Ca^{2+}-dependent manner, suggesting a role of TRPML1 in lysosomal exocytosis and phagosome formation (**Fig 6.2**.). This result, together with recent studies indicating that the induction of lysosomal exocytosis promotes cellular waste clearance (Medina et al., 2011; Settembre et al., 2013), suggests that TRPML1 may serve as an important therapeutic target for disorders associated with intracellular storage, for example, Lysosomal Storage diseases.

6.2 The missing piece in the puzzle-what's the NAADP receptor?

Ever since the discovery of NAADP signaling, intense efforts have been made to search for the NAADP receptor(s). Recently a large body of literature have claimed that TPCs are NAADP receptors, which appeared to be a breakthrough. However, the conclusion was largely based on indirect measurements, and the reported properties of TPC channels are inconsistent among the studies. In sharp contrast, our direct measurements have demonstrated that TPCs are NAADP-insensitive $PI(3,5)P_2$-activated Na^+-selective channels. How should we perceive the dramatically different conclusions?

Let's take a look at their results first. Although different in details, three major lines of evidence for TPCs as NAADP receptors can be summarized from the initial reports in 2009 (Brailoiu et al., 2009; Calcraft et al., 2009; Zong et al., 2009). First, membrane prepared from TPC-overexpressing cells exhibited higher affinity binding to $^{[32P]}$NAADP compared to those from wild-type HEK293 cells. However, this result was challenged by more recent photoaffinity labeling studies (Lin-Moshier et al., 2012; Walseth et al., 2012), which suggested that TPCs are unlikely to be the *bona fide* NAADP binding sites. Although the photolabeled NAADP recapitulated the essential properties of NAADP as a Ca^{2+}-mobilizing messenger, surprisingly, there was no direct labeling of either endogenous or overexpressed TPC channels in the sea urchin egg (Walseth et al., 2011), mammalian cell lines (HEK293 and SKBR3) or mouse pancreas (Lin-Moshier et al., 2011). Moreover, labeling of high affinity NAADP-binding sites was preserved in pancreatic samples from TPC1 and TPC2 knockout mice. Instead, a 22- and 23-KD pair of proteins was identified as NAADP-binding proteins in mammalian cells.

The second evidence came from Ca^{2+} imaging results showing that the NAADP-induced

intracellular Ca^{2+} response was increased in TPC-overexpressing cells, while disrupting TPC-expressions attenuated the effect. This evidence can be challenged from three aspects. First, the enhance NAADP response caused by TPC overexpression may be explained by indirect mechanisms, for example those that are secondary to endolysosomal enlargement associated with TPC overexpression (**Fig. 6.1**). Second, since NAADP is membrane-impermeable, this chemical is usually delivered into intact cells by microinjection/intracellular dialysis (Brailoiu et al., 2009; Calcraft et al., 2009; Zong et al., 2009). The operation itself may cause some artifacts, for example, it may induce mechanically-sensitive Ca^{2+} response. Some other groups, including ours, employed NAADP-AM, a membrane-permeable form of NAADP (Aley et al., 2010; Ruas et al., 2010), although this chemical is not very stable and tends to get hydrolyzed (Parkesh et al., 2008). Third, in our hands, although we observed NAADP-evoked Ca^{2+} response in pancreatic β-cell lines (INS1 and MIN6), surprisingly, TPC currents were absent in the endolysosomes from these cells.

The third and apparently most convincing evidence was from TPC2 knockout studies. Whole-cell patch clamp recordings showed that a NAADP-induced plasma membrane cation conductance was lost in TPC2 knockout pancreatic β cells (Calcraft et al., 2009). However, this plasma membrane conductance is uncharacterized and the molecular mechanism is unidentified. Also, there was no evidence that this conductance is specifically dependent on NAADP-induced intracellular Ca^{2+} release. In contrast, we observed largely comparable NAADP Ca^{2+} response in TPC1/TPC2 KO pancreatic islets, compared with that in WT islets, suggesting that NAADP Ca^{2+} response may not be dependent on TPCs.

The NAADP-activated TPC currents were subsequently reported by three groups (Brailoiu et al., 2010; Pitt et al., 2010; Schieder et al., 2010), by employing different ways to examine the intracellularly-localized TPC channels using electrophysiology. The first group (Schieder et al., 2010) used a planar patch-clamp technique to record from isolated lysosomes enlarged by vacuolin-1, a method similar to ours. Lysosomes from TPC2-overexpressing cells displayed NAADP-evoked currents with a Ca^{2+} selectivity over K^+ by >1000 folds, and the currents were only observed with intraluminal low pH, but not neutral pH. However, K^+ and Ca^{2+} were the only cations included in the recording solution, and the current size might be too small for the TPC-overexpressing system (at least 50 folds smaller compared with our results). Based on the small current size, it would be difficult to distinguish the NAADP-induced response and possible endogenous background currents. Another group (Pitt et al., 2010)

incorporated immunopurified TPC2 into artificial planar lipid bilayer membranes, an approach traditionally used to study IP_3 and RyRs. Results from single channel recordings indicated that the NAADP-evoked TPC2 current is K^+-permeable, and the luminal pH has little effects on the current size. While the artificial lipid bilayer technique may provide advantages to show that TPC2 itself is the pore-forming channel without contaminating from other membrane proteins, although it requires a series of control experiments to verify the purity of the incorporated proteins. Further, more control experiments are required to establish that TPC2 protein is responsible to the single channel conductance, such as pore mutations causing the changes of conductance or selectivity. The third group (Brailoiu et al., 2010) found that deletion of a di-leucine motif in the N terminus of TPC2 resulted in its mistargeting to the plasma membrane, where the traditional whole-cell patch clamp technique could be applied. Results from this study concluded that TPC2 is a Cs^+-permeable channel, although the experiments raised a few concerns, including the possible changes of channel properties in the non-native location, and using an inappropriately-controlled pipette solution, i.e., with no Ca^{2+} buffer, which may induce endogenous Ca^{2+}-sensitive currents. In summary, all three channel studies suggested TPC2 is activated by NAADP, although the TPC2 currents were shown to be K^+-permeable (Pitt et al., 2010), Cs^+- permeable (Brailoiu et al., 2010), or Ca^{2+}-selective (Schieder et al., 2010).

Using our established lysosome-recording method, we directly measured that TPCs are $PI(3,5)P_2$ activated Na^+-selective channels. However, we found that NAADP failed to induce or modify TPC currents in either endogenous or overexpression systems, although NAADP activated the plasma membrane TRPM2 at μM level, suggesting that TPC2 is not activated by NAADP. One concern about our approach is that the NAADP- sensitive conductance might be lost due to vacuolin-1 treatment. However, we have also tested a plasma membrane expressed TPC2 mutant, which underwent no vacuolin-1 treatment. The plasma membrane TPC2 mutant has the same electrophysiological properties as WT TPC2 (lysosomal TPC2), and consistently, this mutant was only activated by $PI(3,5)P_2$, but not NAADP. Thus our results showed that TPCs are $PI(3,5)P_2$-activated Na^+-selective channels, and they are unlikely to be NAADP receptors, although they may be involved in NAADP signaling indirectly.

Thus the molecular identity of NAADP receptor(s) remains elusive. Besides TPCs, TRPML1, TRPM2 and RyRs have been proposed to be involved in NAADP signaling, however, none of them has been conclusively proved to be NAADP receptors. Recently, Lin-Moshier et al. discovered an NAADP-bound 22-23-kDa lysosomal proteins (Lin-Moshier et al., 2011) which

may be involved in NAADP signaling or serve as the NAADP receptor, but the molecular identity of the protein remains enigmatic. Putative NAADP receptors may be lysosomal Ca^{2+}-permeable channels activated by NAADP, and can be blocked by Ned-19 (Naylor et al., 2009a; Rosen et al., 2009; Thai et al., 2009). Further, the dose-dependence curve for NAADP response was proposed to be "bell-shaped" (Galione, 2011), with maximal responses at ~ 100 nM of NAADP, whereas no response at > 1 μM. It's also possible that NAADP might target other non-Ca^{2+} conductances (e.g. anion conductance), and indirectly induces lysosomal Ca^{2+} release.

Since we have not been able to detect any NAADP-activated whole-endolysosome current, it is also possible that NAADP, like Bafilomycin-A1 and Glycyl-L-phenylalanine 2-naphthylamide (GPN) (Morgan et al., 2011), might act via non- channel-mediated Ca^{2+} release mechanisms. Or NAADP might inhibit putative Ca^{2+} pump responsible for lysosomal Ca^{2+} refilling and cause Ca^{2+} leak. In addition, NAADP might also induce Ca^{2+} release from non-lysosomal Ca^{2+} stores, but in a lysosome-dependent manner. Molecular identification of the NAADP-bound 22-23-kDa lysosomal proteins (Lin-Moshier et al., 2011) may prove helpful distinguishing these possibilities.

6.3 TPC proteins mediated Na^+-efflux from lysosomes

We have demonstrated that TPC proteins form $PI(3,5)P_2$-activated Na^+-selective ion channels in the lysosome, However, the *in vivo* function of $PI(3,5)P_2$ – TPCs pathway is still largely unknown. Here I will discuss its potential roles in regulating lysosomal Na^+ dynamics and lysosomal membrane depolarization.

Lysosomes are abundant with Na^+ ions. Using cellular fractionation combined with atomic absorption spectroscopy, we measured that the major cation in the lysosomal lumen is Na^+, with the K^+/Na^+ ratio around 0.01. Assuming that lysosome lumen is water-based, iso-osmotic relative to the cytosol, and all the cations are osmotically active (free ions), we estimated the luminal Na^+ concentration to be ~150 mM. If we assume the average lysosome size is 0.5 μm - the lysosome size varies from 0.1 μm to 1.2 μm (Luzio et al., 2007b) - then each lysosome may contain ~ 10^{-17} mol of Na^+, *i.e.* 6×10^6 of Na^+ ions per lysosome.

Is $PI(3,5)P_2$ level high enough *in vivo* to activate TPCs? Very likely, especially under the stimulated condition. $PI(3,5)P_2$ makes up ~0.04% of total cellular PIs in non-stimulated condition (Dove et al., 2009; Zolov et al., 2012), and is ~0.2-1% of $PI(4,5)P_2$, whose

concentration is estimated to be 4~10 μM on the plasma membrane. (Lemmon, 2008; Zolov et al., 2012). In a 10 μm-diameter cell with 200 late endosomes/lysosomes (0.5 μm- diameter), the total surface area of late endosomes/ lysosomes where $PI(3,5)P_2$ localized, is roughly half of the surface area of plasma membrane where $PI(4,5)P_2$ localized. Thus in such modal cell, $PI(3,5)P_2$ concentration in the LELs under resting condition could range from 4 nM (4 μM × 1/2 × 0.2%) to 50 nM (10 μM × 1/2 × 1%). This estimation assumed the even distribution of $PI(3,5)P_2$ in endolysosomes. However, $PI(3,5)P_2$ is enriched in microdomains where PIKfyve complex is localized (Dove et al., 2009). Further, $PI(3,5)P_2$ level can rapidly increase by 2-20 folds upon stimulation in mammalian cells or yeast cells (Lemmon, 2008; Suh and Hille, 2008). Thus upon stimulation, $PI(3,5)P_2$ concentration enriched in microdomains may reach ~μM range, a concentration high enough to induce appreciable TPCs-mediated Na^+ efflux from lysosomes.

$PI(3,5)P_2$-dependent Na^+ efflux through TPCs may cause a rapid lysosomal membrane depolarization, at a time course of milliseconds range. Based on the lysosomal recordings results, 1 μM $PI(3,5)P_2$ activated ~100 pA of endogenous I_{TPC} at -50 mV (see **Fig. 2.5**) in macrophages (the transmembrane potential is estimated to be +30 ~ +110 mV relative to the cytosol, and here 50 mV was simply picked as an example). Thus the channel conductance is $g = 2 \times 10^{-9}$ S. The average capacitance of enlarged endolysosomes we recorded is ~ 1 pF. Based on the membrane specific capacitance $C_M = 1$ μF/cm^2, we can calculate the specific conductance of a 1-cm^2 area of membrane g_M, and further get the membrane time constant $\tau_M = C_M/g_M = 0.5$ ms. Thus, upon the opening of TPCs, and along an exponential time course with a time constant of 0.5 ms (τ_M):

$$E = [1 - \exp(-t / 0.5\ \text{ms})] \cdot (-50\ \text{mV})$$

A membrane potential change from -50 mV to 0 mV takes only a few milliseconds (t). During this process, an excess charge of $Q = EC_M = 50 \times C_M = 5 \times 10^{-8}$ C/cm^2 has been separated across the membrane. Assuming this charge is all carried by Na^+ ions, this amount is equivalent to an efflux of $Q/F = 5 \times 10^{-13}$ mole of Na^+ ions per cm^2 of membrane. As calculated above, each lysosome contains roughly 10^{-17} mole of Na^+, which, if divided by the lysosomal surface area (4π (0.5 μm)^2), give us an estimate of 5×10^{-9} mole of Na^+ per cm^2 of lysosomal membrane. Therefore, in a few milliseconds, TPCs –mediated membrane depolarization (50 mV) might move 5×10^{-13} mole/ 5×10^{-9} mole = 0.01% of the Na^+ ions out of the lysosomal lumen.

Downstream effects of TPCs-mediated Na^+ efflux

The above discussions demonstrate that the activation of the Na^+-selective channels (TPCs) may

also activate other unidentified voltage-sensitive proteins in the lysosome, such as voltage-dependent ion channels or voltage-dependent phosphatases (Schroder et al., 2010), and thus regulate endolysosomal functions.

Further, since TPCs barely have voltage-dependent inactivation (especially at -50 mV for TPC2, see **Fig 2.6**), and are not desensitized with constant presence of $PI(3,5)P_2$, in the absence an rapid "shut down" mechanism, the opening of TPCs may cause massive Na^+ efflux, and thereby dramatically changing of the local ionic milieu. It is possible that a substantial amount of Na^+ efflux into the cytosol from a pool of lysosomes in the close vicinity of the plasma membrane (including dendrites and axons) in excitable cells may induce or modulate the formation of action potentials. The identification of membrane-permeable activators of TPCs may prove helpful to test this possibility.

The change in Na^+ composition may also have impacts on other luminal ions through different transporters, e.g. pH regulation (see the discussion below). It's also conceivable that a large Na^+ efflux may cause the local decrease the luminal osmolality and subsequent change in endolysosome morphology, and potentially influence their functions (Manneville et al., 2008).

"Shut down" mechanism of TPC proteins

Because of the rapid membrane depolarization and the lack of efficient inactivation mechanisms, TPCs need to be turned on or turned off in a rapid and tightly regulated manner. One possible regulatory mechanism is through the fast turnover of activation signals. The level of $PI(3,5)P_2$ is tightly regulated both spatially and temporally by a protein complex enriched in microdomains, including the PI 5-kinase PIKfyve, the scaffolding protein Vac14, the phosphatase Fig4 and regulators Vac7 and Atg18 (Dove et al., 2009; Ho et al., 2012). It is likely that constitutive signals or acute stimuli may recruit or activate PIKfyve present in microdomains, result in a rapid and transient increase in $PI(3,5)P_2$ level, and thereby induce TPCs-mediated Na^+ efflux. It is worth mentioning that when we assay TPC channel activities using lysosomal recordings, a water soluble form of $PI(3,5)P_2$ (diC8) is applied globally, while *in vivo* form of $PI(3,5)P_2$ (diC16-$PI(3,5)P_2$) might be less potent compare to the diC8-$PI(3,5)P_2$ (Dong et al., 2010a). Therefore higher concentration of $PI(3,5)P_2$ may be needed to activate TPCs in physiological condition. Alternatively TPCs may be negatively regulated by either cytosolic factors or lysosomal luminal factors. For example, ATP is proposed to inhibit TPC activities related with metabolic status (Cang et al., 2013). It remains to be tested whether other signal lipids/proteins

can inhibit TPCs.

$PI(3,5)P_2$: an activator or a permissive factor

The precise concentration of local $PI(3,5)P_2$ in endolysosomes under basal or stimulated conditions is not known. Therefore the $PI(3,5)P_2$ regulation mechanism for TPCs remains unclear. A rapid increase of PI(3,5)P2 up to μM range may transiently induce large TPC conductance, or a high nM basal level of PI(3,5)P2 may cause constitutive small Na+ leak through TPCs (Cang et al., 2013). Moreover, it is also possible that $PI(3,5)P_2$ may play a permissive role to sensitize, yet not fully activate TPCs, and other activation mechanisms may be exist. As an example, the plasma membrane isoform $PI(4,5)P_2$ has been shown to be a permissive factor for the activation of voltage-gated Ca^{2+} channels in response to depolarization (Suh and Hille, 2008; Wu et al., 2002).

6.4 The potential functions of TPCs

Based on our studies, the large Na^+ gradient across the endolysosomal membrane, together with the presence of Na^+-selective channels have clearly suggested important roles of the Na^+ efflux conductance, although our knowledge about the regulations and functions of TPCs are very primitive. Here are some speculations on the possible cellular functions of TPCs (see **Fig. 6.1**).

TPCs may regulate membrane trafficking

First, TPCs-mediated Na^+ influx may be involved in defining compartmental specificity and determining the fusogenic potential of endolysosomes. A bold hypothesis is that, similar to the scenario on the plasma membrane, the efflux of Na^+ may cause lysosomal membrane depolarization, and act as intracellular signals, since lysosomes are presumed to be luminal-side positive at rest (estimated to be +30 to +110 mV) (Dong et al., 2010b; Morgan et al., 2011). In addition, the local, transient Na^+ efflux in response to the $PI(3,5)P_2$ increase may rapidly reduce and reverse the endolysosomal potential, and promote its fusion with the oppositely charged lipid bilayer of another vesicle in contact (Anzai et al., 1993; Epand and Hui, 1986). Indeed, consistent with a previous report (Ruas et al., 2010), we found that TPC overexpression results in enlarged endolysosomes, which might be caused by enhanced endolysosomal fusion, decreased fission, or both. Second, TPCs may contribute to the formations of special membrane structures. It has long been known that Na^+ and K^+ exhibit differential effects on membrane curvature *in*

vitro (Kraayenhof et al., 1996). If this is also true *in vivo*, it's conceivable that the enrichment of Na^+ channels in microdomains and the resultant Na^+ flux may help the formation or maintenance of tubular structures for sorting or intraluminal vesicles for degradation. Third, as we discussed in section 6.3, $PI(3,5)P_2$ may play a permissive role to prepare TPCs for opening. In that case, TPCs may integrate multiple trafficking cues, together with $PI(3,5)P_2$ to regulate membrane trafficking. For example, TPCs might be activated by mechanical force generated by the membrane curvature. Finally, unlike TRPML1 (Shen et al., 2011), TPCs are not expressed in every cell type, suggesting that their role in membrane trafficking is more specific. Furthermore, because membrane fusion could occur even in *in vitro* reconstitution systems, neither TPCs nor TRPMLs might be required as direct participants in the basic membrane fusion machinery (Shen et al., 2011). However, they may regulate the direction and specificity of lysosomal trafficking *in vivo*. Indeed, lysosomal trafficking is significantly delayed, although not blocked in cells lacking TRPML1 (Shen et al., 2011). Future research may reveal the relative importance of Na^+ *versus* Ca^{2+}, and TRPMLs *versus* TPCs in spatial and temporal regulation of lysosomal trafficking.

TPCs may participate in luminal pH regulations in endolysosomes

A putative efflux of monovalent cation (K^+ or Na^+), together with our demonstration of a large Na^+ gradient across the endolysosomal membrane, suggests that Na^+-permeable TPCs, but not K^+ release conductance, may contribute to endolysosomal pH regulation at rest condition or in a transient and localized manner. In addition, rapid changes in Na^+ content will drive Na^+/H^+ exchangers (NHEs, expressed in endosomes but not in lysosomes) in the organelle membrane, thus changing organellar pH. To understand the exact sequence of events, it is crucial to identify the putative transporters in endolysosomal membranes and devise more accurate methods to measure endolysosomal potentials in intact cells.

TPCs are ATP-sensitive channels regulated by mTOR

A follow up study from Cang et al. (Cang et al., 2013) agreed with our demonstration that TPC proteins form NAADP-insensitive $PI(3,5)P_2$ activated Na^+-selective channels. Moreover they proposed that TPCs may associate with mTOR complex to sense cellular nutrient level. They hypothesized that TPCs have a basal channel activity, and are inhibited by sub-mM level of ATP. The inhibitory effect requires the mTOR complex. Their working model is that at nutrient replete status, TPCs are inhibited, while during cell starvation, ATP level falls, mTOR dissociates from

the lysosomal membrane, and TPCs are released from inhibition. Interestingly, TPCs-knockout mice are found to have severely reduced endurance after fasting. However, the involvement of TPCs in mTOR signaling at cellular and animal level remains to be uncovered.

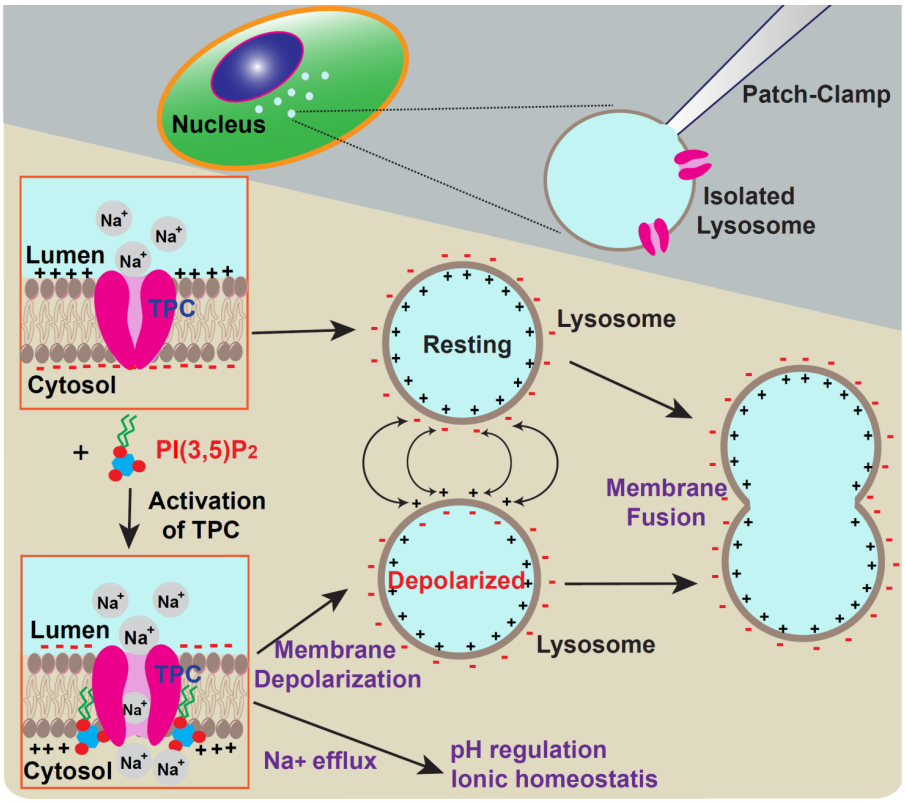

Figure 6.1. TPC-mediated Na^+ flux may be involved in membrane trafficking and pH regulation in endolysosomes

TPC proteins are Na^+-selective channels in lysosomes, specifically activated by $PI(3,5)P_2$. TPC-mediated Na^+ flux in response to a localized increase in $PI(3,5)P_2$ may rapidly depolarize endolysosomal membranes and promote fusion, since lysosomes are presumed to be luminal-side positive at rest (estimated to be +30 to +110 mV). In addition, the TPC mediated Na^+ efflux may serve as cation counterflux to support the maintenance of lysosomal acidification, and may also actively participate in pH regulation in a transient and localized manner.

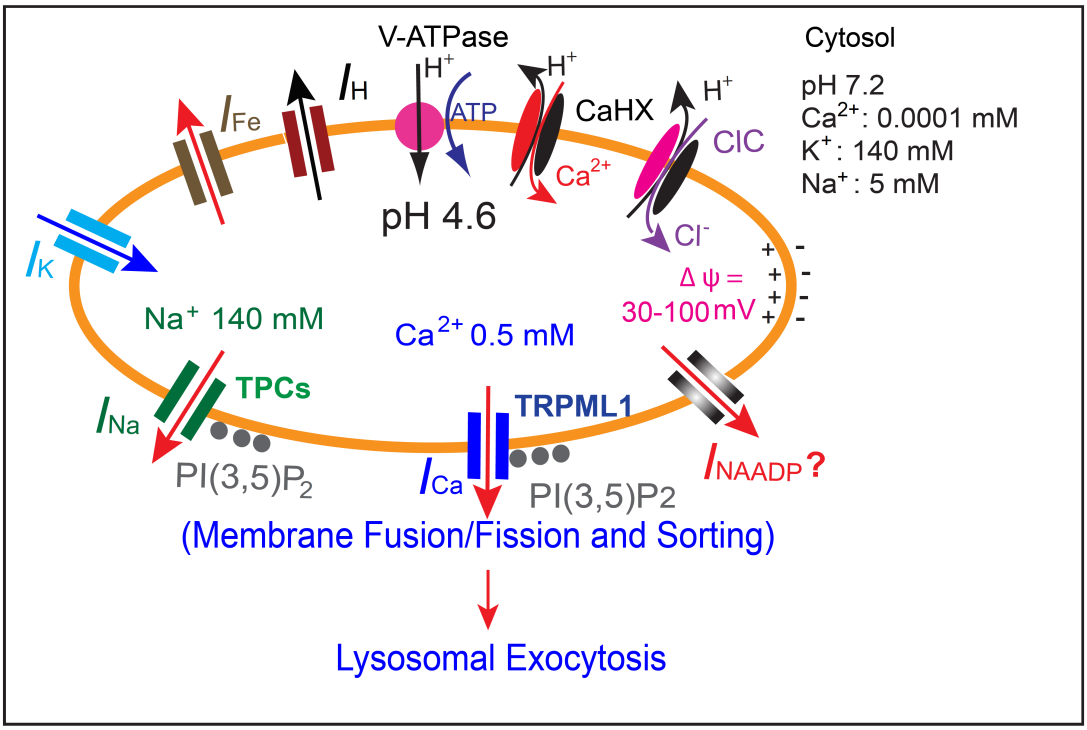

Figure. 6.2. TRPML1 and TPCs in the endolysosome

My thesis work has identified that Two-Pore Channels (TPCs) are Na^+-selective channels, activated by $PI(3,5)P_2$, but not by NAADP, although the function of TPCs remains uncovered. Since TPCs are unlikely to be the NAADP receptors, the proteins mediating NAADP-evoked Ca^{2+} signaling remain enigmatic. In addition, my work has contributed to the discovery that $PI(3,5)P_2$ controls membrane trafficking by directly activating the lysosomal Ca^{2+}-release channel TRPML1. Also, I found that TRPML1 is involved in Ca^{2+}-dependent lysosomal exocytosis, a fundamental process important for cellular clearance, phagocytosis and plasma membrane repair.

Reference

Abe, K., and Puertollano, R. (2011). Role of TRP channels in the regulation of the endosomal pathway. Physiology *26*, 14-22.

Ahluwalia, J.P., Topp, J.D., Weirather, K., Zimmerman, M., and Stamnes, M. (2001). A role for calcium in stabilizing transport vesicle coats. The Journal of biological chemistry *276*, 34148-34155.

Aley, P.K., Mikolajczyk, A.M., Munz, B., Churchill, G.C., Galione, A., and Berger, F. (2010). Nicotinic acid adenine dinucleotide phosphate regulates skeletal muscle differentiation via action at two-pore channels. Proceedings of the National Academy of Sciences of the United States of America *107*, 19927-19932.

Altarescu, G., Sun, M., Moore, D.F., Smith, J.A., Wiggs, E.A., Solomon, B.I., Patronas, N.J., Frei, K.P., Gupta, S., Kaneski, C.R.*, et al.* (2002). The neurogenetics of mucolipidosis type IV. Neurology *59*, 306-313.

Altimimi, H.F., and Schnetkamp, P.P. (2007). Na+/Ca2+-K+ exchangers (NCKX): functional properties and physiological roles. Channels *1*, 62-69.

Alzamora, R., Thali, R.F., Gong, F., Smolak, C., Li, H., Baty, C.J., Bertrand, C.A., Auchli, Y., Brunisholz, R.A., Neumann, D.*, et al.* (2010). PKA regulates vacuolar H+-ATPase localization and activity via direct phosphorylation of the a subunit in kidney cells. The Journal of biological chemistry *285*, 24676-24685.

Andrews, N.W. (2000). Regulated secretion of conventional lysosomes. Trends in cell biology *10*, 316-321.

Andrews, N.W. (2005). Membrane resealing: synaptotagmin VII keeps running the show. Science's STKE : signal transduction knowledge environment *2005*, pe19.

Andrews, N.W., and Chakrabarti, S. (2005). There's more to life than neurotransmission: the regulation of exocytosis by synaptotagmin VII. Trends in cell biology *15*, 626-631.

Anzai, K., Masumi, M., Kawasaki, K., and Kirino, Y. (1993). Frequent fusion of liposomes to a positively charged planar bilayer without calcium ions. Journal of biochemistry *114*, 487-491.

Arantes, R.M., and Andrews, N.W. (2006). A role for synaptotagmin VII-regulated exocytosis of lysosomes in neurite outgrowth from primary sympathetic neurons. The Journal of neuroscience : the official journal of the Society for Neuroscience *26*, 4630-4637.

Arredouani, A., Evans, A.M., Ma, J., Parrington, J., Zhu, M.X., and Galione, A. (2010). An emerging role for NAADP-mediated Ca2+ signaling in the pancreatic beta-cell. Islets *2*, 323-330.

Bargal, R., Avidan, N., Ben-Asher, E., Olender, Z., Zeigler, M., Frumkin, A., Raas-Rothschild,

A., Glusman, G., Lancet, D., and Bach, G. (2000). Identification of the gene causing mucolipidosis type IV. Nature genetics *26*, 118-123.

Bassi, M.T., Manzoni, M., Monti, E., Pizzo, M.T., Ballabio, A., and Borsani, G. (2000). Cloning of the gene encoding a novel integral membrane protein, mucolipidin-and identification of the two major founder mutations causing mucolipidosis type IV. American journal of human genetics *67*, 1110-1120.

Bassil, E., Ohto, M.A., Esumi, T., Tajima, H., Zhu, Z., Cagnac, O., Belmonte, M., Peleg, Z., Yamaguchi, T., and Blumwald, E. (2011). The Arabidopsis intracellular Na+/H+ antiporters NHX5 and NHX6 are endosome associated and necessary for plant growth and development. The Plant cell *23*, 224-239.

Beck, A., Kolisek, M., Bagley, L.A., Fleig, A., and Penner, R. (2006). Nicotinic acid adenine dinucleotide phosphate and cyclic ADP-ribose regulate TRPM2 channels in T lymphocytes. FASEB journal : official publication of the Federation of American Societies for Experimental Biology *20*, 962-964.

Berg, I., Potter, B.V., Mayr, G.W., and Guse, A.H. (2000). Nicotinic acid adenine dinucleotide phosphate (NAADP(+)) is an essential regulator of T-lymphocyte Ca(2+)-signaling. The Journal of cell biology *150*, 581-588.

Berridge, M.J., Lipp, P., and Bootman, M.D. (2000). The versatility and universality of calcium signalling. Nature reviews Molecular cell biology *1*, 11-21.

Boittin, F.X., Galione, A., and Evans, A.M. (2002). Nicotinic acid adenine dinucleotide phosphate mediates Ca2+ signals and contraction in arterial smooth muscle via a two-pool mechanism. Circulation research *91*, 1168-1175.

Bonangelino, C.J., Catlett, N.L., and Weisman, L.S. (1997). Vac7p, a novel vacuolar protein, is required for normal vacuole inheritance and morphology. Molecular and cellular biology *17*, 6847-6858.

Bonangelino, C.J., Nau, J.J., Duex, J.E., Brinkman, M., Wurmser, A.E., Gary, J.D., Emr, S.D., and Weisman, L.S. (2002). Osmotic stress-induced increase of phosphatidylinositol 3,5-bisphosphate requires Vac14p, an activator of the lipid kinase Fab1p. The Journal of cell biology *156*, 1015-1028.

Botelho, R.J., Efe, J.A., Teis, D., and Emr, S.D. (2008). Assembly of a Fab1 phosphoinositide kinase signaling complex requires the Fig4 phosphoinositide phosphatase. Molecular biology of the cell *19*, 4273-4286.

Brailoiu, E., Churamani, D., Cai, X., Schrlau, M.G., Brailoiu, G.C., Gao, X., Hooper, R., Boulware, M.J., Dun, N.J., Marchant, J.S*., et al.* (2009). Essential requirement for two-pore channel 1 in NAADP-mediated calcium signaling. The Journal of cell biology *186*, 201-209.

Brailoiu, E., Churamani, D., Pandey, V., Brailoiu, G.C., Tuluc, F., Patel, S., and Dun, N.J. (2006). Messenger-specific role for nicotinic acid adenine dinucleotide phosphate in neuronal differentiation. The Journal of biological chemistry *281*, 15923-15928.

Brailoiu, E., Patel, S., and Dun, N.J. (2003). Modulation of spontaneous transmitter release from the frog neuromuscular junction by interacting intracellular Ca(2+) stores: critical role for nicotinic acid-adenine dinucleotide phosphate (NAADP). The Biochemical journal *373*, 313-318.

Brailoiu, E., Rahman, T., Churamani, D., Prole, D.L., Brailoiu, G.C., Hooper, R., Taylor, C.W., and Patel, S. (2010). An NAADP-gated two-pore channel targeted to the plasma membrane uncouples triggering from amplifying Ca2+ signals. The Journal of biological chemistry *285*, 38511-38516.

Brandt, S., and Jentsch, T.J. (1995). ClC-6 and ClC-7 are two novel broadly expressed members of the CLC chloride channel family. FEBS letters *377*, 15-20.

Braun, V., Fraisier, V., Raposo, G., Hurbain, I., Sibarita, J.B., Chavrier, P., Galli, T., and Niedergang, F. (2004). TI-VAMP/VAMP7 is required for optimal phagocytosis of opsonised particles in macrophages. The EMBO journal *23*, 4166-4176.

Burgoyne, R.D., and Clague, M.J. (2003). Calcium and calmodulin in membrane fusion. Biochimica et biophysica acta *1641*, 137-143.

Byrne, S.L., Steere, A.N., Chasteen, N.D., and Mason, A.B. (2010). Identification of a kinetically significant anion binding (KISAB) site in the N-lobe of human serum transferrin. Biochemistry *49*, 4200-4207.

Calcraft, P.J., Ruas, M., Pan, Z., Cheng, X., Arredouani, A., Hao, X., Tang, J., Rietdorf, K., Teboul, L., Chuang, K.T.*, et al.* (2009). NAADP mobilizes calcium from acidic organelles through two-pore channels. Nature *459*, 596-600.

Cancela, J.M., Churchill, G.C., and Galione, A. (1999). Coordination of agonist-induced Ca2+-signalling patterns by NAADP in pancreatic acinar cells. Nature *398*, 74-76.

Cang, C., Zhou, Y., Navarro, B., Seo, Y.J., Aranda, K., Shi, L., Battaglia-Hsu, S., Nissim, I., Clapham, D.E., and Ren, D. (2013). mTOR regulates lysosomal ATP-sensitive two-pore Na(+) channels to adapt to metabolic state. Cell *152*, 778-790.

Carrithers, M.D., Dib-Hajj, S., Carrithers, L.M., Tokmoulina, G., Pypaert, M., Jonas, E.A., and Waxman, S.G. (2007). Expression of the voltage-gated sodium channel NaV1.5 in the macrophage late endosome regulates endosomal acidification. J Immunol *178*, 7822-7832.

Caterina, M.J., Rosen, T.A., Tominaga, M., Brake, A.J., and Julius, D. (1999). A capsaicin-receptor homologue with a high threshold for noxious heat. Nature *398*, 436-441.

Chakrabarti, S., Kobayashi, K.S., Flavell, R.A., Marks, C.B., Miyake, K., Liston, D.R., Fowler, K.T., Gorelick, F.S., and Andrews, N.W. (2003). Impaired membrane resealing and autoimmune myositis in synaptotagmin VII-deficient mice. The Journal of cell biology *162*, 543-549.

Chen, C.S., Bach, G., and Pagano, R.E. (1998). Abnormal transport along the lysosomal pathway in mucolipidosis, type IV disease. Proceedings of the National Academy of Sciences of the United States of America *95*, 6373-6378.

Chen, G., Zhang, Z., Wei, Z., Cheng, Q., Li, X., Li, W., Duan, S., and Gu, X. (2012). Lysosomal

exocytosis in Schwann cells contributes to axon remyelination. Glia *60*, 295-305.

Chen, J.L., Ahluwalia, J.P., and Stamnes, M. (2002). Selective effects of calcium chelators on anterograde and retrograde protein transport in the cell. The Journal of biological chemistry *277*, 35682-35687.

Chen, X., Wang, L., Zhou, Y., Zheng, L.H., and Zhou, Z. (2005). "Kiss-and-run" glutamate secretion in cultured and freshly isolated rat hippocampal astrocytes. The Journal of neuroscience : the official journal of the Society for Neuroscience *25*, 9236-9243.

Chen, Y., and Yu, L. (2013). Autophagic lysosome reformation. Experimental cell research *319*, 142-146.

Cheng, X., Shen, D., Samie, M., and Xu, H. (2010). Mucolipins: Intracellular TRPML1-3 channels. FEBS letters *584*, 2013-2021.

Chow, C.W., Downey, G.P., and Grinstein, S. (2004). Measurements of phagocytosis and phagosomal maturation. Current protocols in cell biology / editorial board, Juan S Bonifacino [et al] *Chapter 15*, Unit 15 17.

Chow, C.Y., Zhang, Y., Dowling, J.J., Jin, N., Adamska, M., Shiga, K., Szigeti, K., Shy, M.E., Li, J., Zhang, X.*, et al.* (2007). Mutation of FIG4 causes neurodegeneration in the pale tremor mouse and patients with CMT4J. Nature *448*, 68-72.

Christensen, K.A., Myers, J.T., and Swanson, J.A. (2002). pH-dependent regulation of lysosomal calcium in macrophages. Journal of cell science *115*, 599-607.

Churchill, G.C., Okada, Y., Thomas, J.M., Genazzani, A.A., Patel, S., and Galione, A. (2002). NAADP mobilizes Ca(2+) from reserve granules, lysosome-related organelles, in sea urchin eggs. Cell *111*, 703-708.

Clague, M.J., Urbe, S., Aniento, F., and Gruenberg, J. (1994). Vacuolar ATPase activity is required for endosomal carrier vesicle formation. The Journal of biological chemistry *269*, 21-24.

Clapper, D.L., Walseth, T.F., Dargie, P.J., and Lee, H.C. (1987). Pyridine nucleotide metabolites stimulate calcium release from sea urchin egg microsomes desensitized to inositol trisphosphate. The Journal of biological chemistry *262*, 9561-9568.

Coen, K., Flannagan, R.S., Baron, S., Carraro-Lacroix, L.R., Wang, D., Vermeire, W., Michiels, C., Munck, S., Baert, V., Sugita, S.*, et al.* (2012). Lysosomal calcium homeostasis defects, not proton pump defects, cause endo-lysosomal dysfunction in PSEN-deficient cells. The Journal of cell biology *198*, 23-35.

Cohn, D.V., Bawdon, R., Newman, R.R., and Hamilton, J.W. (1968). Effect of calcium chelation on the ion content of liver mitochondria in carbon tetrachloride-poisoned rats. J Biol Chem *243*, 1089-1095.

Colombo, C., Porzio, O., Liu, M., Massa, O., Vasta, M., Salardi, S., Beccaria, L., Monciotti, C., Toni, S., Pedersen, O.*, et al.* (2008). Seven mutations in the human insulin gene linked to

permanent neonatal/infancy-onset diabetes mellitus. J Clin Invest *118*, 2148-2156.

Cooke, F.T., Dove, S.K., McEwen, R.K., Painter, G., Holmes, A.B., Hall, M.N., Michell, R.H., and Parker, P.J. (1998). The stress-activated phosphatidylinositol 3-phosphate 5-kinase Fab1p is essential for vacuole function in S. cerevisiae. Current biology : CB *8*, 1219-1222.

Coorssen, J.R., Schmitt, H., and Almers, W. (1996). Ca2+ triggers massive exocytosis in Chinese hamster ovary cells. The EMBO journal *15*, 3787-3791.

Cosker, F., Cheviron, N., Yamasaki, M., Menteyne, A., Lund, F.E., Moutin, M.J., Galione, A., and Cancela, J.M. (2010). The ecto-enzyme CD38 is a nicotinic acid adenine dinucleotide phosphate (NAADP) synthase that couples receptor activation to Ca2+ mobilization from lysosomes in pancreatic acinar cells. The Journal of biological chemistry *285*, 38251-38259.

Cuajungco, M.P., and Samie, M.A. (2008). The varitint-waddler mouse phenotypes and the TRPML3 ion channel mutation: cause and consequence. Pflugers Archiv : European journal of physiology *457*, 463-473.

Cunningham, K.W. (2011). Acidic calcium stores of Saccharomyces cerevisiae. Cell calcium *50*, 129-138.

Cuppoletti, J., Aures-Fischer, D., and Sachs, G. (1987). The lysosomal H+ pump: 8-azido-ATP inhibition and the role of chloride in H+ transport. Biochimica et biophysica acta *899*, 276-284.

Curcio-Morelli, C., Charles, F.A., Micsenyi, M.C., Cao, Y., Venugopal, B., Browning, M.F., Dobrenis, K., Cotman, S.L., Walkley, S.U., and Slaugenhaupt, S.A. (2010). Macroautophagy is defective in mucolipin-1-deficient mouse neurons. Neurobiology of disease *40*, 370-377.

Czibener, C., Sherer, N.M., Becker, S.M., Pypaert, M., Hui, E., Chapman, E.R., Mothes, W., and Andrews, N.W. (2006). Ca2+ and synaptotagmin VII-dependent delivery of lysosomal membrane to nascent phagosomes. The Journal of cell biology *174*, 997-1007.

Dammermann, W., and Guse, A.H. (2005). Functional ryanodine receptor expression is required for NAADP-mediated local Ca2+ signaling in T-lymphocytes. The Journal of biological chemistry *280*, 21394-21399.

de Brito, O.M., and Scorrano, L. (2008). Mitofusin 2 tethers endoplasmic reticulum to mitochondria. Nature *456*, 605-610.

De Duve, C. (1963). The lysosome. Sci Am *208*, 64-72.

De Duve, C.a.W., R. (1966). Functions of lysosomes. Annu Rev Physiol *28*, 435-492.

de Lartigue, J., Polson, H., Feldman, M., Shokat, K., Tooze, S.A., Urbe, S., and Clague, M.J. (2009). PIKfyve regulation of endosome-linked pathways. Traffic *10*, 883-893.

Dellis, O., Dedos, S.G., Tovey, S.C., Taufiq Ur, R., Dubel, S.J., and Taylor, C.W. (2006). Ca2+ entry through plasma membrane IP3 receptors. Science *313*, 229-233.

Demaurex, N. (2002). pH Homeostasis of cellular organelles. News in physiological sciences :

an international journal of physiology produced jointly by the International Union of Physiological Sciences and the American Physiological Society *17*, 1-5.

Dewitt, S., Tian, W., and Hallett, M.B. (2006). Localised PtdIns(3,4,5)P3 or PtdIns(3,4)P2 at the phagocytic cup is required for both phagosome closure and Ca2+ signalling in HL60 neutrophils. Journal of cell science *119*, 443-451.

Di Paolo, G., and De Camilli, P. (2006). Phosphoinositides in cell regulation and membrane dynamics. Nature *443*, 651-657.

Dong, X.P., Cheng, X., Mills, E., Delling, M., Wang, F., Kurz, T., and Xu, H. (2008). The type IV mucolipidosis-associated protein TRPML1 is an endolysosomal iron release channel. Nature *455*, 992-996.

Dong, X.P., Shen, D., Wang, X., Dawson, T., Li, X., Zhang, Q., Cheng, X., Zhang, Y., Weisman, L.S., Delling, M.*, et al.* (2010a). PI(3,5)P(2) controls membrane trafficking by direct activation of mucolipin Ca(2+) release channels in the endolysosome. Nature communications *1*, 38.

Dong, X.P., Wang, X., Shen, D., Chen, S., Liu, M., Wang, Y., Mills, E., Cheng, X., Delling, M., and Xu, H. (2009). Activating mutations of the TRPML1 channel revealed by proline-scanning mutagenesis. The Journal of biological chemistry *284*, 32040-32052.

Dong, X.P., Wang, X., and Xu, H. (2010b). TRP channels of intracellular membranes. Journal of neurochemistry *113*, 313-328.

Dou, Y., Wu, H.J., Li, H.Q., Qin, S., Wang, Y.E., Li, J., Lou, H.F., Chen, Z., Li, X.M., Luo, Q.M.*, et al.* (2012). Microglial migration mediated by ATP-induced ATP release from lysosomes. Cell research *22*, 1022-1033.

Dove, S.K., Dong, K., Kobayashi, T., Williams, F.K., and Michell, R.H. (2009). Phosphatidylinositol 3,5-bisphosphate and Fab1p/PIKfyve underPPIn endo-lysosome function. The Biochemical journal *419*, 1-13.

Dove, S.K., McEwen, R.K., Mayes, A., Hughes, D.C., Beggs, J.D., and Michell, R.H. (2002). Vac14 controls PtdIns(3,5)P(2) synthesis and Fab1-dependent protein trafficking to the multivesicular body. Current biology : CB *12*, 885-893.

Dove, S.K., Piper, R.C., McEwen, R.K., Yu, J.W., King, M.C., Hughes, D.C., Thuring, J., Holmes, A.B., Cooke, F.T., Michell, R.H.*, et al.* (2004). Svp1p defines a family of phosphatidylinositol 3,5-bisphosphate effectors. The EMBO journal *23*, 1922-1933.

Du, J., Xie, J., and Yue, L. (2009). Intracellular calcium activates TRPM2 and its alternative spliced isoforms. Proceedings of the National Academy of Sciences of the United States of America *106*, 7239-7244.

Duex, J.E., Nau, J.J., Kauffman, E.J., and Weisman, L.S. (2006a). Phosphoinositide 5-phosphatase Fig 4p is required for both acute rise and subsequent fall in stress-induced phosphatidylinositol 3,5-bisphosphate levels. Eukaryotic cell *5*, 723-731.

Duex, J.E., Tang, F., and Weisman, L.S. (2006b). The Vac14p-Fig4p complex acts

independently of Vac7p and couples PI3,5P2 synthesis and turnover. The Journal of cell biology *172*, 693-704.

Edwards, J.C., and Kahl, C.R. (2010). Chloride channels of intracellular membranes. FEBS letters *584*, 2102-2111.

Efe, J.A., Botelho, R.J., and Emr, S.D. (2007). Atg18 regulates organelle morphology and Fab1 kinase activity independent of its membrane recruitment by phosphatidylinositol 3,5-bisphosphate. Molecular biology of the cell *18*, 4232-4244.

Eichelsdoerfer, J.L., Evans, J.A., Slaugenhaupt, S.A., and Cuajungco, M.P. (2010). Zinc dyshomeostasis is linked with the loss of mucolipidosis IV-associated TRPML1 ion channel. The Journal of biological chemistry *285*, 34304-34308.

El Chemaly, A., and Demaurex, N. (2012). Do Hv1 proton channels regulate the ionic and redox homeostasis of phagosomes? Molecular and cellular endocrinology *353*, 82-87.

Epand, R.M., and Hui, S.W. (1986). Effect of electrostatic repulsion on the morphology and thermotropic transitions of anionic phospholipids. FEBS letters *209*, 257-260.

Ezaki, J., Himeno, M., and Kato, K. (1992). Purification and characterization of (Ca2+-Mg2+)-ATPase in rat liver lysosomal membranes. Journal of biochemistry *112*, 33-39.

Falguieres, T., Luyet, P.P., Bissig, C., Scott, C.C., Velluz, M.C., and Gruenberg, J. (2008). In vitro budding of intralumenal vesicles into late endosomes is regulated by Alix and Tsg101. Molecular biology of the cell *19*, 4942-4955.

Fares, H., and Greenwald, I. (2001). Regulation of endocytosis by CUP-5, the Caenorhabditis elegans mucolipin-1 homolog. Nature genetics *28*, 64-68.

Favre, I., Moczydlowski, E., and Schild, L. (1996). On the structural basis for ionic selectivity among Na+, K+, and Ca2+ in the voltage-gated sodium channel. Biophys J *71*, 3110-3125.

Ferguson, C.J., Lenk, G.M., and Meisler, M.H. (2009). Defective autophagy in neurons and astrocytes from mice deficient in PI(3,5)P2. Human molecular genetics *18*, 4868-4878.

Flannagan, R.S., Jaumouille, V., and Grinstein, S. (2012). The cell biology of phagocytosis. Annual review of pathology *7*, 61-98.

Forgac, M. (2007). Vacuolar ATPases: rotary proton pumps in physiology and pathophysiology. Nature reviews Molecular cell biology *8*, 917-929.

Friedman, J.R., Dibenedetto, J.R., West, M., Rowland, A.A., and Voeltz, G.K. (2013). Endoplasmic reticulum-endosome contact increases as endosomes traffic and mature. Molecular biology of the cell *24*, 1030-1040.

Galione, A. (2011). NAADP receptors. Cold Spring Harbor perspectives in biology *3*, a004036.

Galione, A., and Churchill, G.C. (2002). Interactions between calcium release pathways: multiple messengers and multiple stores. Cell calcium *32*, 343-354.

Galione, A., Evans, A.M., Ma, J., Parrington, J., Arredouani, A., Cheng, X., and Zhu, M.X. (2009). The acid test: the discovery of two-pore channels (TPCs) as NAADP-gated endolysosomal Ca(2+) release channels. Pflugers Archiv : European journal of physiology *458*, 869-876.

Galione, A., Morgan, A.J., Arredouani, A., Davis, L.C., Rietdorf, K., Ruas, M., and Parrington, J. (2010). NAADP as an intracellular messenger regulating lysosomal calcium-release channels. Biochemical Society transactions *38*, 1424-1431.

Gao, Z., Reavey-Cantwell, J., Young, R.A., Jegier, P., and Wolf, B.A. (2000). Synaptotagmin III/VII isoforms mediate Ca2+-induced insulin secretion in pancreatic islet beta -cells. The Journal of biological chemistry *275*, 36079-36085.

Gary, J.D., Sato, T.K., Stefan, C.J., Bonangelino, C.J., Weisman, L.S., and Emr, S.D. (2002). Regulation of Fab1 phosphatidylinositol 3-phosphate 5-kinase pathway by Vac7 protein and Fig4, a polyphosphoinositide phosphatase family member. Molecular biology of the cell *13*, 1238-1251.

Gary, J.D., Wurmser, A.E., Bonangelino, C.J., Weisman, L.S., and Emr, S.D. (1998). Fab1p is essential for PtdIns(3)P 5-kinase activity and the maintenance of vacuolar size and membrane homeostasis. The Journal of cell biology *143*, 65-79.

Gerasimenko, J.V., Lur, G., Sherwood, M.W., Ebisui, E., Tepikin, A.V., Mikoshiba, K., Gerasimenko, O.V., and Petersen, O.H. (2009). Pancreatic protease activation by alcohol metabolite depends on Ca2+ release via acid store IP3 receptors. Proceedings of the National Academy of Sciences of the United States of America *106*, 10758-10763.

Gerasimenko, J.V., Maruyama, Y., Yano, K., Dolman, N.J., Tepikin, A.V., Petersen, O.H., and Gerasimenko, O.V. (2003). NAADP mobilizes Ca2+ from a thapsigargin-sensitive store in the nuclear envelope by activating ryanodine receptors. The Journal of cell biology *163*, 271-282.

Gerasimenko, J.V., Tepikin, A.V., Petersen, O.H., and Gerasimenko, O.V. (1998). Calcium uptake via endocytosis with rapid release from acidifying endosomes. Current biology : CB *8*, 1335-1338.

Giacomello, M., Hudec, R., and Lopreiato, R. (2011). Huntington's disease, calcium, and mitochondria. BioFactors *37*, 206-218.

Gomez-Suaga, P., Churchill, G.C., Patel, S., and Hilfiker, S. (2012). A link between LRRK2, autophagy and NAADP-mediated endolysosomal calcium signalling. Biochemical Society transactions *40*, 1140-1146.

Goncalves, P.P., Meireles, S.M., Neves, P., and Vale, M.G. (2000). Distinction between Ca(2+) pump and Ca(2+)/H(+) antiport activities in synaptic vesicles of sheep brain cortex. Neurochemistry international *37*, 387-396.

Graves, A.R., Curran, P.K., Smith, C.L., and Mindell, J.A. (2008). The Cl-/H+ antiporter ClC-7 is the primary chloride permeation pathway in lysosomes. Nature *453*, 788-792.

Grimm, C., Cuajungco, M.P., van Aken, A.F., Schnee, M., Jors, S., Kros, C.J., Ricci, A.J., and Heller, S. (2007). A helix-breaking mutation in TRPML3 leads to constitutive activity underlying deafness in the varitint-waddler mouse. Proceedings of the National Academy of Sciences of the United States of America *104*, 19583-19588.

Grimm, C., Hassan, S., Wahl-Schott, C., and Biel, M. (2012). Role of TRPML and two-pore channels in endolysosomal cation homeostasis. The Journal of pharmacology and experimental therapeutics *342*, 236-244.

Grimm, C., Jors, S., Saldanha, S.A., Obukhov, A.G., Pan, B., Oshima, K., Cuajungco, M.P., Chase, P., Hodder, P., and Heller, S. (2010). Small molecule activators of TRPML3. Chemistry & biology *17*, 135-148.

Gunther, W., Luchow, A., Cluzeaud, F., Vandewalle, A., and Jentsch, T.J. (1998). ClC-5, the chloride channel mutated in Dent's disease, colocalizes with the proton pump in endocytotically active kidney cells. Proceedings of the National Academy of Sciences of the United States of America *95*, 8075-8080.

Guse, A.H. (2009). Second messenger signaling: multiple receptors for NAADP. Current biology : CB *19*, R521-523.

Guse, A.H., and Lee, H.C. (2008). NAADP: a universal Ca2+ trigger. Science signaling *1*, re10.

Gut, A., Kiraly, C.E., Fukuda, M., Mikoshiba, K., Wollheim, C.B., and Lang, J. (2001). Expression and localisation of synaptotagmin isoforms in endocrine beta-cells: their function in insulin exocytosis. Journal of cell science *114*, 1709-1716.

Haggie, P.M., and Verkman, A.S. (2009a). Defective organellar acidification as a cause of cystic fibrosis lung disease: reexamination of a recurring hypothesis. American journal of physiology Lung cellular and molecular physiology *296*, L859-867.

Haggie, P.M., and Verkman, A.S. (2009b). Unimpaired lysosomal acidification in respiratory epithelial cells in cystic fibrosis. The Journal of biological chemistry *284*, 7681-7686.

Hara-Chikuma, M., Yang, B., Sonawane, N.D., Sasaki, S., Uchida, S., and Verkman, A.S. (2005). ClC-3 chloride channels facilitate endosomal acidification and chloride accumulation. The Journal of biological chemistry *280*, 1241-1247.

Harikumar, P., and Reeves, J.P. (1983). The lysosomal proton pump is electrogenic. The Journal of biological chemistry *258*, 10403-10410.

Harris, H., and Rubinsztein, D.C. (2012). Control of autophagy as a therapy for neurodegenerative disease. Nature reviews Neurology *8*, 108-117.

Hay, J.C. (2007). Calcium: a fundamental regulator of intracellular membrane fusion? EMBO reports *8*, 236-240.

He, C., and Klionsky, D.J. (2009). Regulation mechanisms and signaling pathways of autophagy. Annual review of genetics *43*, 67-93.

Hers, H.G. (1963). α-glucosidase deficiency in generalized glycogen storage disease (Pompe's disease). Biochem J *86*, 11-16.

Hersh, B.M., Hartwieg, E., and Horvitz, H.R. (2002). The Caenorhabditis elegans mucolipin-like gene cup-5 is essential for viability and regulates lysosomes in multiple cell types. Proceedings of the National Academy of Sciences of the United States of America *99*, 4355-4360.

Hicks, B.W., and Parsons, S.M. (1992). Characterization of the P-type and V-type ATPases of cholinergic synaptic vesicles and coupling of nucleotide hydrolysis to acetylcholine transport. Journal of neurochemistry *58*, 1211-1220.

Hille, B. (1972). The permeability of the sodium channel to metal cations in myelinated nerve. J Gen Physiol *59*, 637-658.

Ho, C.Y., Alghamdi, T.A., and Botelho, R.J. (2012). Phosphatidylinositol-3,5-bisphosphate: no longer the poor PIP2. Traffic *13*, 1-8.

Holevinsky, K.O., and Nelson, D.J. (1998). Membrane capacitance changes associated with particle uptake during phagocytosis in macrophages. Biophysical journal *75*, 2577-2586.

Huotari, J., and Helenius, A. (2011). Endosome maturation. The EMBO journal *30*, 3481-3500.

Huynh, C., and Andrews, N.W. (2005). The small chemical vacuolin-1 alters the morphology of lysosomes without inhibiting Ca2+-regulated exocytosis. EMBO Rep *6*, 843-847.

Huynh, K.K., Kay, J.G., Stow, J.L., and Grinstein, S. (2007). Fusion, fission, and secretion during phagocytosis. Physiology *22*, 366-372.

Idone, V., Tam, C., and Andrews, N.W. (2008). Two-way traffic on the road to plasma membrane repair. Trends in cell biology *18*, 552-559.

Ikonomov, O.C., Sbrissa, D., Delvecchio, K., Xie, Y., Jin, J.P., Rappolee, D., and Shisheva, A. (2011). The phosphoinositide kinase PIKfyve is vital in early embryonic development: preimplantation lethality of PIKfyve-/- embryos but normality of PIKfyve+/- mice. The Journal of biological chemistry *286*, 13404-13413.

Ikonomov, O.C., Sbrissa, D., Ijuin, T., Takenawa, T., and Shisheva, A. (2009). Sac3 is an insulin-regulated phosphatidylinositol 3,5-bisphosphate phosphatase: gain in insulin responsiveness through Sac3 down-regulation in adipocytes. The Journal of biological chemistry *284*, 23961-23971.

Ikonomov, O.C., Sbrissa, D., and Shisheva, A. (2001). Mammalian cell morphology and endocytic membrane homeostasis require enzymatically active phosphoinositide 5-kinase PIKfyve. The Journal of biological chemistry *276*, 26141-26147.

Ishibashi, K., Suzuki, M., and Imai, M. (2000). Molecular cloning of a novel form (two-repeat) protein related to voltage-gated sodium and calcium channels. Biochemical and biophysical research communications *270*, 370-376.

Jain, P., Slama, J.T., Perez-Haddock, L.A., and Walseth, T.F. (2010). Nicotinic acid adenine

dinucleotide phosphate analogues containing substituted nicotinic acid: effect of modification on Ca(2+) release. J Med Chem *53*, 7599-7612.

Jaiswal, J.K., Andrews, N.W., and Simon, S.M. (2002). Membrane proximal lysosomes are the major vesicles responsible for calcium-dependent exocytosis in nonsecretory cells. The Journal of cell biology *159*, 625-635.

Jefferies, H.B., Cooke, F.T., Jat, P., Boucheron, C., Koizumi, T., Hayakawa, M., Kaizawa, H., Ohishi, T., Workman, P., Waterfield, M.D.*, et al.* (2008). A selective PIKfyve inhibitor blocks PtdIns(3,5)P(2) production and disrupts endomembrane transport and retroviral budding. EMBO reports *9*, 164-170.

Jentsch, T.J., Neagoe, I., and Scheel, O. (2005). CLC chloride channels and transporters. Current opinion in neurobiology *15*, 319-325.

Jin, N., Chow, C.Y., Liu, L., Zolov, S.N., Bronson, R., Davisson, M., Petersen, J.L., Zhang, Y., Park, S., Duex, J.E.*, et al.* (2008). VAC14 nucleates a protein complex essential for the acute interconversion of PI3P and PI(3,5)P(2) in yeast and mouse. The EMBO journal *27*, 3221-3234.

Johnson, R.G., Beers, M.F., and Scarpa, A. (1982). H+ ATPase of chromaffin granules. Kinetics, regulation, and stoichiometry. The Journal of biological chemistry *257*, 10701-10707.

Kane, P.M. (1995). Disassembly and reassembly of the yeast vacuolar H(+)-ATPase in vivo. The Journal of biological chemistry *270*, 17025-17032.

Kanzaki, M., Zhang, Y.Q., Mashima, H., Li, L., Shibata, H., and Kojima, I. (1999). Translocation of a calcium-permeable cation channel induced by insulin-like growth factor-I. Nature cell biology *1*, 165-170.

Kasper, D., Planells-Cases, R., Fuhrmann, J.C., Scheel, O., Zeitz, O., Ruether, K., Schmitt, A., Poet, M., Steinfeld, R., Schweizer, M.*, et al.* (2005a). Loss of the chloride channel ClC-7 leads to lysosomal storage disease and neurodegeneration. The EMBO journal *24*, 1079-1091.

Kasper, G., Vogel, A., Klaman, I., Grone, J., Petersen, I., Weber, B., Castanos-Velez, E., Staub, E., and Mennerich, D. (2005b). The human LAPTM4b transcript is upregulated in various types of solid tumours and seems to play a dual functional role during tumour progression. Cancer letters *224*, 93-103.

Kawasaki-Nishi, S., Nishi, T., and Forgac, M. (2001). Yeast V-ATPase complexes containing different isoforms of the 100-kDa a-subunit differ in coupling efficiency and in vivo dissociation. The Journal of biological chemistry *276*, 17941-17948.

Kerr, M.C., Wang, J.T., Castro, N.A., Hamilton, N.A., Town, L., Brown, D.L., Meunier, F.A., Brown, N.F., Stow, J.L., and Teasdale, R.D. (2010). Inhibition of the PtdIns(5) kinase PIKfyve disrupts intracellular replication of Salmonella. The EMBO journal *29*, 1331-1347.

Kettner, C., Bertl, A., Obermeyer, G., Slayman, C., and Bihler, H. (2003). Electrophysiological analysis of the yeast V-type proton pump: variable coupling ratio and proton shunt. Biophysical journal *85*, 3730-3738.

Kilpatrick, B.S., Eden, E.R., Schapira, A.H., Futter, C.E., and Patel, S. (2013). Direct mobilisation of lysosomal Ca2+ triggers complex Ca2+ signals. Journal of cell science *126*, 60-66.

Kim, H.J., Li, Q., Tjon-Kon-Sang, S., So, I., Kiselyov, K., and Muallem, S. (2007). Gain-of-function mutation in TRPML3 causes the mouse Varitint-Waddler phenotype. The Journal of biological chemistry *282*, 36138-36142.

Kim, H.J., Li, Q., Tjon-Kon-Sang, S., So, I., Kiselyov, K., Soyombo, A.A., and Muallem, S. (2008). A novel mode of TRPML3 regulation by extracytosolic pH absent in the varitint-waddler phenotype. The EMBO journal *27*, 1197-1205.

Kim, H.J., Soyombo, A.A., Tjon-Kon-Sang, S., So, I., and Muallem, S. (2009). The Ca(2+) channel TRPML3 regulates membrane trafficking and autophagy. Traffic *10*, 1157-1167.

Kinnear, N.P., Boittin, F.X., Thomas, J.M., Galione, A., and Evans, A.M. (2004). Lysosome-sarcoplasmic reticulum junctions. A trigger zone for calcium signaling by nicotinic acid adenine dinucleotide phosphate and endothelin-1. The Journal of biological chemistry *279*, 54319-54326.

Kiselyov, K., Colletti, G.A., Terwilliger, A., Ketchum, K., Lyons, C.W., Quinn, J., and Muallem, S. (2011). TRPML: transporters of metals in lysosomes essential for cell survival? Cell calcium *50*, 288-294.

Koivusalo, M., Steinberg, B.E., Mason, D., and Grinstein, S. (2011). In situ measurement of the electrical potential across the lysosomal membrane using FRET. Traffic *12*, 972-982.

Kornak, U., Kasper, D., Bosl, M.R., Kaiser, E., Schweizer, M., Schulz, A., Friedrich, W., Delling, G., and Jentsch, T.J. (2001). Loss of the ClC-7 chloride channel leads to osteopetrosis in mice and man. Cell *104*, 205-215.

Kraayenhof, R., Sterk, G.J., Wong Fong Sang, H.W., Krab, K., and Epand, R.M. (1996). Monovalent cations differentially affect membrane surface properties and membrane curvature, as revealed by fluorescent probes and dynamic light scattering. Biochimica et biophysica acta *1282*, 293-302.

Kurz, T., Terman, A., Gustafsson, B., and Brunk, U.T. (2008). Lysosomes in iron metabolism, ageing and apoptosis. Histochemistry and cell biology *129*, 389-406.

Kwon, Y., Hofmann, T., and Montell, C. (2007). Integration of phosphoinositide- and calmodulin-mediated regulation of TRPC6. Molecular cell *25*, 491-503.

Lamason, R.L., Mohideen, M.A., Mest, J.R., Wong, A.C., Norton, H.L., Aros, M.C., Jurynec, M.J., Mao, X., Humphreville, V.R., Humbert, J.E., *et al.* (2005). SLC24A5, a putative cation exchanger, affects pigmentation in zebrafish and humans. Science *310*, 1782-1786.

Lange, I., Yamamoto, S., Partida-Sanchez, S., Mori, Y., Fleig, A., and Penner, R. (2009). TRPM2 functions as a lysosomal Ca2+-release channel in beta cells. Science signaling *2*, ra23.

Lange, P.F., Wartosch, L., Jentsch, T.J., and Fuhrmann, J.C. (2006). ClC-7 requires Ostm1 as a

beta-subunit to support bone resorption and lysosomal function. Nature *440*, 220-223.

LaPlante, J.M., Sun, M., Falardeau, J., Dai, D., Brown, E.M., Slaugenhaupt, S.A., and Vassilev, P.M. (2006). Lysosomal exocytosis is impaired in mucolipidosis type IV. Molecular genetics and metabolism *89*, 339-348.

Laporte, R., Hui, A., and Laher, I. (2004). Pharmacological modulation of sarcoplasmic reticulum function in smooth muscle. Pharmacological reviews *56*, 439-513.

Lawrence, S.P., Bright, N.A., Luzio, J.P., and Bowers, K. (2010). The sodium/proton exchanger NHE8 regulates late endosomal morphology and function. Molecular biology of the cell *21*, 3540-3551.

Lee, H.C., and Aarhus, R. (1995). A derivative of NADP mobilizes calcium stores insensitive to inositol trisphosphate and cyclic ADP-ribose. The Journal of biological chemistry *270*, 2152-2157.

Lee, W.L., Mason, D., Schreiber, A.D., and Grinstein, S. (2007). Quantitative analysis of membrane remodeling at the phagocytic cup. Molecular biology of the cell *18*, 2883-2892.

Lemmon, M.A. (2008). Membrane recognition by phospholipid-binding domains. Nature reviews Molecular cell biology *9*, 99-111.

Levine, T.P., and Munro, S. (1998). The pleckstrin homology domain of oxysterol-binding protein recognises a determinant specific to Golgi membranes. Curr Biol *8*, 729-739.

Lewis, C.A. (1979). Ion-concentration dependence of the reversal potential and the single channel conductance of ion channels at the frog neuromuscular junction. The Journal of physiology *286*, 417-445.

Li, D.S., Yuan, Y.H., Tu, H.J., Liang, Q.L., and Dai, L.J. (2009). A protocol for islet isolation from mouse pancreas. Nat Protoc *4*, 1649-1652.

Li, Y., Zou, L., Li, Q., Haibe-Kains, B., Tian, R., Desmedt, C., Sotiriou, C., Szallasi, Z., Iglehart, J.D., Richardson, A.L.*, et al.* (2010). Amplification of LAPTM4B and YWHAZ contributes to chemotherapy resistance and recurrence of breast cancer. Nature medicine *16*, 214-218.

Lin-Moshier, Y., Walseth, T.F., Churamani, D., Davidson, S.M., Slama, J.T., Hooper, R., Brailoiu, E., Patel, S., and Marchant, J.S. (2011). Photoaffinity labeling of nicotinic acid adenine dinucleotide phosphate (NAADP) targets in mammalian cells. J Biol Chem.

Lin-Moshier, Y., Walseth, T.F., Churamani, D., Davidson, S.M., Slama, J.T., Hooper, R., Brailoiu, E., Patel, S., and Marchant, J.S. (2012). Photoaffinity labeling of nicotinic acid adenine dinucleotide phosphate (NAADP) targets in mammalian cells. The Journal of biological chemistry *287*, 2296-2307.

Link, T.M., Park, U., Vonakis, B.M., Raben, D.M., Soloski, M.J., and Caterina, M.J. (2010). TRPV2 has a pivotal role in macrophage particle binding and phagocytosis. Nature immunology *11*, 232-239.

Liu, T., Sun, L., Xiong, Y., Shang, S., Guo, N., Teng, S., Wang, Y., Liu, B., Wang, C., Wang, L., *et al.* (2011). Calcium triggers exocytosis from two types of organelles in a single astrocyte. The Journal of neuroscience : the official journal of the Society for Neuroscience *31*, 10593-10601.

Lloyd-Evans, E., Morgan, A.J., He, X., Smith, D.A., Elliot-Smith, E., Sillence, D.J., Churchill, G.C., Schuchman, E.H., Galione, A., and Platt, F.M. (2008). Niemann-Pick disease type C1 is a sphingosine storage disease that causes deregulation of lysosomal calcium. Nature medicine *14*, 1247-1255.

Long, S.B., Campbell, E.B., and Mackinnon, R. (2005). Voltage sensor of Kv1.2: structural basis of electromechanical coupling. Science *309*, 903-908.

Lopez, J.J., Camello-Almaraz, C., Pariente, J.A., Salido, G.M., and Rosado, J.A. (2005). Ca2+ accumulation into acidic organelles mediated by Ca2+- and vacuolar H+-ATPases in human platelets. The Biochemical journal *390*, 243-252.

Lopez, J.J., Redondo, P.C., Salido, G.M., Pariente, J.A., and Rosado, J.A. (2006). Two distinct Ca2+ compartments show differential sensitivity to thrombin, ADP and vasopressin in human platelets. Cellular signalling *18*, 373-381.

Lopez-Sanjurjo, C.I., Tovey, S.C., Prole, D.L., and Taylor, C.W. (2013). Lysosomes shape Ins(1,4,5)P3-evoked Ca2+ signals by selectively sequestering Ca2+ released from the endoplasmic reticulum. Journal of cell science *126*, 289-300.

Luzio, J.P., Bright, N.A., and Pryor, P.R. (2007a). The role of calcium and other ions in sorting and delivery in the late endocytic pathway. Biochemical Society transactions *35*, 1088-1091.

Luzio, J.P., Pryor, P.R., and Bright, N.A. (2007b). Lysosomes: fusion and function. Nature reviews Molecular cell biology *8*, 622-632.

Lytton, J. (2007). Na+/Ca2+ exchangers: three mammalian gene families control Ca2+ transport. The Biochemical journal *406*, 365-382.

Macgregor, A., Yamasaki, M., Rakovic, S., Sanders, L., Parkesh, R., Churchill, G.C., Galione, A., and Terrar, D.A. (2007). NAADP controls cross-talk between distinct Ca2+ stores in the heart. The Journal of biological chemistry *282*, 15302-15311.

Macia, E., Ehrlich, M., Massol, R., Boucrot, E., Brunner, C., and Kirchhausen, T. (2006). Dynasore, a cell-permeable inhibitor of dynamin. Developmental cell *10*, 839-850.

Majumdar, A., Capetillo-Zarate, E., Cruz, D., Gouras, G.K., and Maxfield, F.R. (2011). Degradation of Alzheimer's amyloid fibrils by microglia requires delivery of ClC-7 to lysosomes. Molecular biology of the cell *22*, 1664-1676.

Majumdar, A., Chung, H., Dolios, G., Wang, R., Asamoah, N., Lobel, P., and Maxfield, F.R. (2008). Degradation of fibrillar forms of Alzheimer's amyloid beta-peptide by macrophages. Neurobiology of aging *29*, 707-715.

Majumdar, A., Cruz, D., Asamoah, N., Buxbaum, A., Sohar, I., Lobel, P., and Maxfield, F.R. (2007). Activation of microglia acidifies lysosomes and leads to degradation of Alzheimer

amyloid fibrils. Molecular biology of the cell *18*, 1490-1496.

Manneville, J.B., Casella, J.F., Ambroggio, E., Gounon, P., Bertherat, J., Bassereau, P., Cartaud, J., Antonny, B., and Goud, B. (2008). COPI coat assembly occurs on liquid-disordered domains and the associated membrane deformations are limited by membrane tension. Proceedings of the National Academy of Sciences of the United States of America *105*, 16946-16951.

Manolson, M.F., Wu, B., Proteau, D., Taillon, B.E., Roberts, B.T., Hoyt, M.A., and Jones, E.W. (1994). STV1 gene encodes functional homologue of 95-kDa yeast vacuolar H(+)-ATPase subunit Vph1p. The Journal of biological chemistry *269*, 14064-14074.

Marshansky, V., and Futai, M. (2008). The V-type H+-ATPase in vesicular trafficking: targeting, regulation and function. Current opinion in cell biology *20*, 415-426.

Martens, S., and McMahon, H.T. (2008). Mechanisms of membrane fusion: disparate players and common principles. Nature reviews Molecular cell biology *9*, 543-556.

Martina, J.A., Lelouvier, B., and Puertollano, R. (2009). The calcium channel mucolipin-3 is a novel regulator of trafficking along the endosomal pathway. Traffic *10*, 1143-1156.

Martinez, I., Chakrabarti, S., Hellevik, T., Morehead, J., Fowler, K., and Andrews, N.W. (2000). Synaptotagmin VII regulates Ca(2+)-dependent exocytosis of lysosomes in fibroblasts. The Journal of cell biology *148*, 1141-1149.

Masgrau, R., Churchill, G.C., Morgan, A.J., Ashcroft, S.J., and Galione, A. (2003). NAADP: a new second messenger for glucose-induced Ca2+ responses in clonal pancreatic beta cells. Current biology : CB *13*, 247-251.

Maxfield, F.R., and McGraw, T.E. (2004). Endocytic recycling. Nature reviews Molecular cell biology *5*, 121-132.

Mazzulli, J.R., Xu, Y.H., Sun, Y., Knight, A.L., McLean, P.J., Caldwell, G.A., Sidransky, E., Grabowski, G.A., and Krainc, D. (2011). Gaucher disease glucocerebrosidase and alpha-synuclein form a bidirectional pathogenic loop in synucleinopathies. Cell *146*, 37-52.

Medina, D.L., Fraldi, A., Bouche, V., Annunziata, F., Mansueto, G., Spampanato, C., Puri, C., Pignata, A., Martina, J.A., Sardiello, M.*, et al.* (2011). Transcriptional activation of lysosomal exocytosis promotes cellular clearance. Developmental cell *21*, 421-430.

Menteyne, A., Burdakov, A., Charpentier, G., Petersen, O.H., and Cancela, J.M. (2006). Generation of specific Ca(2+) signals from Ca(2+) stores and endocytosis by differential coupling to messengers. Current biology : CB *16*, 1931-1937.

Micsenyi, M.C., Dobrenis, K., Stephney, G., Pickel, J., Vanier, M.T., Slaugenhaupt, S.A., and Walkley, S.U. (2009). Neuropathology of the Mcoln1(-/-) knockout mouse model of mucolipidosis type IV. Journal of neuropathology and experimental neurology *68*, 125-135.

Miedel, M.T., Rbaibi, Y., Guerriero, C.J., Colletti, G., Weixel, K.M., Weisz, O.A., and Kiselyov, K. (2008). Membrane traffic and turnover in TRP-ML1-deficient cells: a revised model for mucolipidosis type IV pathogenesis. The Journal of experimental medicine *205*, 1477-1490.

Mindell, J.A. (2012). Lysosomal acidification mechanisms. Annual review of physiology *74*, 69-86.

Mitchell, K.J., Lai, F.A., and Rutter, G.A. (2003). Ryanodine receptor type I and nicotinic acid adenine dinucleotide phosphate receptors mediate Ca2+ release from insulin-containing vesicles in living pancreatic beta-cells (MIN6). The Journal of biological chemistry *278*, 11057-11064.

Miyawaki, A., Llopis, J., Heim, R., McCaffery, J.M., Adams, J.A., Ikura, M., and Tsien, R.Y. (1997). Fluorescent indicators for Ca2+ based on green fluorescent proteins and calmodulin. Nature *388*, 882-887.

Moccia, F., Lim, D., Kyozuka, K., and Santella, L. (2004). NAADP triggers the fertilization potential in starfish oocytes. Cell calcium *36*, 515-524.

Mohammad-Panah, R., Harrison, R., Dhani, S., Ackerley, C., Huan, L.J., Wang, Y., and Bear, C.E. (2003). The chloride channel ClC-4 contributes to endosomal acidification and trafficking. The Journal of biological chemistry *278*, 29267-29277.

Morgan, A.J. (2011). Sea urchin eggs in the acid reign. Cell calcium *50*, 147-156.

Morgan, A.J., Platt, F.M., Lloyd-Evans, E., and Galione, A. (2011). Molecular mechanisms of endolysosomal Ca2+ signalling in health and disease. The Biochemical journal *439*, 349-374.

Nagata, K., Zheng, L., Madathany, T., Castiglioni, A.J., Bartles, J.R., and Garcia-Anoveros, J. (2008). The varitint-waddler (Va) deafness mutation in TRPML3 generates constitutive, inward rectifying currents and causes cell degeneration. Proceedings of the National Academy of Sciences of the United States of America *105*, 353-358.

Nakamura, N., Tanaka, S., Teko, Y., Mitsui, K., and Kanazawa, H. (2005). Four Na+/H+ exchanger isoforms are distributed to Golgi and post-Golgi compartments and are involved in organelle pH regulation. The Journal of biological chemistry *280*, 1561-1572.

Nanda, A., Gukovskaya, A., Tseng, J., and Grinstein, S. (1992). Activation of vacuolar-type proton pumps by protein kinase C. Role in neutrophil pH regulation. The Journal of biological chemistry *267*, 22740-22746.

Naylor, E., Arredouani, A., Vasudevan, S.R., Lewis, A.M., Parkesh, R., Mizote, A., Rosen, D., Thomas, J.M., Izumi, M., Ganesan, A.*, et al.* (2009a). Identification of a chemical probe for NAADP by virtual screening. Nature chemical biology *5*, 220-226.

Naylor, E., Arredouani, A., Vasudevan, S.R., Lewis, A.M., Parkesh, R., Mizote, A., Rosen, D., Thomas, J.M., Izumi, M., Ganesan, A.*, et al.* (2009b). Identification of a chemical probe for NAADP by virtual screening. Nat Chem Biol *5*, 220-226.

Neher, E. (1992). Correction for liquid junction potentials in patch clamp experiments. Methods in enzymology *207*, 123-131.

Nilius, B., Owsianik, G., and Voets, T. (2008). Transient receptor potential channels meet phosphoinositides. The EMBO journal *27*, 2809-2816.

Ninomiya, Y., Kishimoto, T., Miyashita, Y., and Kasai, H. (1996). Ca2+-dependent exocytotic pathways in Chinese hamster ovary fibroblasts revealed by a caged-Ca2+ compound. The Journal of biological chemistry *271*, 17751-17754.

Novarino, G., Weinert, S., Rickheit, G., and Jentsch, T.J. (2010). Endosomal chloride-proton exchange rather than chloride conductance is crucial for renal endocytosis. Science *328*, 1398-1401.

Obara, K., Sekito, T., Niimi, K., and Ohsumi, Y. (2008). The Atg18-Atg2 complex is recruited to autophagic membranes via phosphatidylinositol 3-phosphate and exerts an essential function. The Journal of biological chemistry *283*, 23972-23980.

Ohkuma, S., Moriyama, Y., and Takano, T. (1982). Identification and characterization of a proton pump on lysosomes by fluorescein-isothiocyanate-dextran fluorescence. Proceedings of the National Academy of Sciences of the United States of America *79*, 2758-2762.

Ohkuma, S., Moriyama, Y., and Takano, T. (1983). Electrogenic nature of lysosomal proton pump as revealed with a cyanine dye. Journal of biochemistry *94*, 1935-1943.

Orlowski, J., and Grinstein, S. (2007). Emerging roles of alkali cation/proton exchangers in organellar homeostasis. Current opinion in cell biology *19*, 483-492.

Pan, C.Y., Tsai, L.L., Jiang, J.H., Chen, L.W., and Kao, L.S. (2008). The co-presence of Na+/Ca2+-K+ exchanger and Na+/Ca2+ exchanger in bovine adrenal chromaffin cells. Journal of neurochemistry *107*, 658-667.

Papp, B., Enyedi, A., Paszty, K., Kovacs, T., Sarkadi, B., Gardos, G., Magnier, C., Wuytack, F., and Enouf, J. (1992). Simultaneous presence of two distinct endoplasmic-reticulum-type calcium-pump isoforms in human cells. Characterization by radio-immunoblotting and inhibition by 2,5-di-(t-butyl)-1,4-benzohydroquinone. The Biochemical journal *288 (Pt 1)*, 297-302.

Parkesh, R., Lewis, A.M., Aley, P.K., Arredouani, A., Rossi, S., Tavares, R., Vasudevan, S.R., Rosen, D., Galione, A., Dowden, J*., et al.* (2007). Cell-permeant NAADP: A novel chemical tool enabling the study of Ca(2+) signalling in intact cells. Cell Calcium.

Parkesh, R., Lewis, A.M., Aley, P.K., Arredouani, A., Rossi, S., Tavares, R., Vasudevan, S.R., Rosen, D., Galione, A., Dowden, J*., et al.* (2008). Cell-permeant NAADP: a novel chemical tool enabling the study of Ca2+ signalling in intact cells. Cell calcium *43*, 531-538.

Parnas, H., Segel, L., Dudel, J., and Parnas, I. (2000). Autoreceptors, membrane potential and the regulation of transmitter release. Trends Neurosci *23*, 60-68.

Paroutis, P., Touret, N., and Grinstein, S. (2004). The pH of the secretory pathway: measurement, determinants, and regulation. Physiology *19*, 207-215.

Patel, S., Marchant, J.S., and Brailoiu, E. (2010). Two-pore channels: Regulation by NAADP and customized roles in triggering calcium signals. Cell calcium *47*, 480-490.

Peiter, E., Maathuis, F.J., Mills, L.N., Knight, H., Pelloux, J., Hetherington, A.M., and Sanders, D. (2005). The vacuolar Ca2+-activated channel TPC1 regulates germination and stomatal

movement. Nature *434*, 404-408.

Perraud, A.L., Fleig, A., Dunn, C.A., Bagley, L.A., Launay, P., Schmitz, C., Stokes, A.J., Zhu, Q., Bessman, M.J., Penner, R.*, et al.* (2001). ADP-ribose gating of the calcium-permeable LTRPC2 channel revealed by Nudix motif homology. Nature *411*, 595-599.

Peters, C., and Mayer, A. (1998). Ca2+/calmodulin signals the completion of docking and triggers a late step of vacuole fusion. Nature *396*, 575-580.

Pitt, S.J., Funnell, T.M., Sitsapesan, M., Venturi, E., Rietdorf, K., Ruas, M., Ganesan, A., Gosain, R., Churchill, G.C., Zhu, M.X.*, et al.* (2010). TPC2 is a novel NAADP-sensitive Ca2+ release channel, operating as a dual sensor of luminal pH and Ca2+. The Journal of biological chemistry *285*, 35039-35046.

Pittman, J.K. (2011). Vacuolar Ca(2+) uptake. Cell calcium *50*, 139-146.

Piwon, N., Gunther, W., Schwake, M., Bosl, M.R., and Jentsch, T.J. (2000). ClC-5 Cl- -channel disruption impairs endocytosis in a mouse model for Dent's disease. Nature *408*, 369-373.

Planells-Cases, R., and Jentsch, T.J. (2009). Chloride channelopathies. Biochimica et biophysica acta *1792*, 173-189.

Platt, F.M., Boland, B., and van der Spoel, A.C. (2012). The cell biology of disease: lysosomal storage disorders: the cellular impact of lysosomal dysfunction. The Journal of cell biology *199*, 723-734.

Poccia, D., and Larijani, B. (2009). Phosphatidylinositol metabolism and membrane fusion. The Biochemical journal *418*, 233-246.

Poupetova, H., Ledvinova, J., Berna, L., Dvorakova, L., Kozich, V., and Elleder, M. (2010). The birth prevalence of lysosomal storage disorders in the Czech Republic: comparison with data in different populations. Journal of inherited metabolic disease *33*, 387-396.

Pryor, P.R., Mullock, B.M., Bright, N.A., Gray, S.R., and Luzio, J.P. (2000). The role of intraorganellar Ca(2+) in late endosome-lysosome heterotypic fusion and in the reformation of lysosomes from hybrid organelles. The Journal of cell biology *149*, 1053-1062.

Pryor, P.R., Reimann, F., Gribble, F.M., and Luzio, J.P. (2006). Mucolipin-1 is a lysosomal membrane protein required for intracellular lactosylceramide traffic. Traffic *7*, 1388-1398.

Puertollano, R., and Kiselyov, K. (2009). TRPMLs: in sickness and in health. American journal of physiology Renal physiology *296*, F1245-1254.

Qiu, Q.S., and Fratti, R.A. (2010). The Na+/H+ exchanger Nhx1p regulates the initiation of Saccharomyces cerevisiae vacuole fusion. Journal of cell science *123*, 3266-3275.

Qureshi, O.S., Paramasivam, A., Yu, J.C., and Murrell-Lagnado, R.D. (2007). Regulation of P2X4 receptors by lysosomal targeting, glycan protection and exocytosis. Journal of cell science *120*, 3838-3849.

Radhakrishnan, A., Goldstein, J.L., McDonald, J.G., and Brown, M.S. (2008). Switch-like control of SREBP-2 transport triggered by small changes in ER cholesterol: a delicate balance. Cell Metab *8*, 512-521.

Rao, S.K., Huynh, C., Proux-Gillardeaux, V., Galli, T., and Andrews, N.W. (2004). Identification of SNAREs involved in synaptotagmin VII-regulated lysosomal exocytosis. The Journal of biological chemistry *279*, 20471-20479.

Reddy, A., Caler, E.V., and Andrews, N.W. (2001). Plasma membrane repair is mediated by Ca(2+)-regulated exocytosis of lysosomes. Cell *106*, 157-169.

Rienmuller, F., Dreyer, I., Schonknecht, G., Schulz, A., Schumacher, K., Nagy, R., Martinoia, E., Marten, I., and Hedrich, R. (2012). Luminal and cytosolic pH feedback on proton pump activity and ATP affinity of V-type ATPase from Arabidopsis. The Journal of biological chemistry *287*, 8986-8993.

Rizzuto, R., Marchi, S., Bonora, M., Aguiari, P., Bononi, A., De Stefani, D., Giorgi, C., Leo, S., Rimessi, A., Siviero, R.*, et al.* (2009). Ca(2+) transfer from the ER to mitochondria: when, how and why. Biochimica et biophysica acta *1787*, 1342-1351.

Roczniak-Ferguson, A., Petit, C.S., Froehlich, F., Qian, S., Ky, J., Angarola, B., Walther, T.C., and Ferguson, S.M. (2012). The transcription factor TFEB links mTORC1 signaling to transcriptional control of lysosome homeostasis. Science signaling *5*, ra42.

Rodriguez, A., Martinez, I., Chung, A., Berlot, C.H., and Andrews, N.W. (1999). cAMP regulates Ca2+-dependent exocytosis of lysosomes and lysosome-mediated cell invasion by trypanosomes. The Journal of biological chemistry *274*, 16754-16759.

Rodriguez, A., Webster, P., Ortego, J., and Andrews, N.W. (1997). Lysosomes behave as Ca2+-regulated exocytic vesicles in fibroblasts and epithelial cells. The Journal of cell biology *137*, 93-104.

Rodriguez-Rosales, M.P., Galvez, F.J., Huertas, R., Aranda, M.N., Baghour, M., Cagnac, O., and Venema, K. (2009). Plant NHX cation/proton antiporters. Plant signaling & behavior *4*, 265-276.

Rosen, D., Lewis, A.M., Mizote, A., Thomas, J.M., Aley, P.K., Vasudevan, S.R., Parkesh, R., Galione, A., Izumi, M., Ganesan, A.*, et al.* (2009). Analogues of the nicotinic acid adenine dinucleotide phosphate (NAADP) antagonist Ned-19 indicate two binding sites on the NAADP receptor. The Journal of biological chemistry *284*, 34930-34934.

Roth, M.G. (2004). Phosphoinositides in constitutive membrane traffic. Physiological reviews *84*, 699-730.

Roy, D., Liston, D.R., Idone, V.J., Di, A., Nelson, D.J., Pujol, C., Bliska, J.B., Chakrabarti, S., and Andrews, N.W. (2004). A process for controlling intracellular bacterial infections induced by membrane injury. Science *304*, 1515-1518.

Ruas, M., Rietdorf, K., Arredouani, A., Davis, L.C., Lloyd-Evans, E., Koegel, H., Funnell, T.M., Morgan, A.J., Ward, J.A., Watanabe, K.*, et al.* (2010). Purified TPC isoforms form NAADP

receptors with distinct roles for Ca(2+) signaling and endolysosomal trafficking. Current biology : CB *20*, 703-709.

Rudge, S.A., Anderson, D.M., and Emr, S.D. (2004). Vacuole size control: regulation of PtdIns(3,5)P2 levels by the vacuole-associated Vac14-Fig4 complex, a PtdIns(3,5)P2-specific phosphatase. Molecular biology of the cell *15*, 24-36.

Rusten, T.E., Vaccari, T., Lindmo, K., Rodahl, L.M., Nezis, I.P., Sem-Jacobsen, C., Wendler, F., Vincent, J.P., Brech, A., Bilder, D.*, et al.* (2007). ESCRTs and Fab1 regulate distinct steps of autophagy. Current biology : CB *17*, 1817-1825.

Rutherford, A.C., Traer, C., Wassmer, T., Pattni, K., Bujny, M.V., Carlton, J.G., Stenmark, H., and Cullen, P.J. (2006). The mammalian phosphatidylinositol 3-phosphate 5-kinase (PIKfyve) regulates endosome-to-TGN retrograde transport. Journal of cell science *119*, 3944-3957.

Rybalchenko, V., Ahuja, M., Coblentz, J., Churamani, D., Patel, S., Kiselyov, K., and Muallem, S. (2012). Membrane potential regulates nicotinic acid adenine dinucleotide phosphate (NAADP) dependence of the pH- and Ca2+-sensitive organellar two-pore channel TPC1. The Journal of biological chemistry *287*, 20407-20416.

Saftig, P., and Klumperman, J. (2009). Lysosome biogenesis and lysosomal membrane proteins: trafficking meets function. Nature reviews Molecular cell biology *10*, 623-635.

Saito, M., Hanson, P.I., and Schlesinger, P. (2007). Luminal chloride-dependent activation of endosome calcium channels: patch clamp study of enlarged endosomes. The Journal of biological chemistry *282*, 27327-27333.

Sardiello, M., Palmieri, M., di Ronza, A., Medina, D.L., Valenza, M., Gennarino, V.A., Di Malta, C., Donaudy, F., Embrione, V., Polishchuk, R.S.*, et al.* (2009). A gene network regulating lysosomal biogenesis and function. Science *325*, 473-477.

Savalas, L.R., Gasnier, B., Damme, M., Lubke, T., Wrocklage, C., Debacker, C., Jezegou, A., Reinheckel, T., Hasilik, A., Saftig, P.*, et al.* (2011). Disrupted in renal carcinoma 2 (DIRC2), a novel transporter of the lysosomal membrane, is proteolytically processed by cathepsin L. The Biochemical journal *439*, 113-128.

Sbrissa, D., Ikonomov, O.C., and Shisheva, A. (1999). PIKfyve, a mammalian ortholog of yeast Fab1p lipid kinase, synthesizes 5-phosphoinositides. Effect of insulin. The Journal of biological chemistry *274*, 21589-21597.

Schieder, M., Rotzer, K., Bruggemann, A., Biel, M., and Wahl-Schott, C.A. (2010). Characterization of two-pore channel 2 (TPCN2)-mediated Ca2+ currents in isolated lysosomes. The Journal of biological chemistry *285*, 21219-21222.

Schmidt, R., Zimmermann, H., and Whittaker, V.P. (1980). Metal ion content of cholinergic synaptic vesicles isolated from the electric organ of Torpedo: effect of stimulation-induced transmitter release. Neuroscience *5*, 625-638.

Schroder, B.A., Wrocklage, C., Hasilik, A., and Saftig, P. (2010). The proteome of lysosomes.

Proteomics *10*, 4053-4076.

Scott, C.C., and Gruenberg, J. (2011). Ion flux and the function of endosomes and lysosomes: pH is just the start: the flux of ions across endosomal membranes influences endosome function not only through regulation of the luminal pH. BioEssays : news and reviews in molecular, cellular and developmental biology *33*, 103-110.

Seby, F., Gagean, M., Garraud, H., Castetbon, A., and Donard, O.F. (2003). Development of analytical procedures for determination of total chromium by quadrupole ICP-MS and high-resolution ICP-MS, and hexavalent chromium by HPLC-ICP-MS, in different materials used in the automotive industry. Anal Bioanal Chem *377*, 685-694.

Settembre, C., Fraldi, A., Medina, D.L., and Ballabio, A. (2013). Signals from the lysosome: a control centre for cellular clearance and energy metabolism. Nature reviews Molecular cell biology *14*, 283-296.

Shao, G.Z., Zhou, R.L., Zhang, Q.Y., Zhang, Y., Liu, J.J., Rui, J.A., Wei, X., and Ye, D.X. (2003). Molecular cloning and characterization of LAPTM4B, a novel gene upregulated in hepatocellular carcinoma. Oncogene *22*, 5060-5069.

Shen, D., Wang, X., Li, X., Zhang, X., Yao, Z., Dibble, S., Dong, X.P., Yu, T., Lieberman, A.P., Showalter, H.D.*, et al.* (2012). Lipid storage disorders block lysosomal trafficking by inhibiting a TRP channel and lysosomal calcium release. Nature communications *3*, 731.

Shen, D., Wang, X., and Xu, H. (2011). Pairing phosphoinositides with calcium ions in endolysosomal dynamics: phosphoinositides control the direction and specificity of membrane trafficking by regulating the activity of calcium channels in the endolysosomes. BioEssays : news and reviews in molecular, cellular and developmental biology *33*, 448-457.

Shen, J., Yu, W.M., Brotto, M., Scherman, J.A., Guo, C., Stoddard, C., Nosek, T.M., Valdivia, H.H., and Qu, C.K. (2009). Deficiency of MIP/MTMR14 phosphatase induces a muscle disorder by disrupting Ca(2+) homeostasis. Nature cell biology *11*, 769-776.

Slaugenhaupt, S.A. (2002). The molecular basis of mucolipidosis type IV. Current molecular medicine *2*, 445-450.

Soyombo, A.A., Tjon-Kon-Sang, S., Rbaibi, Y., Bashllari, E., Bisceglia, J., Muallem, S., and Kiselyov, K. (2006). TRP-ML1 regulates lysosomal pH and acidic lysosomal lipid hydrolytic activity. The Journal of biological chemistry *281*, 7294-7301.

Steinberg, B.E., Huynh, K.K., Brodovitch, A., Jabs, S., Stauber, T., Jentsch, T.J., and Grinstein, S. (2010). A cation counterflux supports lysosomal acidification. The Journal of cell biology *189*, 1171-1186.

Steinberg, B.E., Touret, N., Vargas-Caballero, M., and Grinstein, S. (2007). In situ measurement of the electrical potential across the phagosomal membrane using FRET and its contribution to the proton-motive force. Proceedings of the National Academy of Sciences of the United States of America *104*, 9523-9528.

Stenmark, H. (2009). Rab GTPases as coordinators of vesicle traffic. Nature reviews Molecular cell biology *10*, 513-525.

Sudhof, T.C., and Rizo, J. (1996). Synaptotagmins: C2-domain proteins that regulate membrane traffic. Neuron *17*, 379-388.

Suh, B.C., and Hille, B. (2008). PIP2 is a necessary cofactor for ion channel function: how and why? Annual review of biophysics *37*, 175-195.

Sulem, P., Gudbjartsson, D.F., Stacey, S.N., Helgason, A., Rafnar, T., Jakobsdottir, M., Steinberg, S., Gudjonsson, S.A., Palsson, A., Thorleifsson, G.*, et al.* (2008). Two newly identified genetic determinants of pigmentation in Europeans. Nature genetics *40*, 835-837.

Sumoza-Toledo, A., Lange, I., Cortado, H., Bhagat, H., Mori, Y., Fleig, A., Penner, R., and Partida-Sanchez, S. (2011). Dendritic cell maturation and chemotaxis is regulated by TRPM2-mediated lysosomal Ca2+ release. FASEB journal : official publication of the Federation of American Societies for Experimental Biology *25*, 3529-3542.

Sun, M., Goldin, E., Stahl, S., Falardeau, J.L., Kennedy, J.C., Acierno, J.S., Jr., Bove, C., Kaneski, C.R., Nagle, J., Bromley, M.C.*, et al.* (2000). Mucolipidosis type IV is caused by mutations in a gene encoding a novel transient receptor potential channel. Human molecular genetics *9*, 2471-2478.

Suudhof, T.C. (2008). Neurotransmitter release. Handbook of experimental pharmacology, 1-21.

Tam, C., Idone, V., Devlin, C., Fernandes, M.C., Flannery, A., He, X., Schuchman, E., Tabas, I., and Andrews, N.W. (2010). Exocytosis of acid sphingomyelinase by wounded cells promotes endocytosis and plasma membrane repair. The Journal of cell biology *189*, 1027-1038.

Tapper, H., Furuya, W., and Grinstein, S. (2002). Localized exocytosis of primary (lysosomal) granules during phagocytosis: role of Ca2+-dependent tyrosine phosphorylation and microtubules. Journal of immunology *168*, 5287-5296.

Tauber, A.I. (2003). Metchnikoff and the phagocytosis theory. Nature reviews Molecular cell biology *4*, 897-901.

Thai, T.L., Churchill, G.C., and Arendshorst, W.J. (2009). NAADP receptors mediate calcium signaling stimulated by endothelin-1 and norepinephrine in renal afferent arterioles. American journal of physiology Renal physiology *297*, F510-516.

Thompson, E.G., Schaheen, L., Dang, H., and Fares, H. (2007). Lysosomal trafficking functions of mucolipin-1 in murine macrophages. BMC cell biology *8*, 54.

Tieleman, D.P., Shrivastava, I.H., Ulmschneider, M.R., and Sansom, M.S. (2001). Proline-induced hinges in transmembrane helices: possible roles in ion channel gating. Proteins *44*, 63-72.

Toei, M., Saum, R., and Forgac, M. (2010). Regulation and isoform function of the V-ATPases. Biochemistry *49*, 4715-4723.

Tofaris, G.K. (2012). Lysosome-dependent pathways as a unifying theme in Parkinson's disease. Movement disorders : official journal of the Movement Disorder Society *27*, 1364-1369.

Toth, B., and Csanady, L. (2010). Identification of direct and indirect effectors of the transient receptor potential melastatin 2 (TRPM2) cation channel. J Biol Chem *285*, 30091-30102.

Tsien, R.Y., Pozzan, T., and Rink, T.J. (1982). Calcium homeostasis in intact lymphocytes: cytoplasmic free calcium monitored with a new, intracellularly trapped fluorescent indicator. The Journal of cell biology *94*, 325-334.

Tucker, W.C., Weber, T., and Chapman, E.R. (2004). Reconstitution of Ca2+-regulated membrane fusion by synaptotagmin and SNAREs. Science *304*, 435-438.

Tugba Durlu-Kandilci, N., Ruas, M., Chuang, K.T., Brading, A., Parrington, J., and Galione, A. (2010). TPC2 proteins mediate nicotinic acid adenine dinucleotide phosphate (NAADP)- and agonist-evoked contractions of smooth muscle. The Journal of biological chemistry *285*, 24925-24932.

van der Goot, F.G., and Gruenberg, J. (2006). Intra-endosomal membrane traffic. Trends in cell biology *16*, 514-521.

Van der Kloot, W. (2003). Loading and recycling of synaptic vesicles in the Torpedo electric organ and the vertebrate neuromuscular junction. Progress in neurobiology *71*, 269-303.

Van Dyke, R.W. (1993). Acidification of rat liver lysosomes: quantitation and comparison with endosomes. The American journal of physiology *265*, C901-917.

Venkatachalam, K., Long, A.A., Elsaesser, R., Nikolaeva, D., Broadie, K., and Montell, C. (2008). Motor deficit in a Drosophila model of mucolipidosis type IV due to defective clearance of apoptotic cells. Cell *135*, 838-851.

Venugopal, B., Browning, M.F., Curcio-Morelli, C., Varro, A., Michaud, N., Nanthakumar, N., Walkley, S.U., Pickel, J., and Slaugenhaupt, S.A. (2007). Neurologic, gastric, and opthalmologic pathologies in a murine model of mucolipidosis type IV. American journal of human genetics *81*, 1070-1083.

Vergarajauregui, S., Connelly, P.S., Daniels, M.P., and Puertollano, R. (2008). Autophagic dysfunction in mucolipidosis type IV patients. Human molecular genetics *17*, 2723-2737.

Vergarajauregui, S., Martina, J.A., and Puertollano, R. (2009). Identification of the penta-EF-hand protein ALG-2 as a Ca2+-dependent interactor of mucolipin-1. The Journal of biological chemistry *284*, 36357-36366.

Vergarajauregui, S., Martina, J.A., and Puertollano, R. (2011). LAPTMs regulate lysosomal function and interact with mucolipin 1: new clues for understanding mucolipidosis type IV. Journal of cell science *124*, 459-468.

Vergarajauregui, S., and Puertollano, R. (2006). Two di-leucine motifs regulate trafficking of mucolipin-1 to lysosomes. Traffic *7*, 337-353.

Vieira, O.V., Botelho, R.J., and Grinstein, S. (2002). Phagosome maturation: aging gracefully. The Biochemical journal *366*, 689-704.

Walseth, T.F., Lin-Moshier, Y., Jain, P., Ruas, M., Parrington, J., Galione, A., Marchant, J.S., and Slama, J.T. (2011). Photoaffinity labeling of high affinity nicotinic acid adenine dinucleotide 2'-phosphate (NAADP) proteins in sea urchin egg. J Biol Chem.

Walseth, T.F., Lin-Moshier, Y., Jain, P., Ruas, M., Parrington, J., Galione, A., Marchant, J.S., and Slama, J.T. (2012). Photoaffinity labeling of high affinity nicotinic acid adenine dinucleotide phosphate (NAADP)-binding proteins in sea urchin egg. The Journal of biological chemistry *287*, 2308-2315.

Wartosch, L., Fuhrmann, J.C., Schweizer, M., Stauber, T., and Jentsch, T.J. (2009). Lysosomal degradation of endocytosed proteins depends on the chloride transport protein ClC-7. FASEB journal : official publication of the Federation of American Societies for Experimental Biology *23*, 4056-4068.

Weinert, S., Jabs, S., Supanchart, C., Schweizer, M., Gimber, N., Richter, M., Rademann, J., Stauber, T., Kornak, U., and Jentsch, T.J. (2010). Lysosomal pathology and osteopetrosis upon loss of H+-driven lysosomal Cl- accumulation. Science *328*, 1401-1403.

Wieczorek, H., Grber, G., Harvey, W.R., Huss, M., Merzendorfer, H., and Zeiske, W. (2000). Structure and regulation of insect plasma membrane H(+)V-ATPase. The Journal of experimental biology *203*, 127-135.

Wong, C.O., Li, R., Montell, C., and Venkatachalam, K. (2012). Drosophila TRPML is required for TORC1 activation. Current biology : CB *22*, 1616-1621.

Wu, L., Bauer, C.S., Zhen, X.G., Xie, C., and Yang, J. (2002). Dual regulation of voltage-gated calcium channels by PtdIns(4,5)P2. Nature *419*, 947-952.

Xu, H., Delling, M., Li, L., Dong, X., and Clapham, D.E. (2007). Activating mutation in a mucolipin transient receptor potential channel leads to melanocyte loss in varitint-waddler mice. Proceedings of the National Academy of Sciences of the United States of America *104*, 18321-18326.

Yabe, I., Horiuchi, K., Nakahara, K., Hiyama, T., Yamanaka, T., Wang, P.C., Toda, K., Hirata, A., Ohsumi, Y., Hirata, R.*, et al.* (1999). Patch clamp studies on V-type ATPase of vacuolar membrane of haploid Saccharomyces cerevisiae. Preparation and utilization of a giant cell containing a giant vacuole. The Journal of biological chemistry *274*, 34903-34910.

Yamasaki, M., Masgrau, R., Morgan, A.J., Churchill, G.C., Patel, S., Ashcroft, S.J., and Galione, A. (2004). Organelle selection determines agonist-specific Ca2+ signals in pancreatic acinar and beta cells. The Journal of biological chemistry *279*, 7234-7240.

Yamasaki, M., Thomas, J.M., Churchill, G.C., Garnham, C., Lewis, A.M., Cancela, J.M., Patel, S., and Galione, A. (2005). Role of NAADP and cADPR in the induction and maintenance of agonist-evoked Ca2+ spiking in mouse pancreatic acinar cells. Current biology : CB *15*, 874-878.

Yu, F.H., and Catterall, W.A. (2004). The VGL-chanome: a protein superfamily specialized for electrical signaling and ionic homeostasis. Science's STKE : signal transduction knowledge environment *2004*, re15.

Yu, L., McPhee, C.K., Zheng, L., Mardones, G.A., Rong, Y., Peng, J., Mi, N., Zhao, Y., Liu, Z., Wan, F.*, et al.* (2010). Termination of autophagy and reformation of lysosomes regulated by mTOR. Nature *465*, 942-946.

Zeevi, D.A., Frumkin, A., Offen-Glasner, V., Kogot-Levin, A., and Bach, G. (2009). A potentially dynamic lysosomal role for the endogenous TRPML proteins. The Journal of pathology *219*, 153-162.

Zhang, F., and Li, P.L. (2007). Reconstitution and characterization of a nicotinic acid adenine dinucleotide phosphate (NAADP)-sensitive Ca2+ release channel from liver lysosomes of rats. The Journal of biological chemistry *282*, 25259-25269.

Zhang, M., Goforth, P., Bertram, R., Sherman, A., and Satin, L. (2003). The Ca2+ dynamics of isolated mouse beta-cells and islets: implications for mathematical models. Biophys J *84*, 2852-2870.

Zhang, X., Li, X., and Xu, H. (2012a). Phosphoinositide isoforms determine compartment-specific ion channel activity. Proceedings of the National Academy of Sciences of the United States of America *109*, 11384-11389.

Zhang, Y., McCartney, A.J., Zolov, S.N., Ferguson, C.J., Meisler, M.H., Sutton, M.A., and Weisman, L.S. (2012b). Modulation of synaptic function by VAC14, a protein that regulates the phosphoinositides PI(3,5)P(2) and PI(5)P. The EMBO journal *31*, 3442-3456.

Zhang, Y., Zolov, S.N., Chow, C.Y., Slutsky, S.G., Richardson, S.C., Piper, R.C., Yang, B., Nau, J.J., Westrick, R.J., Morrison, S.J.*, et al.* (2007a). Loss of Vac14, a regulator of the signaling lipid phosphatidylinositol 3,5-bisphosphate, results in neurodegeneration in mice. Proceedings of the National Academy of Sciences of the United States of America *104*, 17518-17523.

Zhang, Z., Chen, G., Zhou, W., Song, A., Xu, T., Luo, Q., Wang, W., Gu, X.S., and Duan, S. (2007b). Regulated ATP release from astrocytes through lysosome exocytosis. Nature cell biology *9*, 945-953.

Zhao, H., Ito, Y., Chappel, J., Andrews, N.W., Teitelbaum, S.L., and Ross, F.P. (2008). Synaptotagmin VII regulates bone remodeling by modulating osteoclast and osteoblast secretion. Developmental cell *14*, 914-925.

Zhao, Y., Graeff, R., and Lee, H.C. (2012). Roles of cADPR and NAADP in pancreatic cells. Acta biochimica et biophysica Sinica *44*, 719-729.

Zhao, Y., Yarov-Yarovoy, V., Scheuer, T., and Catterall, W.A. (2004). A gating hinge in Na+ channels; a molecular switch for electrical signaling. Neuron *41*, 859-865.

Zhu, M.X., Evans, A.M., Ma, J., Parrington, J., and Galione, A. (2010a). Two-pore channels for integrative Ca signaling. Communicative & integrative biology *3*, 12-17.

Zhu, M.X., Ma, J., Parrington, J., Calcraft, P.J., Galione, A., and Evans, A.M. (2010b). Calcium signaling via two-pore channels: local or global, that is the question. American journal of physiology Cell physiology *298*, C430-441.

Zhu, M.X., Ma, J., Parrington, J., Galione, A., and Evans, A.M. (2010c). TPCs: Endolysosomal channels for Ca2+ mobilization from acidic organelles triggered by NAADP. FEBS letters *584*, 1966-1974.

Zolov, S.N., Bridges, D., Zhang, Y., Lee, W.W., Riehle, E., Verma, R., Lenk, G.M., Converso-Baran, K., Weide, T., Albin, R.L.*, et al.* (2012). In vivo, Pikfyve generates PI(3,5)P2, which serves as both a signaling lipid and the major precursor for PI5P. Proceedings of the National Academy of Sciences of the United States of America *109*, 17472-17477.

Zoncu, R., Bar-Peled, L., Efeyan, A., Wang, S., Sancak, Y., and Sabatini, D.M. (2011). mTORC1 senses lysosomal amino acids through an inside-out mechanism that requires the vacuolar H(+)-ATPase. Science *334*, 678-683.

Zoncu, R., Perera, R.M., Balkin, D.M., Pirruccello, M., Toomre, D., and De Camilli, P. (2009). A phosphoinositide switch controls the maturation and signaling properties of APPL endosomes. Cell *136*, 1110-1121.

Zong, X., Schieder, M., Cuny, H., Fenske, S., Gruner, C., Rotzer, K., Griesbeck, O., Harz, H., Biel, M., and Wahl-Schott, C. (2009). The two-pore channel TPCN2 mediates NAADP-dependent Ca(2+)-release from lysosomal stores. Pflugers Archiv : European journal of physiology *458*, 891-899.